2013

Increased Gas Recovery Experts in Team, Gullfaks village

Turan Eyyubbali	International master student, Petroleum engineering
Xin Luo	International master student, Statistics
Vegard Skogstad	4th year student, Industrial Chemical engineering
Kjell Andreas Thorud	4th year student, Marine Technology
Chunlei Wang	International master student, Petroleum geoscience
Togi Yonathan	International master student, Petroleum geoscience

Norwegian University of Science and Technology

2/5/2013

Abstract

In this report we have investigated the effect of installing a compression system in connection to the Gullfaks C template. Three different cases have been modeled and analyzed, subsea compressor installation, subsea compressor installation with low pressure modification (LPM) and compressor installation on the platform. Each of the cases has been reviewed and compared to the reference case, in which there is no compressor installation at all. To find the best possible option we have performed an economic evaluation and also done a risk and sensitivity analysis.

In economic analysis we have found that the NPV of the different projects did not differ too much, making our overall conclusions uncertain and very dependent on investment cost.

To confirm that our dry gas basis models were applicable a calculation based on the Modified Black Oil Formulation was also carried out. This showed that the accuracy of our dry gas calculation was good.

Preface

This report is written as part of the subject TPG4851 Experts in Team, Gullfaks Village 2013. The objective of the course is to conduct an interdisciplinary project with students from with different nationalities and backgrounds.

First of all we would like to thank our village leader, Professor Jon Kleppe, and Professor Jan Ivar Jensen for their help and motivation through both the teambuilding and the technical aspects of the project. We would also like to thank Professor Michael Golan, who not only has made us understand how incredible easy it must be to work as a consultant, but also has taught us quite a bit about petroleum technology. We must also mention his talented and helpful Ph.D. students, without their guidance and help with excel files this project would not have been possible. Through this project we have also appreciated the helpful feedback we have gotten from our facilitators, Simon and Heninge.

A special thanks goes out to the representatives from Statoil for providing us with useful and interesting information about the challenges related to increased gas recovery. We are also grateful that we got a chance to hold a presentation during our meeting in Bergen.

Trondheim, May 1st, 2013

Table of Contents

Increased Gas Recovery
for the
Gullfaks South M- and L-template, Norway

In this report we investigate the consequences of installing a subsea compressor in connection to the Gullfaks L and M templates. This report provides quality control and quality assurance for the project, giving optimized production for both templates from 2008 until end of production, economical effects of subsea-compressor installation and decreased separator pressure at Gullfaks C, as well as evaluates the risks of liquid accumulation in the wells for each year of production. Sensitivity analysis and qualitative risk analysis are also included.

The Gullfaks area is a combined oil and gas field located in the Norwegian part of the North Sea, roughly 175 km northwest of Bergen.[1, 2] The main field has been in production since 1986 and today also produces from 6 satellite fields including, Gullfaks South, Gullveig, Gimle, Gulltopp, Rimfaks and Skinfaks. Of these satellite fields Gullfaks South is the largest satellite field in area, and mainly contains natural gas. Gullfaks south has been producing since 1998 and consists of several subsea templates which each is connected to a handful of wells each. The subsea templates transport the resources through pipelines to a platform, either Gullfaks A or Gullfaks C, where the different phases are separated.

In this report it has been focused on two of the templates connected to Gullfaks C: The M- template and the L-template. As of 2008, steady decline in reservoir pressures for the M- and L-templates threatens to decrease the flow rate out of the reservoir. To keep the flow rate constant, and by this increase the total gas recovery from the reservoir, Statoil has decided to install a subsea compressor.

The project was split into two parts, Part A and B, where the first task served as an introduction before meeting with Statoil and Framo Engineering in Bergen. In Part A an initial estimation of the project NPV with and without compressor installation was made using a dry gas basis. To check if the compressor is capable or of delivering the intended pressure a compressor map is used which is the based on our excel calculation. Results for part A is shown in section 3.1 with theory covered briefly in Appendices A and B.

Part B has a broader scope than part A, it has been split into the remaining subsections 3.2-3.7 and Appendices C-F. Here the assumption of a dry gas basis is verified and reservoir optimization for 4 different cases are carried out: No compressor installation, installation of a subsea compression system, installation of a compression system at the platform and installation of a subsea compression system with a lowering of the pressure in the platform separator train.

The results in this report was acquired using excel sheets. The excel sheets was based on transport equations for dry gas which was verified using modified black oil mass balances in section 3.2. The Peng-Robinson thermodynamic package was used with HYSYS[3] to find black oil parameters, densities, and flow characteristics in the wellhead at various reservoir pressures.

2. Conclusions and Recommendation

- If we keep producing after 2030 the low pressure modification might give liquid accumulation in one of the L-template wells.
- The dry gas model and the modified black oil model gave almost identical results which make the dry gas model a good bet for rough estimations.
- The low pressure modification gave the highest project NPV of the three cases with 255 million USD, topside compression gave the lowest at 247.
- Based on sensitivity analysis, the parameter that will impact the NPV mostly is changing gas price.
- Installing the compressor system subsea gave lower risks than installing it on the platform.

Based on reservoir optimization cases and economical calculation, it is clear that the LPM (low pressure modification) case is the best option for Statoil. It will both give the highest economical yield and the lowest risk.

3. Discussion

In section 3.1, transport equations were used to calculate the economically optimized flow out of each of the templates, granted that the combined gas flow would stay at a constant 10×10^6 Sm^3/d. The proportion coming from each template could be adjusted by using either small chokes at each individual wellhead or two larger chokes, directly upstream of the separator system. Both of these possibilities were modeled from 2008 till end of production, defined as the point where total flow fell below 5×10^6 Sm^3/d.

For both cases there was assumed to be only dry gas in the reservoir, and that a subsea compressor system would be installed at an appropriate time to keep the total flow constant some more years. A rough economical evaluation was performed, as well as an analysis of compressor performance. In section 3.2 a modified black oil model was used to get a better optimization than the one found in 3.1. The old and new models were compared, to test the merit of the dry gas assumption and provide additional quality assurance.

Decreasing the pressure in the separator was tested, using a dry gas basis, and is shown in section 3.3. The NPV of the project with the low-pressure modification was also calculated. When the pressure in a reservoir decrease, liquid accumulation is always a possibility; it was tested for using different variations of Turner's droplet model,[4] and is shown in section 3.4. For the models developed in previous sections a parametric analysis was carried out, this is the focus of section 3.5. All the results found in previous subsections are evaluated in section 3.6, this forms the basis for section 2.

3.1. Dry Gas Basis

The first task, named part A, will serve as a more thorough introduction into the Gullfaks case. As mentioned in section 1, the Gullfaks field is surrounded by many subsea templates each belonging at one of Gullfaks several satellite fields. This project is centered on two of these subsea templates, located at Gullfaks South, one of Gullfaks main's biggest satellite fields. The two templates, called the M- and L-template produce almost pure natural gas from 3 and 4 wells respectively, and have reservoir pressures of 210 and 240 bars in 2008. Gas is sent from the templates into either a compression system followed by a towhead, or directly to the towhead without compression. From the towhead the resources are transported through pipelines for 14 km along the seabed, there it reaches a platform, Gullfaks C. At the platform the natural gas is separated from liquids like oil and water, and sent to be processed at the Mongstad gas power plant. Fig. 3.1.1 shows a rough overview of the Subsea-system.

The objective for part A of the project was to find an optimal production plan, including when a subsea compressor should be installed and what year production should be stopped. The key issues for solving the task are:

- To produce a constant 10×10^6 Sm^3/d total from both templates combined. This is because a constant production gives stability and dependability.
- To keep the production at this level as long as possible. To maximize profits and to preserve the dependability this gives.
- When removing gas from the reservoir, the pressure in the reservoir drops; this will cause the flow out of the reservoir to decrease and eventually die out. To compensate for this, a compressor can be used to increase the flow.

For part A, two different models were made. These two differed in what valves where used to control the flow from the reservoir. For the first model, case 1, valves located at each individual wellhead were used to control the flow, gradually opening as the pressure in the reservoir decreased. For the second model, the valves at the wellhead were used to keep the flows going into the template from the wells. Meanwhile, two bigger valves directly upstream of the separator were used to control the flow out of each template. The different cases are shown in Figs. 3.1.2 and 3.1.3, and are discussed in section 3.1.1 and 3.1.2 respectively.

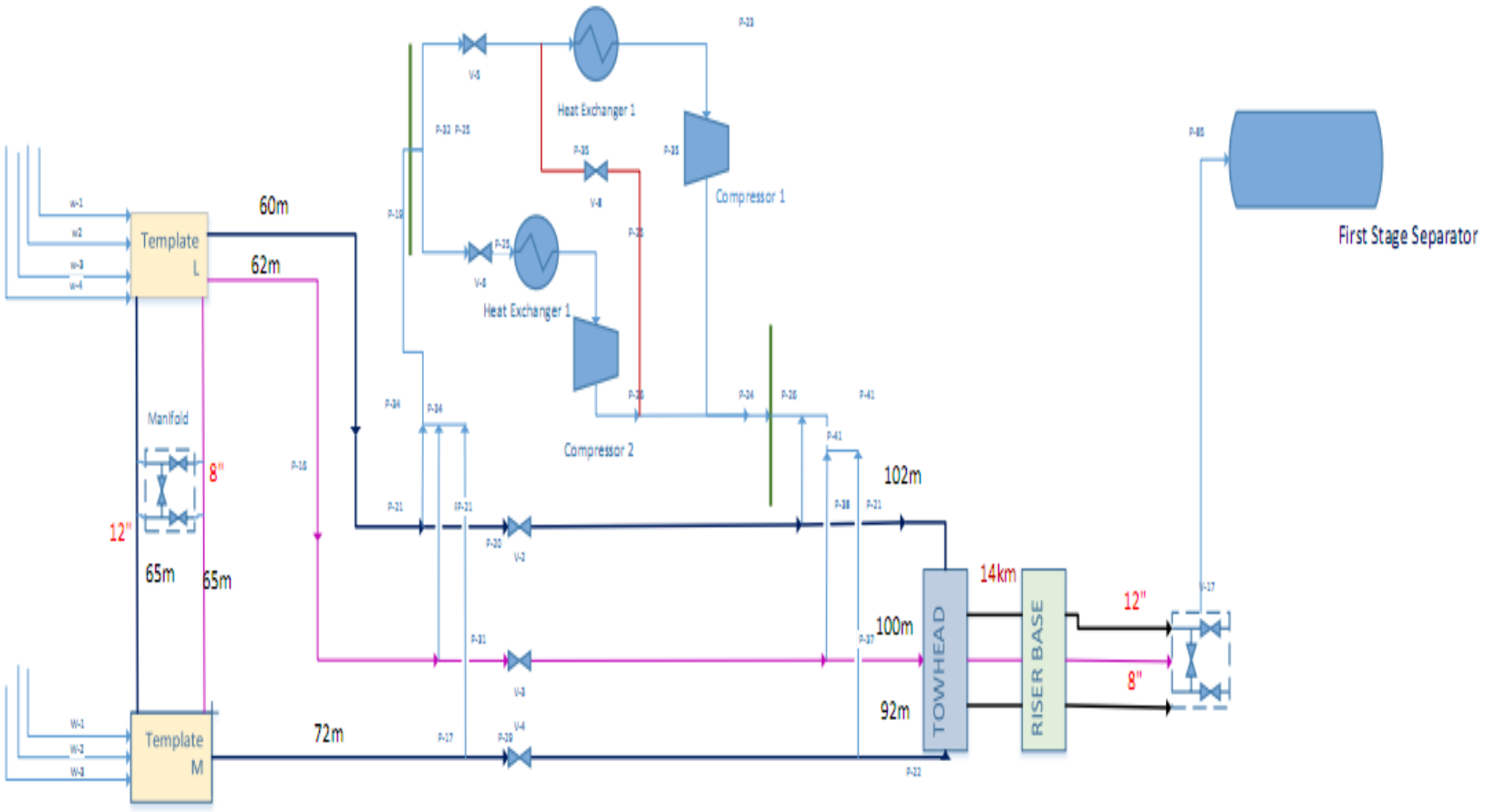

Figure 3.1.1: Flow diagram for subsea compressor cases. The figure demonstrates how the gas flows from the reservoir. First, the gas will flow from the reservoir to the template, and continue the flow to the compressor within 60 m 12" pipe, followed by flow to towhead within the same pipe 100 meters long. The gas will then proceed to flow from The towhead to the separator in platform by 14" pipe-14 km long. With installing the subsea compressor the flow plateau duration can be extended and also optimizing the total flow in the later flow stage after natural plateau and driven plateau.

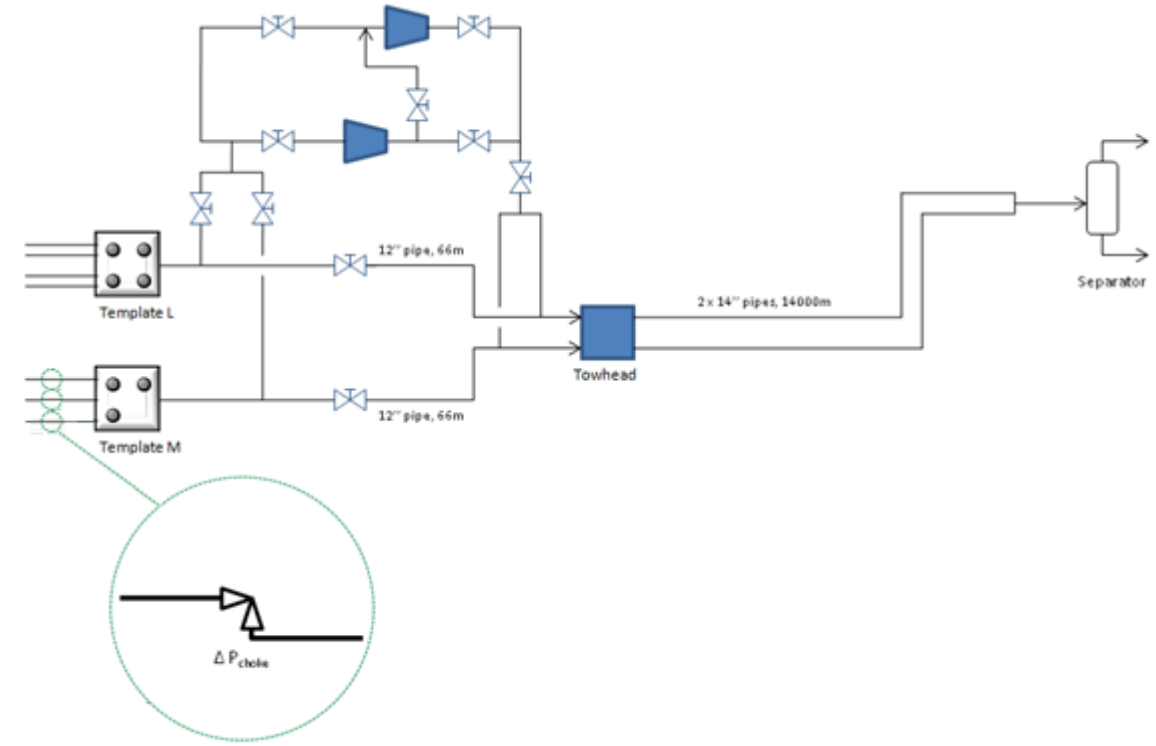

Figure 3.1.2: Flow sequence sketch for case 1 after compressor installation. Here the manipulated chokes are uptream of the templates, shown in green for template M.

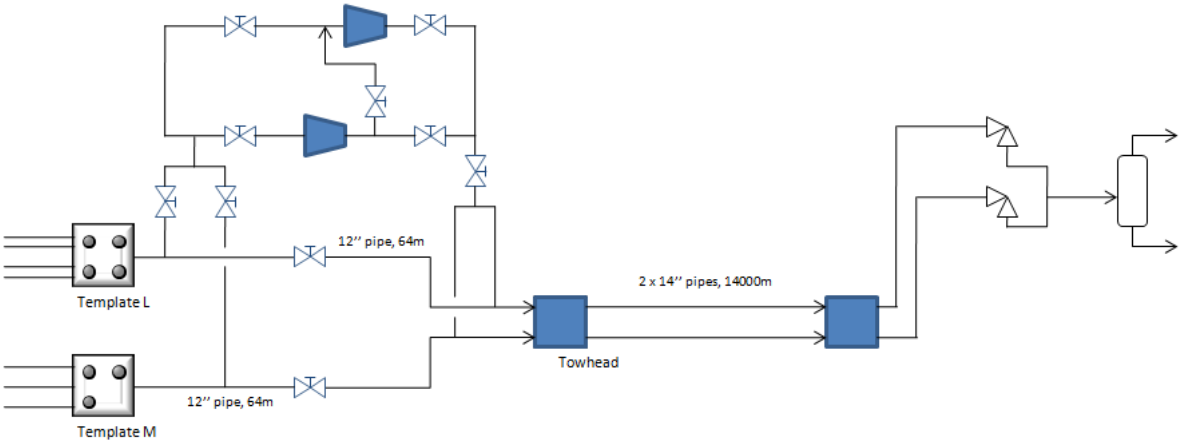

Figure 3.1.3: Flow sequence sketch for case 2 after compressor installation. Here the manipulated chokes are the ones next to the separator.

To find the optimized production plan for case 1 and 2, transport equations and excel programming were used. In Appendix A the theory behind the dry gas model and the transport equations is

shown. Appendix E includes the excel file containing used formulas, tables and all included plots, while the economics are covered in Appendix D. Several simplifications were made for both cases:

- The reservoir was modeled using the tank model.
- The 8'' pipe shown in Fig. 3.1.1, and the connecting pipes between template M and template L were ignored entirely.
- Dry gas was assumed for all equations used in the excel sheet and shown in Appendix A.
- The pressure loss due to lifting gas from the sea floor to the platform was ignored, as it would be mostly light gas in the stream this simplification seems reasonable.
- For case 1 it was assumed that the pressure in the reservoir was identical for each well connected to the same template.
- Each well was assumed to be equally long and deep.

3.1.1. Case 1: Flow Control from the Wellhead Valves

Case 1 can be divided in 2 main periods. The first period lasts until compressor installation, where the gas flows naturally. The second period lasts from compressor installation until end of production. When the natural flow rate falls below the wanted flow rate, here 10×10^6 Sm^3/d, the reservoir has reached the end of the natural plateau. By installing a compressor the actual flow rate falls below the wanted flow rate at a later time; when it does, the reservoir have reached the end of the driven plateau.

In the first period, gas flows from the reservoir to the wellhead and continue to the template, at which the pressure is 73 bars. The flow continues from the template to the towhead through a 64 m long 12" pipe and eventually ends up in the separator. From the towhead to the separator the gs goes through a 14" pipe for 14 kilometers. The pressure difference over the chokes, Δp_{Choke}, is here defined as the difference between the pressure in the wellhead, p_{wh}, and the pressure in the template, $p_{Template}$. Δp_{Choke} decreases with time as the pressure in the reservoir falls. Eventually this causes the flow to decrease. To keep this from happening as long as possible the pressure difference need to be maintained, this have been done by changing the flow rates from each template, $Q_{f,L}$ and $Q_{f,M}$, while keeping the total flow out of the reservoir at 10×10^6 Sm^3/d. The pressure data for each year is shown Figs. 3.1.4 and 3.1.5.

From 2007-2011, the flow rates were kept at 6×10^6 Sm^3/d and 4×10^6 Sm^3/d out of template L and M respectively. After this, the rate from each field needs to be changed to maintain the pressure difference in the M-template. By changing the flows out of each template the natural flow could be maintained until 2016 before the reservoir reached the end of the natural plateau.

From January 2017, a compression system had to be installed to keep the total flow at 10×10^6 Sm^3/d. The primary variable at this stage is the pressure difference between $p_{suction}$ and $p_{towhead}$ which is referred to as $\Delta p_{Compressor}$. The $\Delta p_{Compressor}$ will increase with time but cannot exceed 32 bars, which is considered the maximum pressure the compressor system is able to provide. Calculation showed that $\Delta p_{Compressor}$ will be 32 bars after slightly more than 1 year after compressor installation. That means that early 2018 signify the end of the driven plateau, after this the compressor applied a constant pressure difference to keep the field rate as high as possible. The total flow rate from both

templates will gradually decrease until it reaches the minimum, here defined as 5×10^6 Sm^3/d. This happens in 2026, as shown in Fig. 3.1.6.

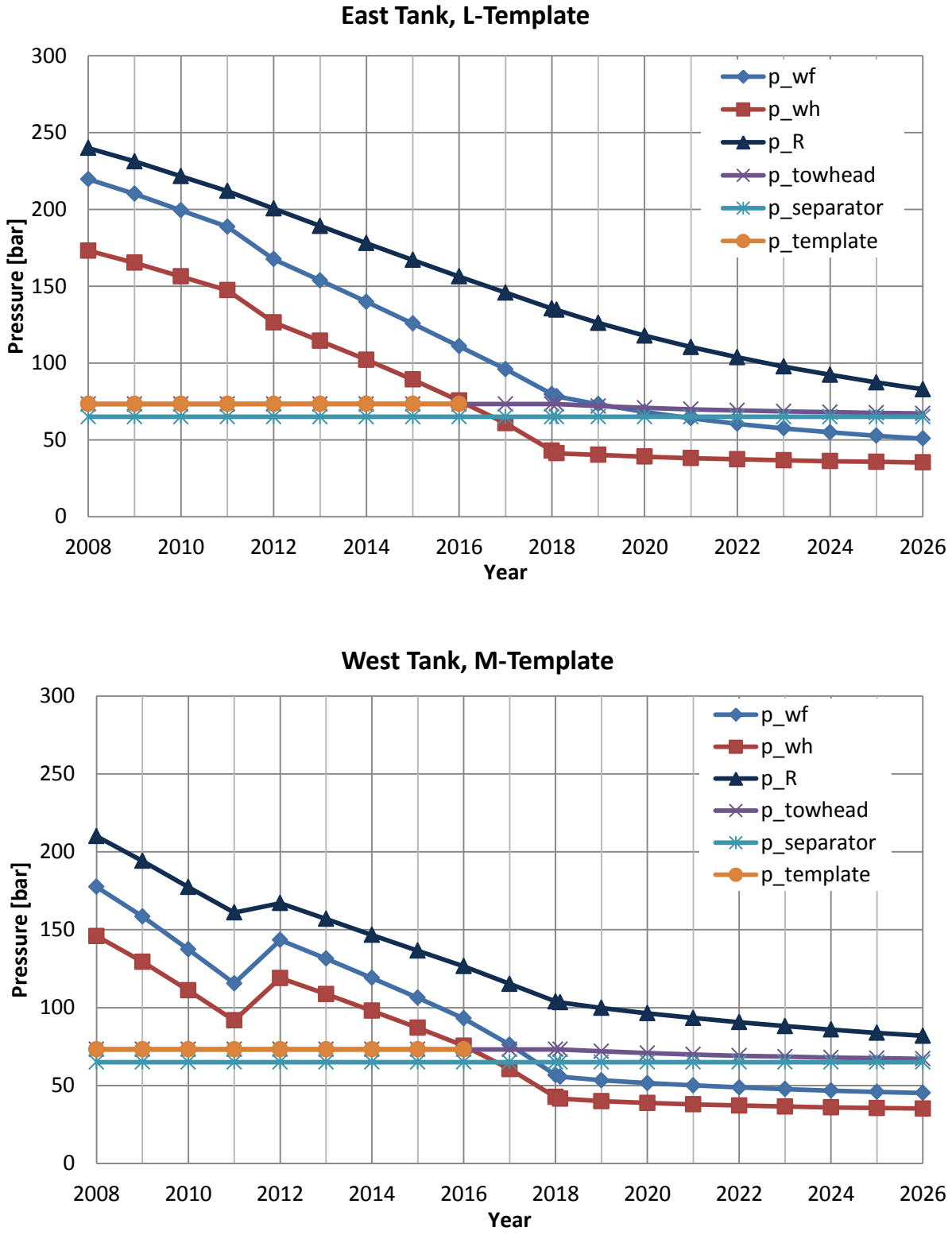

Figure 3.1.4 and 3.1.5: Pressure plots for the east and west tank. The figures show pressure drop through the years of production for the reservoir, p_R, the well bottom, p_{wf} and the wellhead, p_{wh}, while there is constant pressure at the separator and the template. The end of natural plateau is located where p_{wh} and $p_{template}$ crosses, in 2016.

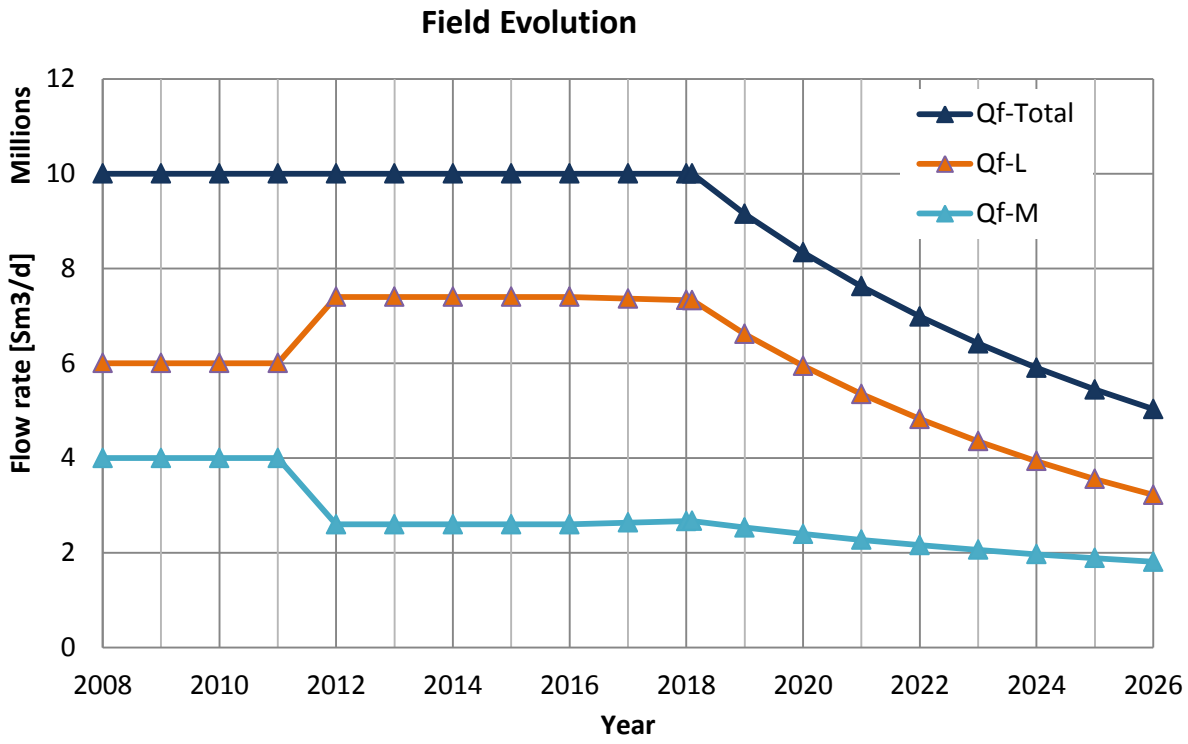

Figure 3.1.6: Field evolution plot. The plot show the total flow rate, Qf, which stays 10×10^6 Sm^3/d from 2008-2018 by changing the partial flows from the M- and L-template.

3.1.2. Case 2: Flow Control from the Platform Valves

For the second case, two chokes directly upstream of the separator were used to manipulate the flow instead of the many chokes at the wellheads, see Fig 3.1.1. Case 2 made it possible to keep the flow at 6.00×10^6 Sm^3/d from template L and 4×10^6 Sm^3/d from template-M through 2012. The ratio was changed in January 2013 to delay the installation of a compressor for some more years. The pressure development is shown in Figs 3.1.7 and 3.1.8, where the increased pressure variation compared to case 1 comes from changing the partial flow rate from the M- and L-templates more often. The partial flow rates are shown in Fig 3.1.9.

In 2015 the natural plateau ended and a compressor system had to be installed upstream of the towhead. The compression kept the total rate at 10×10^6 Sm^3/d for 2.5 extra years. From mid-2017 the total flow out of the reservoir decreased steadily until it reached a total flow of 5×10^6 Sm^3/d at the last half of 2024. The decrease

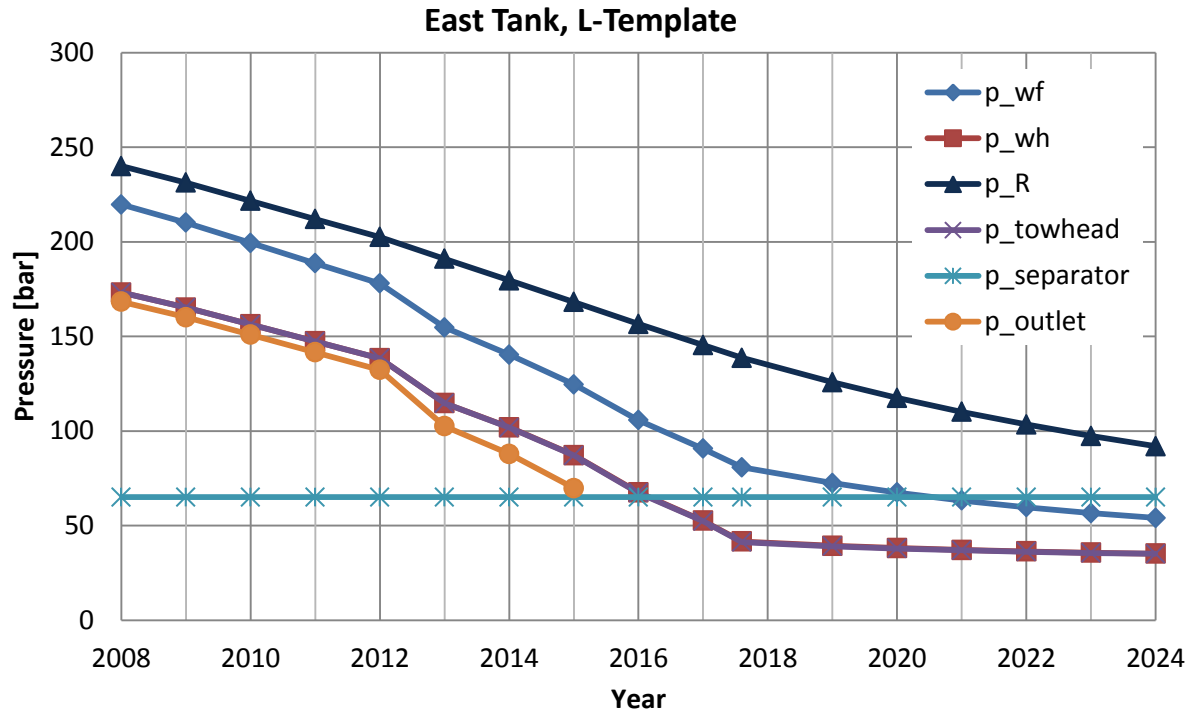

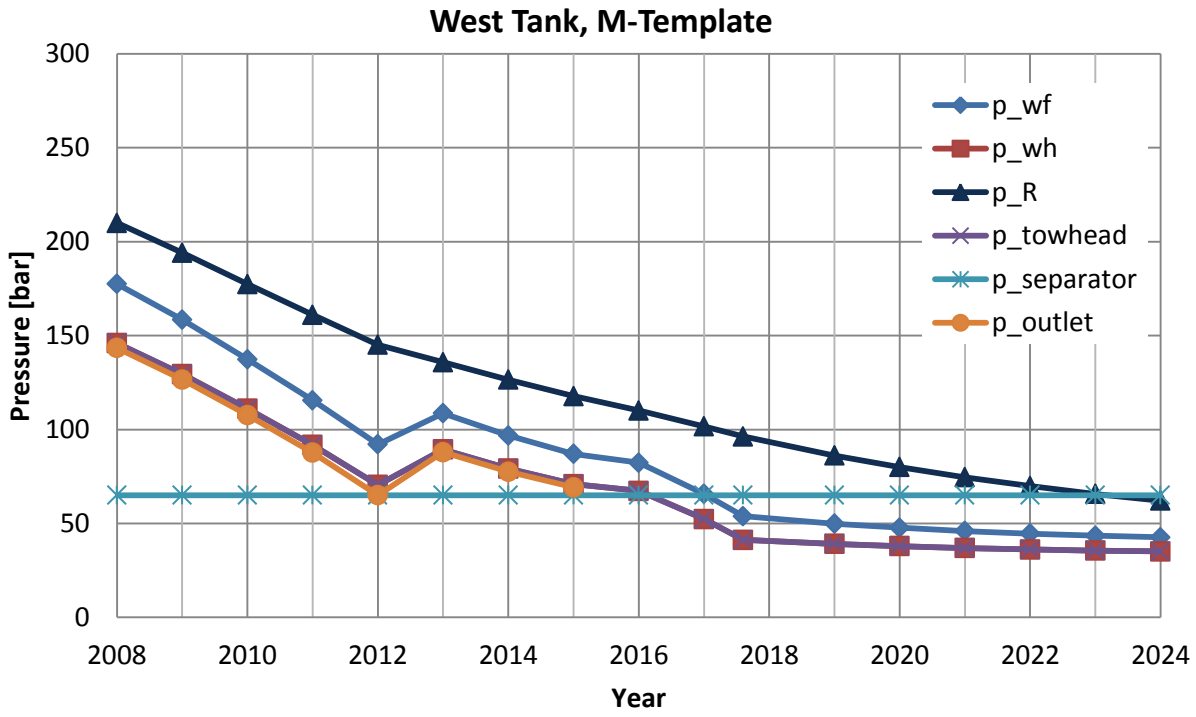

Figure 3.1.7 and 3.1.8: Pressure plots for the east and west tank. The figures show pressure drop through the years of production for the reservoir, the well bottom and the wellhead, while there is constant pressure at the separator and the template. The end of natural plateau is located where p_{wh} and $p_{template}$ crosses, in 2016.

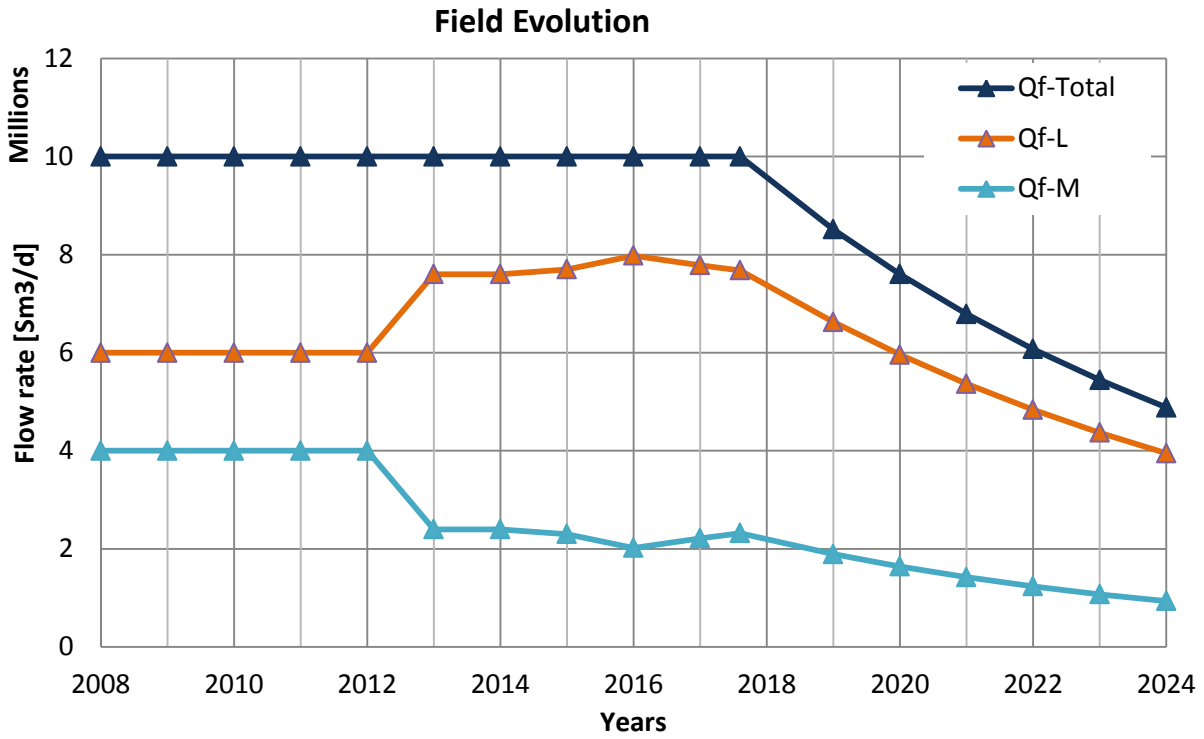

Figure 3.1.9: Field evolution plot. The plot show the total flow rate, Qf, which stays 10×10^6 Sm^3/d from 2008-2017 by changing the partial flows from the M- and L-template.

3.1.4. Financial Summary

The financial calculations showed here gives NPV and total revenue for case 1 and case 2 assuming dry gas bases.

To simplify calculations, we assume that the exchange rate (USD/NOK), inflation rate and discount rate are time-invariant constants equal to 6, 2% and 8%, respectively. The yearly revenue for both cases is shown in Fig. 3.1.10, while the total NPV and yearly NCF is shown in Fig. 3.1.11.

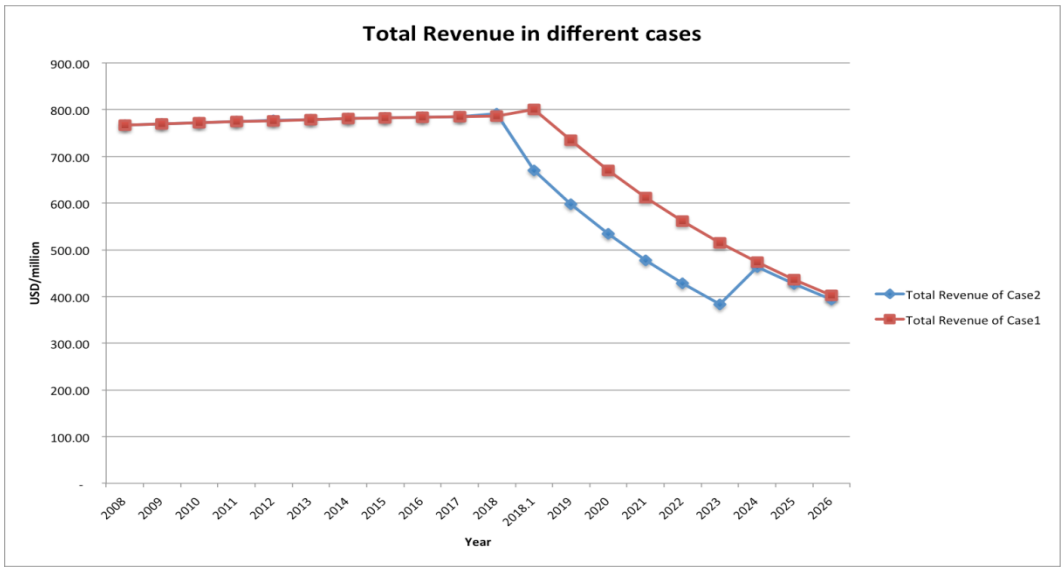

Figure 3.1.10: The yearly revenues for case 1 and case 2 from 2008 to 2026.

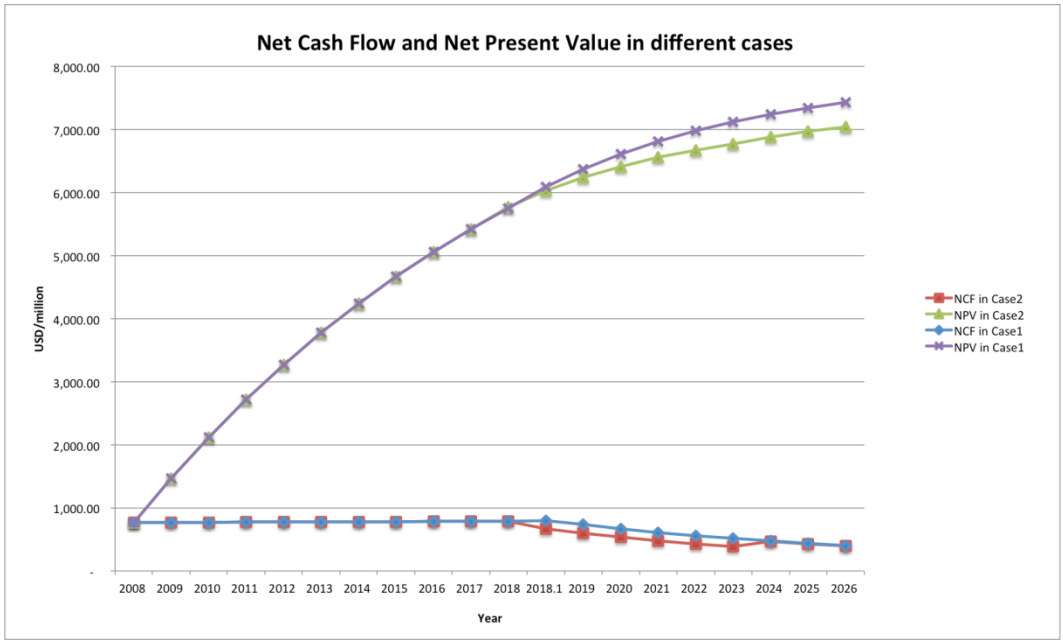

Figure 3.1.11: The NCF and NPV for both cases from 2008 to 2026.

By observing Fig. 3.1.10, it is apparent that case 1 reached plateaus from 2008 to 2018.1, whilst it's counterpart start to dampen 0.1 years in advance. This is due to the different timings for end of the plateau and compressor installation. Except for the years from 2018 to 2024 the two cases almost overlap, signifying that the end of plateau timing is the key difference between the two cases.

For Fig. 3.1.11, the net present value in case 2 is starting to flatten out at the end of production, indicating that there should be a maximum value not too long after year 2027. Compared with case 1 the growth rate decreases a little bit faster, making case 1 economically preferable. From the maximum, both net present values will decrease gradually, but since its value still is positive we still would be generating profits. Meanwhile, the net cash flows hardly differ over the 19 years of production, with the only notable difference occurring from 2018 to 2024, the same time period as the difference in revenue.

Although case 2 is not as good as case 1, both give such promising results that it raises questions whether the expenses involved in the project might have been understated. As the applied parameters are easy to change if we wanted to have more exact calculations, and further economic analysis would be carried out later, this was not prioritized.

3.2. Modified Black Oil Model

For the first part of the project a dry-gas basis was assumed, that means no consideration of condensates or liquids. To improve the model, modified black oil(MBO) properties[5] were used. The modified black oil model is more precise than a dry gas model as it takes into account the oil condensate, while still being a lot simpler than solving the problem using a component by component basis. It is accurate for modeling primary(pressure depletion) and secondary(water injection) recovery[6] but struggles with gas injection.[7] Figure 3.2.1 and 3.2.2 illustrates the difference between the traditional and MBO formulations. And figure 3.2.3 is the comparison of traditional and MBO formulations It can clearly observed that using MBO formulations can play significant role for having more accurate results for gas-condensate reservoirs." Neglecting the surface oil that is produced from flowing reservoir gas may cause gross underestimation of the ultimate stock-tank-oil recovery".[8].

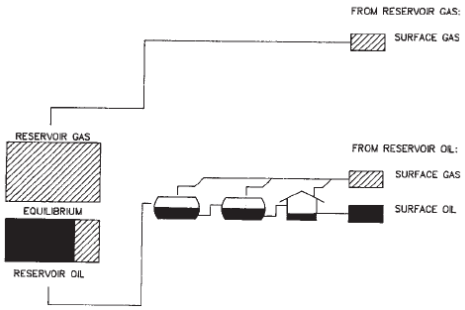

Figure 3.2.1 Traditional Black Oil Formulation between reservoir and surface phases

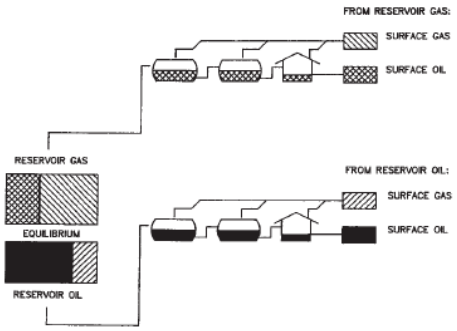

Figure 3.2.2 Modified Traditional Black Oil Formulation between reservoir and surface phases

The BO-model works by creating 2 pseudo components, one combined oil phase and one combined gas phase, and combine these with a liquid water component. The parameters used in the model was found for varying reservoir pressures using Hysys[3] and collected in Tables 3.2.1.1 and 3.2.2.2 .The theory behind the modified BO-model is shown in Appendix C, while stream data for the Hysys case are shown in Appendix G.

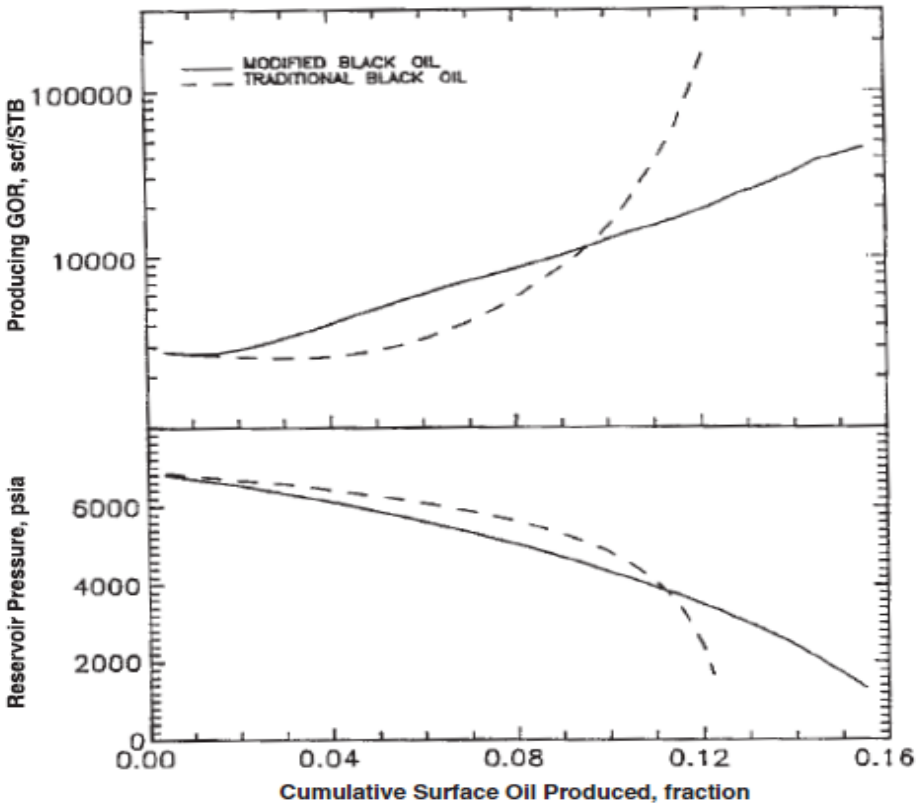

Figure 3.2.2-Average reservoir pressure and producing GOR vs Cumulative surface oil produced.

3.2.1. Hysys-Simulation; Finding the Black Oil Parameters

Hysys simulation was performed to see how the oil and gas fraction at reservoir conditions would change as the liquid was taken to standard conditions, 15.56 ^{0}C and 1 atm.[9] Two different tables had to be created as the reservoir temperature for the L-template differed significantly from that of the M-template, measuring 128 ^{0}C and 112 ^{0}C respectively. Black oil parameters for the L-template are shown in Table 3.2.1.1, while the M-template data shown in Table 3.2.1.2.

Table 3.2.1.1: Black oil parameters for the L-template **using various reservoir pressures.**

p	B_o	B_g	R_s	r_s	μ_o	μ_g	ρ_{og}	ρ_{oo}	γ_o	ρ_{go}	ρ_{gg}	γ_g
[bara]	[m^3/Sm^3]	[m^3/Sm^3]	[m^3/Sm^3]	[Sm^3/Sm^3]	[cp]	[cp]	[kg/m^3]	[kg/m^3]		[kg/m^3]	[kg/m^3]	
240	1,634	5,42E-03	170,206	9,27E-05	0,220	0,023	795,338	803,920	0,989	0,882	0,815	1,081
220	1,574	5,85E-03	149,467	7,46E-05	0,237	0,022	795,068	803,634	0,989	0,889	0,817	1,088
200	1,517	6,39E-03	130,460	5,92E-05	0,254	0,021	794,945	803,332	0,990	0,896	0,817	1,096
180	1,462	7,07E-03	112,905	4,65E-05	0,272	0,020	794,899	803,028	0,990	0,904	0,818	1,105
160	1,411	7,94E-03	96,582	3,62E-05	0,290	0,019	794,776	802,740	0,990	0,912	0,819	1,114
140	1,362	9,09E-03	81,315	2,83E-05	0,310	0,018	794,338	802,501	0,990	0,920	0,819	1,124
120	1,317	1,07E-02	66,971	2,23E-05	0,332	0,018	793,299	802,360	0,989	0,929	0,819	1,134
100	1,275	1,29E-02	53,459	1,82E-05	0,355	0,017	791,394	802,393	0,986	0,938	0,819	1,145
80	1,236	1,63E-02	40,735	1,57E-05	0,381	0,016	788,504	802,715	0,982	0,946	0,819	1,154
65	1,208	2,02E-02	31,713	1,47E-05	0,404	0,016	785,787	803,253	0,978	0,952	0,820	1,161

***Table 3.2.2.2: Black oil parameters for the M-template* using various reservoir pressures.**

p	B_o	B_g	R_s	r_s	μ_o	μ_g	ρ_{og}	ρ_{oo}	γ_o	ρ_{go}	ρ_{gg}	γ_g
[bara]	[m^3/Sm^3]	[m^3/Sm^3]	[m^3/Sm^3]	[Sm^3/Sm^3]	[cp]	[cp]	[kg/m^3]	[kg/m^3]		[kg/m^3]	[kg/m^3]	
240	1.615	5.10E-03	177.564	0.000	0.241	0.023	787.893	802.476	0.982	0.875	0.809	1.082
220	1.557	5.51E-03	156.730	0.000	0.259	0.022	787.377	802.073	0.982	0.882	0.810	1.089
200	1.501	6.01E-03	137.517	0.000	0.277	0.021	787.352	801.632	0.982	0.891	0.812	1.097
180	1.448	6.65E-03	119.652	0.000	0.296	0.020	787.942	801.166	0.983	0.900	0.813	1.106
160	1.398	7.47E-03	102.913	0.000	0.316	0.019	789.151	800.697	0.986	0.909	0.815	1.116
140	1.350	8.56E-03	87.121	0.000	0.337	0.018	790.703	800.263	0.988	0.920	0.815	1.128
120	1.306	1.00E-02	72.142	0.000	0.360	0.017	791.974	799.923	0.990	0.931	0.815	1.141
100	1.263	1.22E-02	57.886	0.000	0.385	0.017	792.165	799.770	0.990	0.942	0.816	1.155
80	1.224	1.54E-02	44.316	0.000	0.415	0.016	790.585	799.946	0.988	0.954	0.816	1.169
65	1.195	1.92E-02	34.604	0.000	0.441	0.015	788.019	800.424	0.985	0.963	0.816	1.179

The Hysys model used for both templates was identical except for the reservoir temperature. The pressure was varied to get good basis parameters for all of the reservoir's lifetime. A screen capture of the simulation is shown in Fig. 3.2.1.1. The resulting BO tables have values that agree well with literature data. The B_o, and R_s terms increase linearly, while the Bg term decreases exponentially, with increasing pressure. All of this is fully consistent with Dake's predictions, in his book "Fundamentals of Reservoir Engineering",[10] which makes it likely that our Hysys model has given decent results.

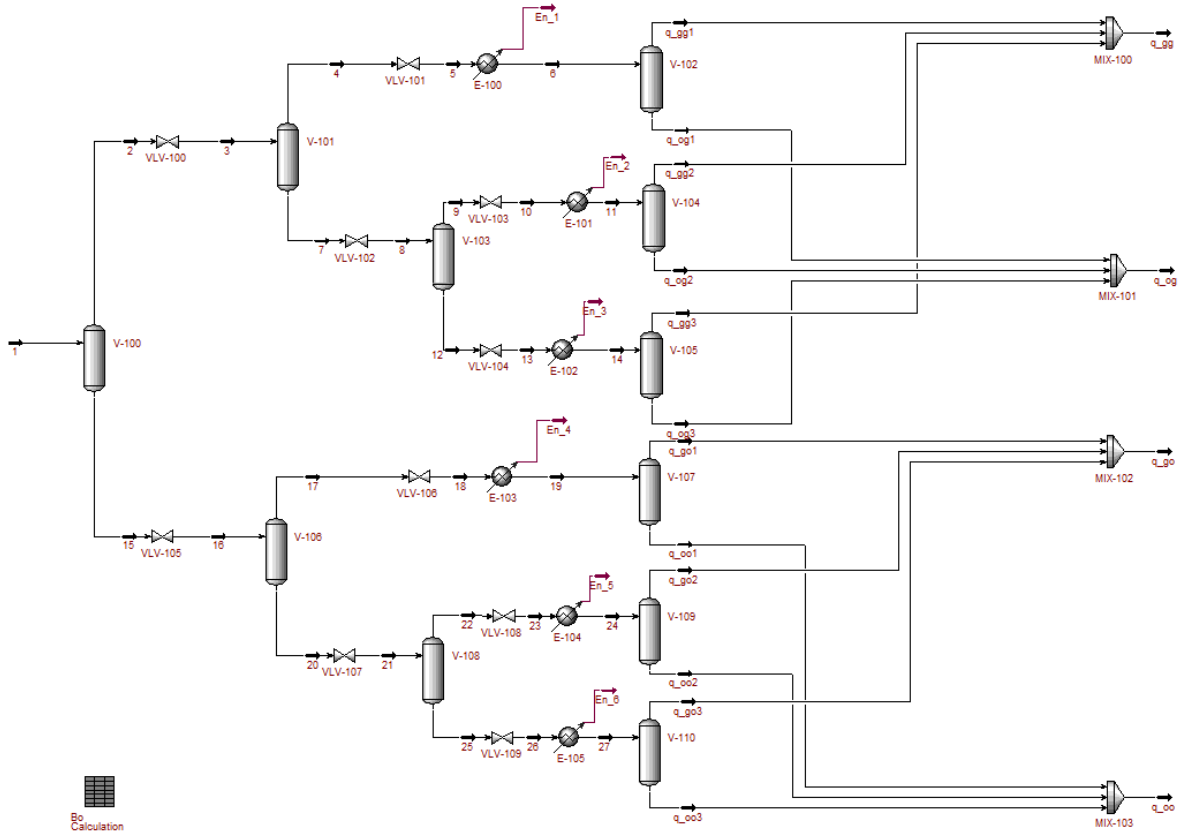

Figure 3.2.1.1: The Hysys-simulation used to find the BO-properties at a given reservoir pressure and temperature.

3.2.2. Modified Black Oil (MBO) Calculations – IPT MATBAL

In this project condensate from reservoir gas is taken into consideration and the calculation method is introduced. Several calculations done for calculating the amount of oil coming from gas for Gullfaks reservoir by using the computer programing called IPT-MATBAL which is based on Microsoft Excel. The formulations and all the steps can be found Appendix C which are used to make computer programming called IPT-MATBAL. IPT-MATBAL is made on Microsoft Excel so in order to fix the material balance error Solver Add-in is used. The calculations are done for both of template L and template M.

Figures 3.2.2.1 and 3.2.2.2 illustrates the gas and condensate production from the after the year 5 we can observe that condensate and gas production decreasing nearly the parallel for both cases. But the amount of condensate compared to gas is quite small when it is compared to gas.

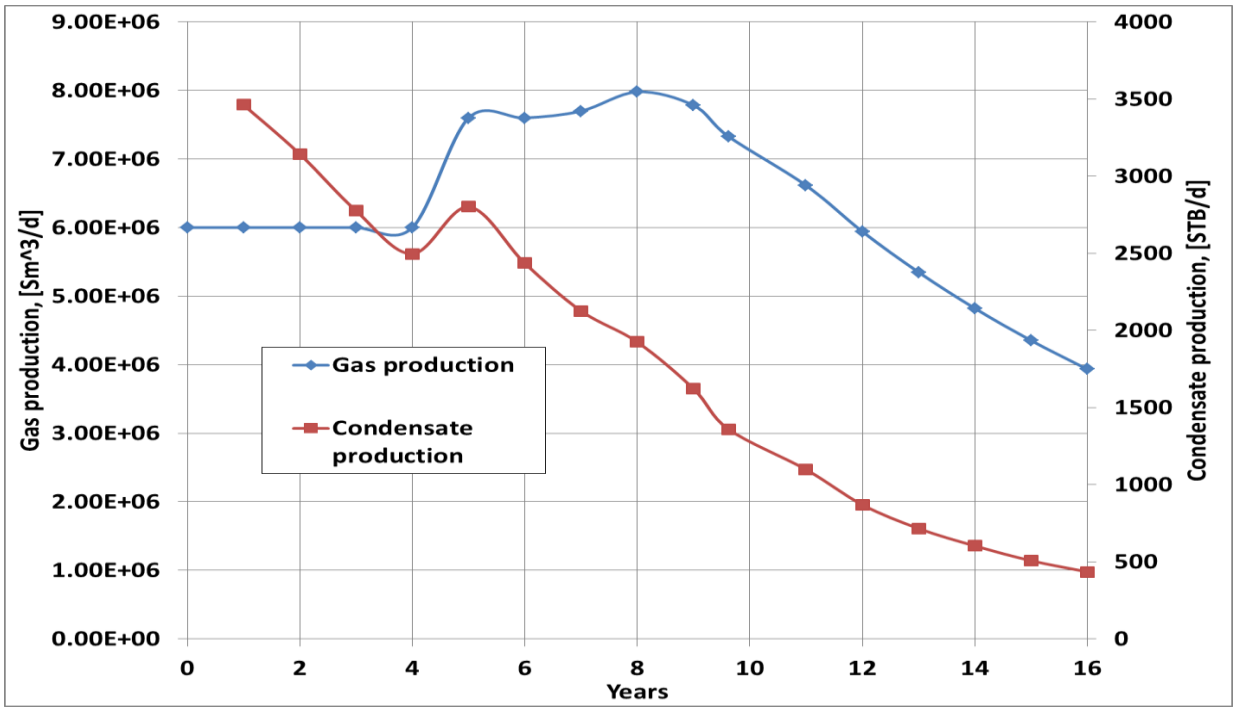

Figure 3.2.2.1 Gas and Condensate production for L template

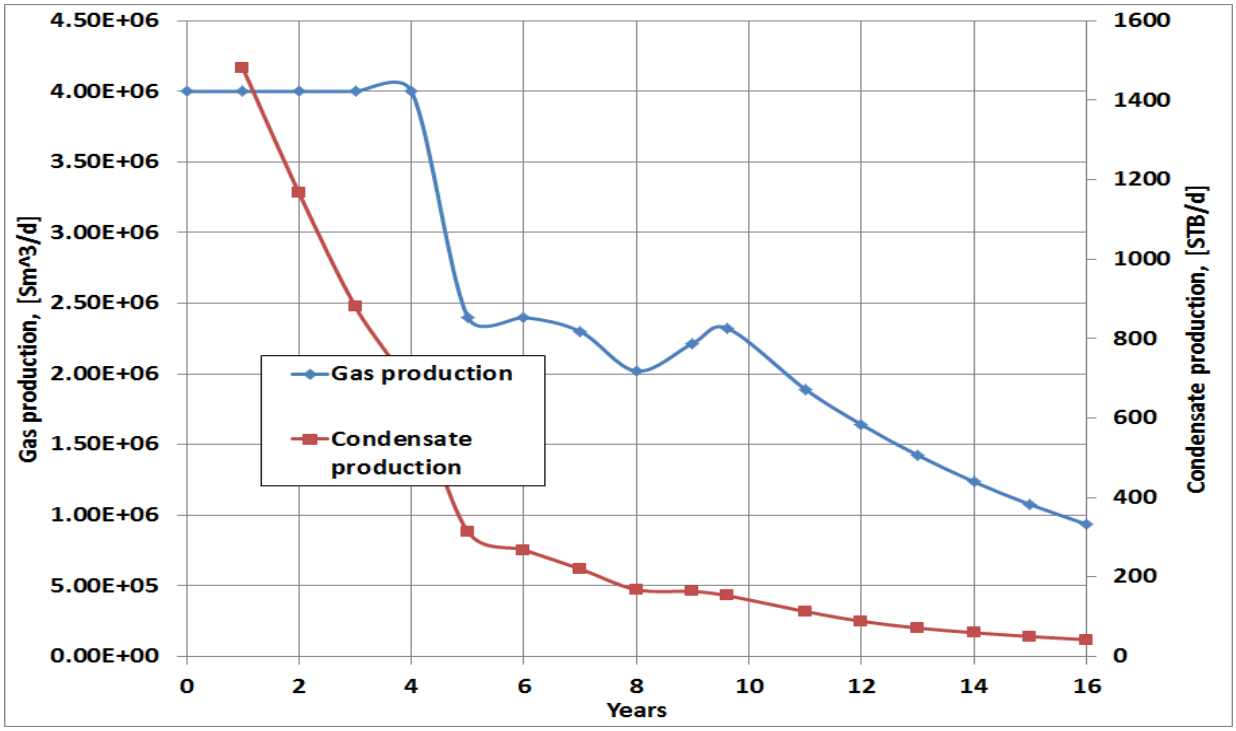

Figure 3.2.2.2: Gas and Condensate production for M template

Figures 3.2.2.3 and 3.2.2.4 show the Oil Gas Ratio of Template L and Template M. Template L and M have different reservoir pressure and it is clear that when the higher reservoir pressures the higher amount of oil dissolved in gas. Therefore, amount of gas coming from L template is bigger than M template.

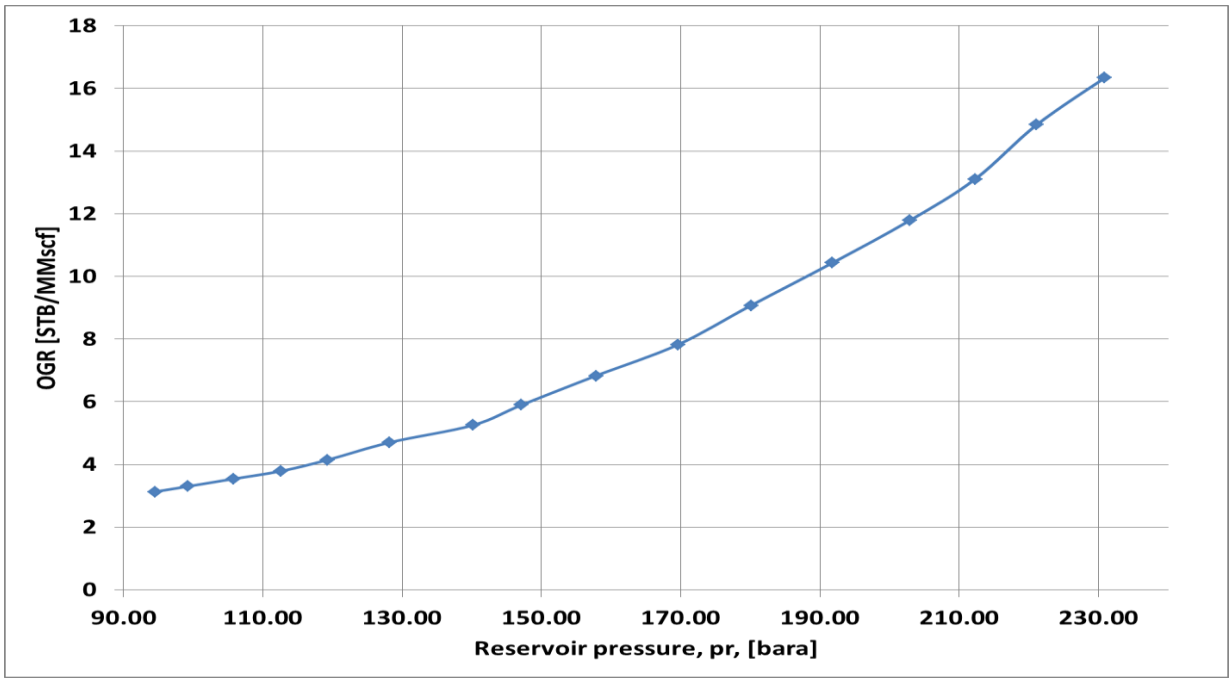

Figure 3.2.2.3: Oil Gas Ratio versus Reservoir Pressure for L template

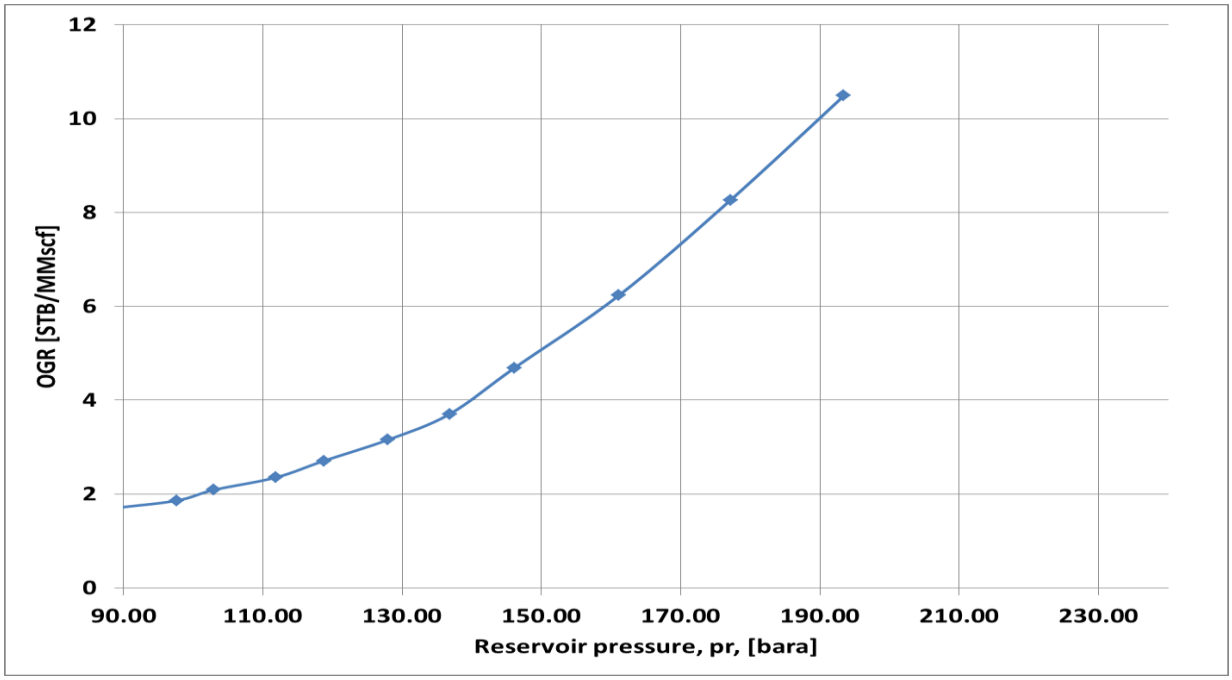

Figure 3.2.2.4: Oil Gas Ratio versus Reservoir Pressure for M template

To compare Dry gas assumption with Modified Black Oil model we plotted our calculation for dry gas and condensate in same figure. The blue and red lines are reservoir pressures when it is assumed dry gas and when the condensate considered. And the green and purple lines show the production for both cases. Figures 3.2.2.5 and 3.2.2.6 is informative enough to see the differences between dry gas and gas with condensate based on our calculation. As we can see from the figures there are not considerable differences between two cases for both templates. There is only bigger distinction in the beginning of the production year which is also not considerable amount. It can be concluded that we can assume our calculation as a dry gas.

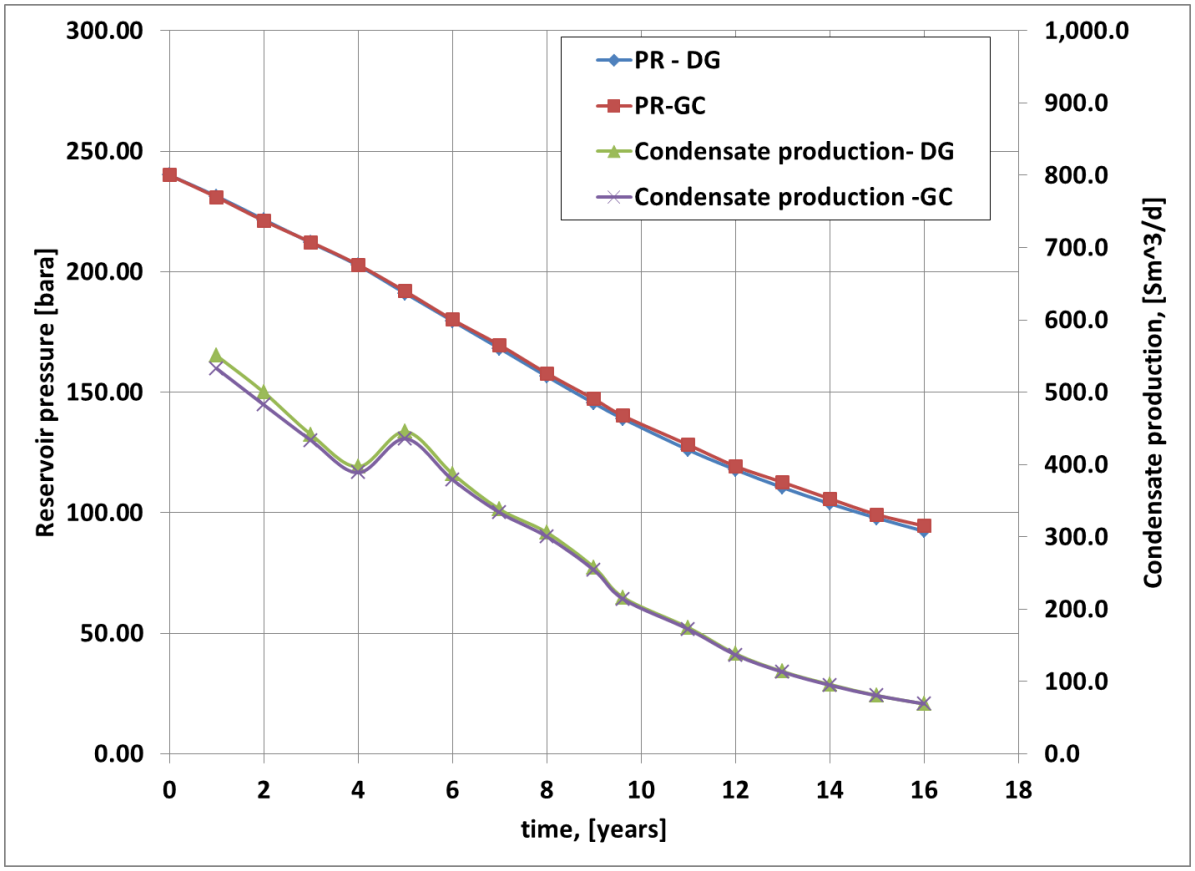

Figure 3.2.2.5: Pressure and Condensate production for Dry gas model and Modified Black Oil Model for Template L

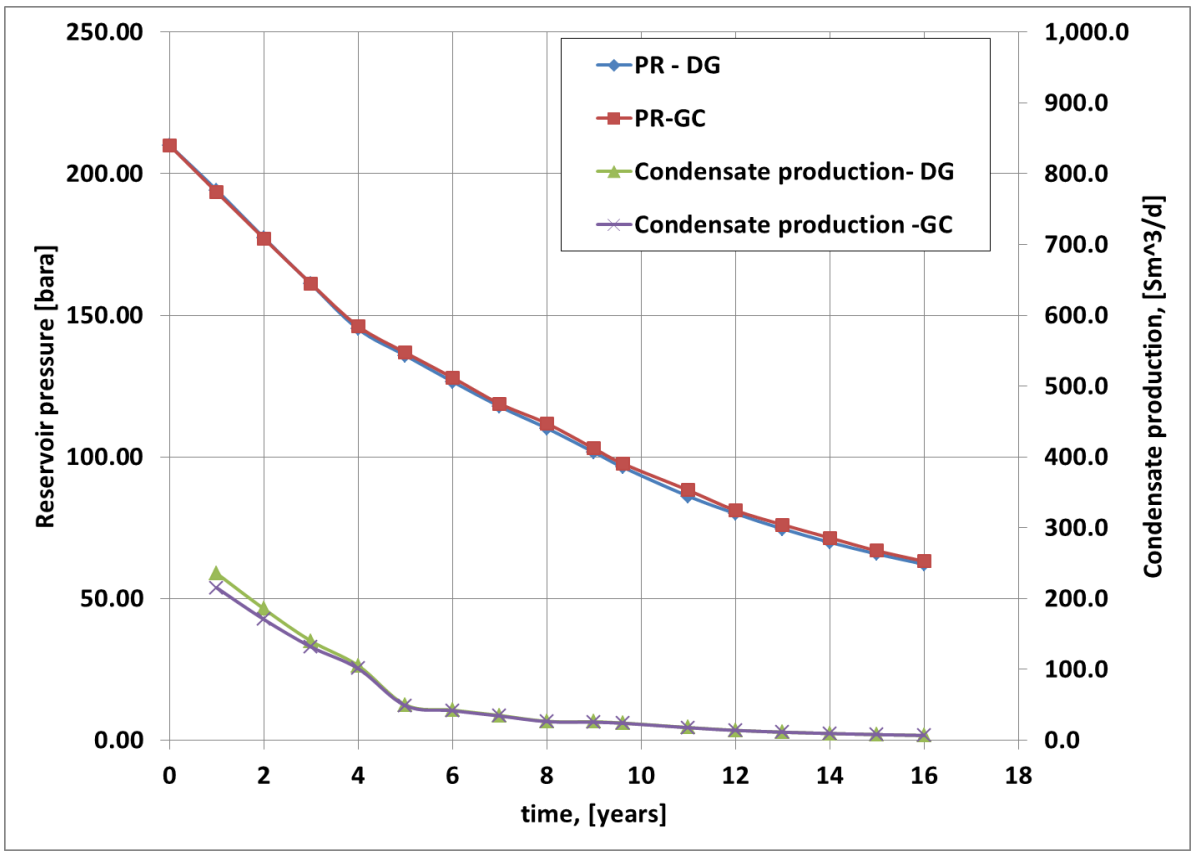

Figure 3.2.2.6: Pressure and Condensate production for Dry gas model and Modified Black Oil Model for Template M

3.3. Reservoir Optimization Cases

In this part, 4 different cases will be described, calculated and compared to figure out the most attractive cases for increasing the production, prolonging the flow plateau and also extending the life time of the field. The cases are:

1. The reference case : the case that use the assumption for doing nothing, neither installing the compressor nor applying low pressure modification (LPM),
2. The subsea compressor case: the compressor is assumed to be installed in subsea with constant separator pressure which is 65 bars,
3. The low pressure modification case (LPM): the subsea compressor case with modification of separator pressure from 65 bars to 28 bars after the driven plateau time exceeded,
4. The topside compressor modification case: the compressor is assumed to be installed in platform.

3.3.1 Reference case

The reference case is based on simple assumption where there is no compressor installation at all and the gas flowing just depend on the natural gas flow from the reservoir. For controlling the pressure difference between the reservoir and separator which is 65 bars, the choke was settled in platform, exactly before the separator.

The calculation made in Excel sheet (see detail result in appendix F table F1) with some input for the calculations that also applied for every other cases (see table 3.3.1). Based on the excel calculation result, the pressure plot (bars) and flow rate (Sm^3/day) plot in time (years) was created to determine how long the flow plateau will be and when is the end of the field (figure .3.3.1& 3.3.2). The total flow (Q_f) constraint was introduced to the calculation which are 10x 10^6 Sm^3/day as the maximum flow and 5 x 10^6 Sm^3/day as minimum economical flow value. Assumption made for this calculation is based on dry gas model where there is only gas fluid phase in reservoir without considering the content of oil in gas. The variables calculated from the excel are Q_f Total and Q from each template (L and M), Recover factor (GP/G), PR (Reservoir pressure), P_{wh} (well head pressure), P_{wf} (well fluid pressure), P_{outlet} from each template.

As the impact of no compressor installed, the natural flow plateau is lasting from 2008-2014.The gas flow constantly 6 x10^6 Sm^3/day from template L and 4 x10^6 Sm^3/day from template M during 2008-2012, continue with 7.5 x10^6 Sm^3/day from template L and 2.5 x10^6 Sm^3/day from template M during 2012-2014, and on the later stage, the flow will gradually decrease until it reach minimum Q_f Total on 2020.

The recovery factor gained from this cases vary from 0.44 (template L) to 0.56 (template M).

Table 3.3.1 The input for excel calculation.

Gullfkas South L-M satellite system Pre-comression Phase (Start Jan 2009)	East Tank L-Template Fault Block 13 Brent Formation	West Tank M-Template Fault Block 14 Brent Formation	Unit
G=GIIP-Gas cap (31 December 2008)		17,5E+9	Sm3
Condensate from Gas Cap (31 December 2008)		4,4E+6	Sm3
oil legs: STOIIP (31 December 2008)		7,5E+6	Sm3
Gas in Solution (from oil leg)		1,9E+9	Sm3
Rs Solution Gas oil Ratio (oil leg) (31 December 2008)		248	Sm3/Sm3
rs Condensate gas ratio (gas cap) (31 December 2008)		251	Sm3/MSm3
STOIIP + Condensate (31 December 2008)	34,5E+6		Sm3
GIIP + diss.gas (31 December 2008)	54,2E+9		Sm3
Daily Plateau production rate (per template)-Pre compression mode	6,0E+6	4,0E+6	Sm3/d
Wells per template (Pre compression)	4	3	
Production days per year	328	330	day
T_R	128	112	^oC
Pi, initial Res pressure (01 Jan 2009)	240	210	bara
Pi, initial Res pressure (1999)	459	446	
C, inflow Back pressure coefficient	1000	700	Sm3/bar^2n
n, backpressure, exponent	0,8	0,8	
Tubing MD	3515	2800	
Tubing TVD	3100	2500	
Ct, Tubing coefficient 7" (ID=6.094")	38152,4	41163	Sm3/bar
Elevation coeff Tubing, S	0,43	0,34	
C_{FL} 12".Template L-to-Towhead 66 m (ID=) Pre-compression spool	1403054		Sm3/bar
C_{FL} 8"Template-to-Towhead 62 m (Id=)	466786		Sm3/bar
C_{FL} 12".Template M-to-Towhead 64 m (ID=) compression spool		1397663	Sm3/bar
$C_{PL\ Pipeline}$ 14" Towhead-to-GFC 14000m (ID=0.32m)	148220	148220	Sm3/bar
$C_{PL\ Pipeline}$ 8" Towhead-to-GFC 14000m (N-Line) (ID=0.197m)	32967	32967	Sm3/bar
Separator pressure GFC (Inlet Sep)	60	60	bara
Tope GFC riser pressure (High pressure mode)	65	65	
Tope GFC riser pressure (Low pressure mode)	25	25	
Gas molecular weight (Methane)	19	19	kg/kmole
Gas specific gravity	0,66	0,66	Gas specific gravity

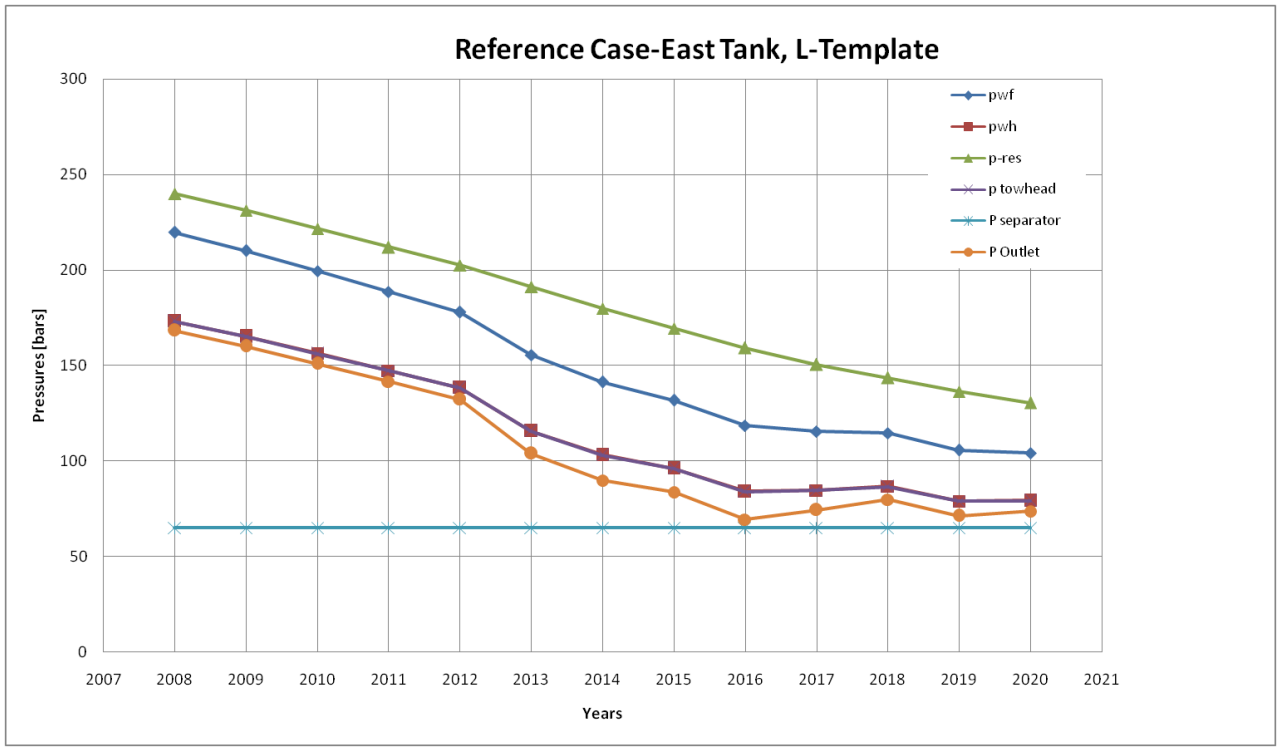

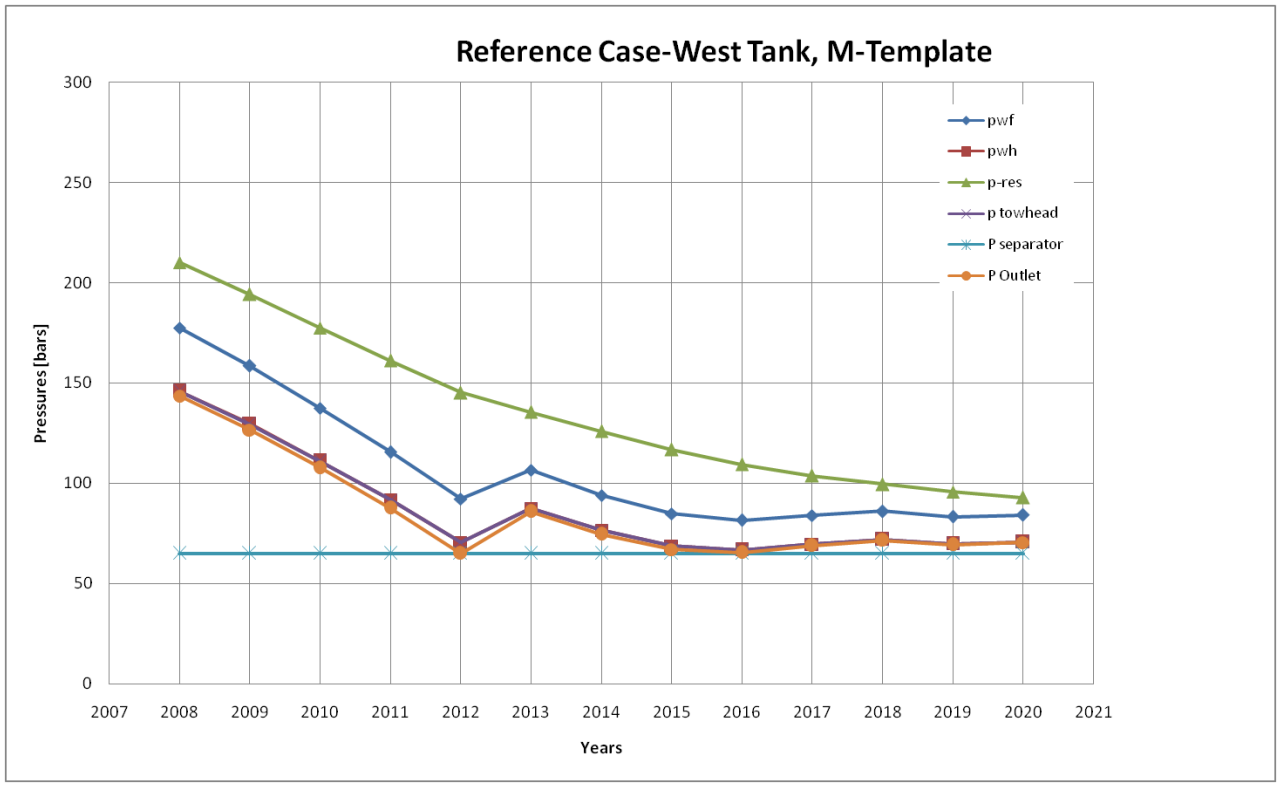

Figure 3.3.1 a (up) -b (bottom).The reference case's pressure plot (bars) in times (years) for both East Tank-L Template and West Tank-M Template. The figure shows that the pressure gradually decrease with times. As the times move on, the pressure difference between the p-outlet and p-separator (Dp choke) become smaller so that Q from each templates need to be controlled for keeping the Dp choke value positive (see also figure 3.3.1.2). Finally, on 2020, the flow reach minimum Qf Total (see also figure 3.3.1.2).

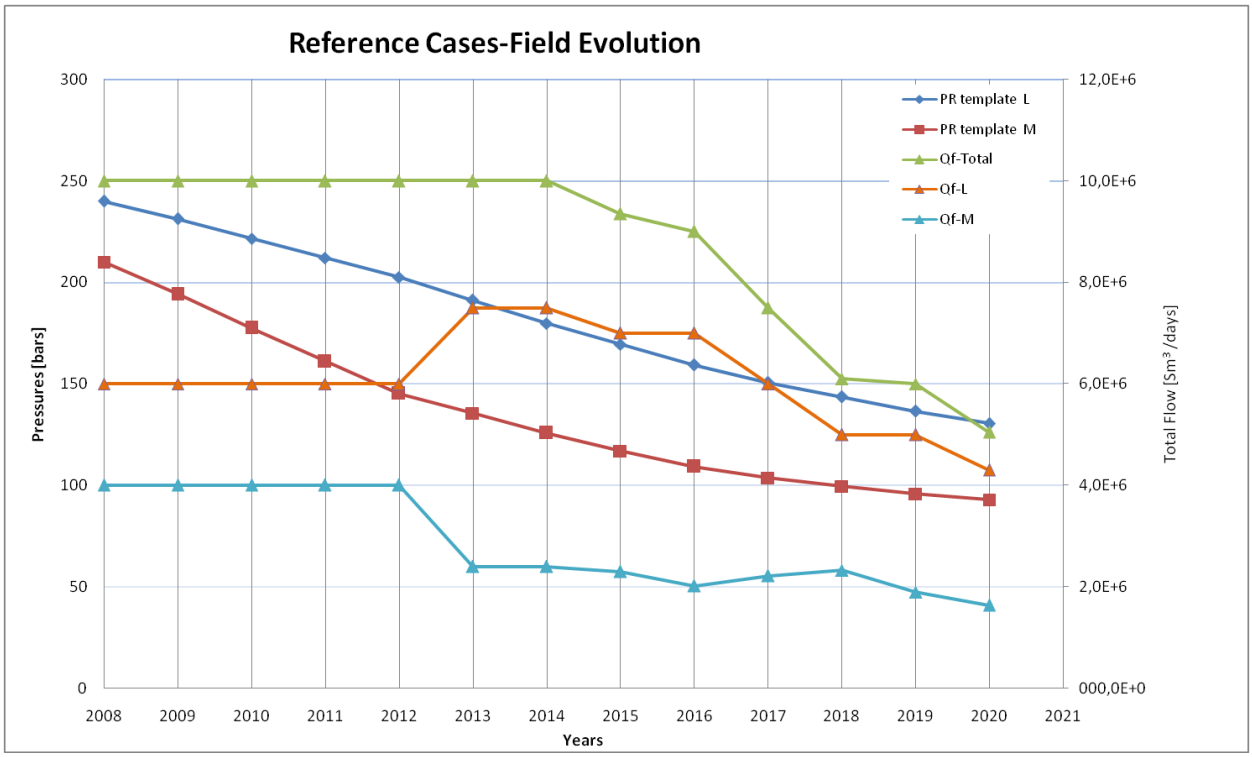

Figure3.3.2The reference case field evolution graphs. The figure demonstrates how the total gas flow (Q-Total) and Qf-L and Qf-M decrease with time as the results of the pressure drop in the reservoir.

3.3.2 Subsea Compressor Installation Case

In this case, the subsea compressor is added to the system to prolong the flow plateau and optimize the flow rate. The subsea compressor will be placed between towhead and wellhead (see figure 3.1.1). The compressor installation actually will help to maintain the pressure difference between the well and the separator in order to keep the same Q_f Total plateau.

The input for excel calculation is exactly the same with the reference case (see table 3.3.1), but the way to calculate the flow is different. As the compressor will play an important role in the system, so the additional columns in excel calculation were added to introduce the new calculation for compressor part such as P discharge, P outlet, and Compression ratio (rp) (see figure 3.3.5).

The same assumption using the dry gas concept was applied to the calculation. In the 2008-2015, the gas will flow with constant (Q_f -Total) plateau 10 $x10^6 Sm^3$/days. The flow is controlled by the choke (same as reference case). In the end of 2015, the pressure difference between P_{wh} and $P_{separator}$ reached its minimum value and no longer can maintain the flow plateau (10 $x10^6 Sm^3$/days), so the compressor need to be installed for increasing this pressure difference. The compressor can keep the maximum flow plateau in 2.6 years (2016-2017.6). On the later stage, the flow is gradually decreased until it reaches the minimum Q_f - Total on 2024 (see figure 3.3.3, 3.3.4 and 3.3.5).

The recovery factor resulted from this cases vary from 0.61 (L template) to 0.71 (M template). For the detail result of the calculation see table F4 in Appendix F.

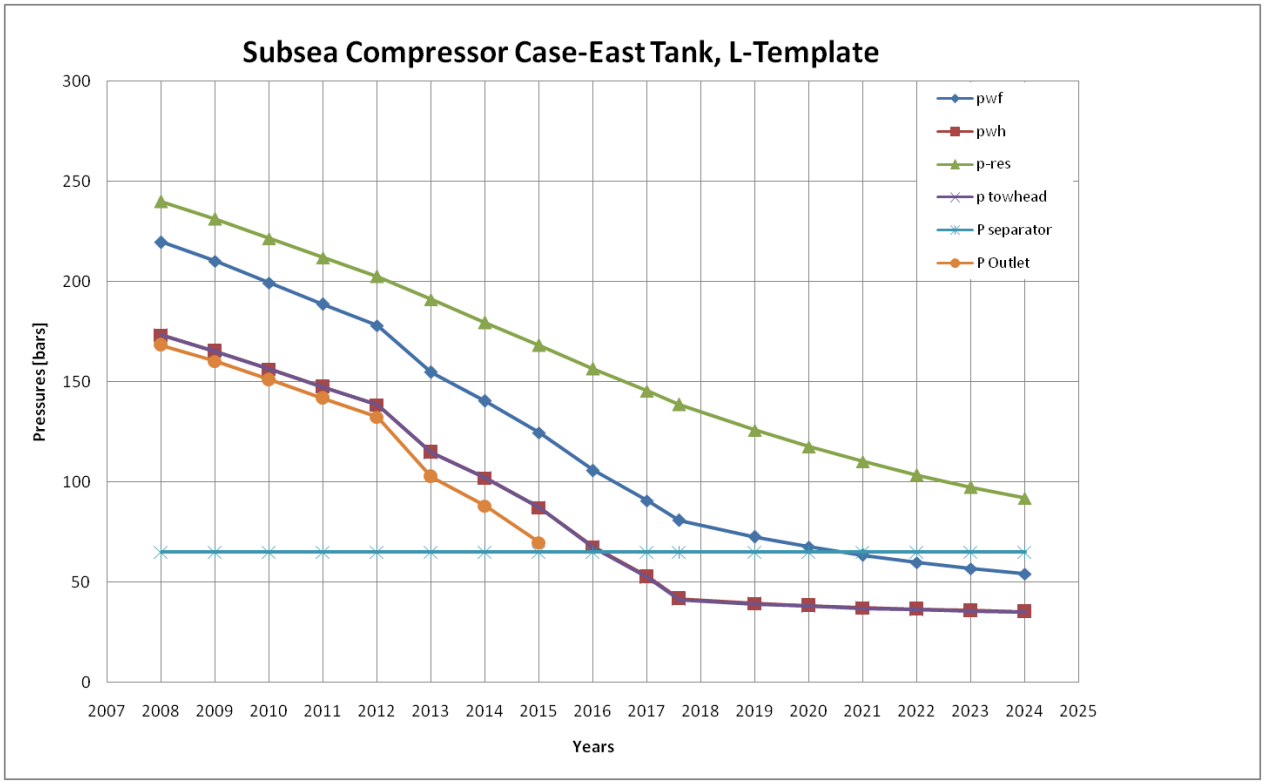

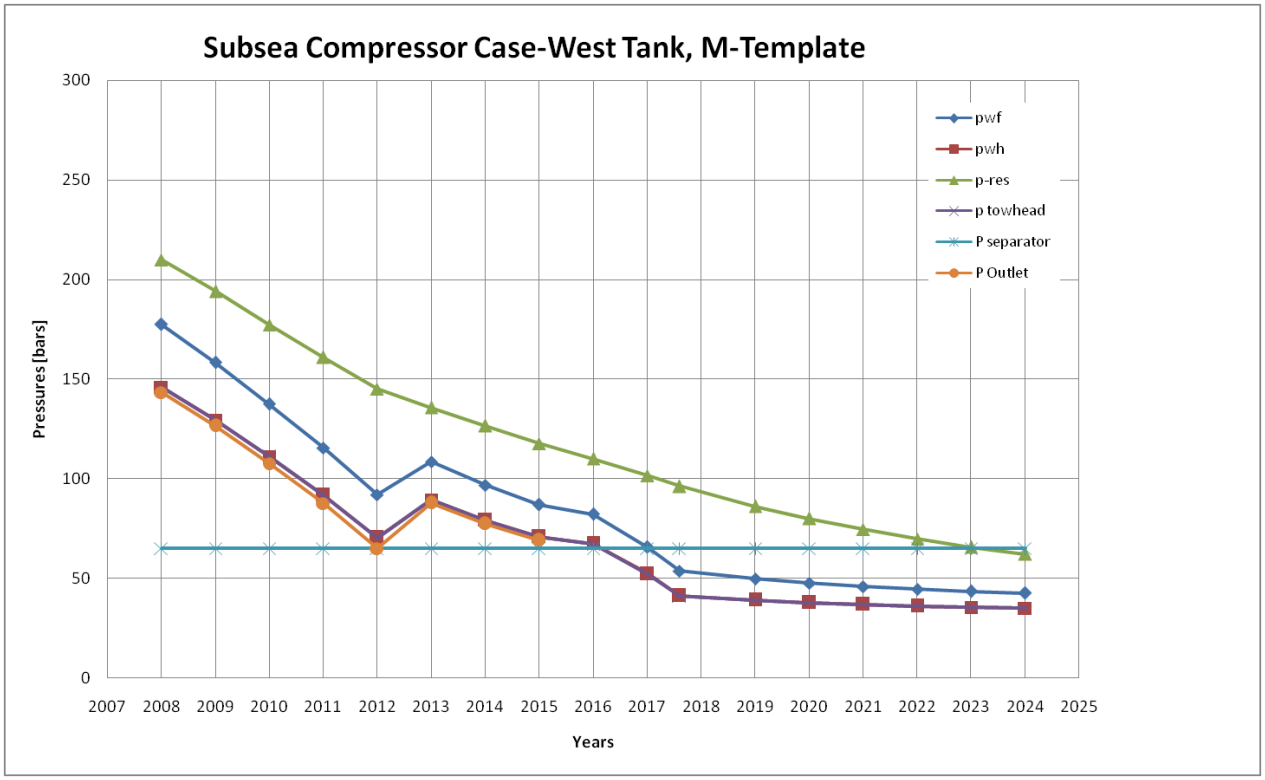

Figure 3.3.3 a (top)-b (bottom). The subsea compressor case's pressure plot (bars) through times (years) for both East Tank-L Template and West Tank-M Template. The figure shows that the pressure is gradually decrease with times. As in the reference case, the choke will be used to control the pressure difference between Poutlet and Pseparator from 2008-2015. From 2016-2017,6, the compressor used to maintain the maximum flow plateau and finally, the flow hit the Q_f minimum on 2024 (see also figure 5 and 6).

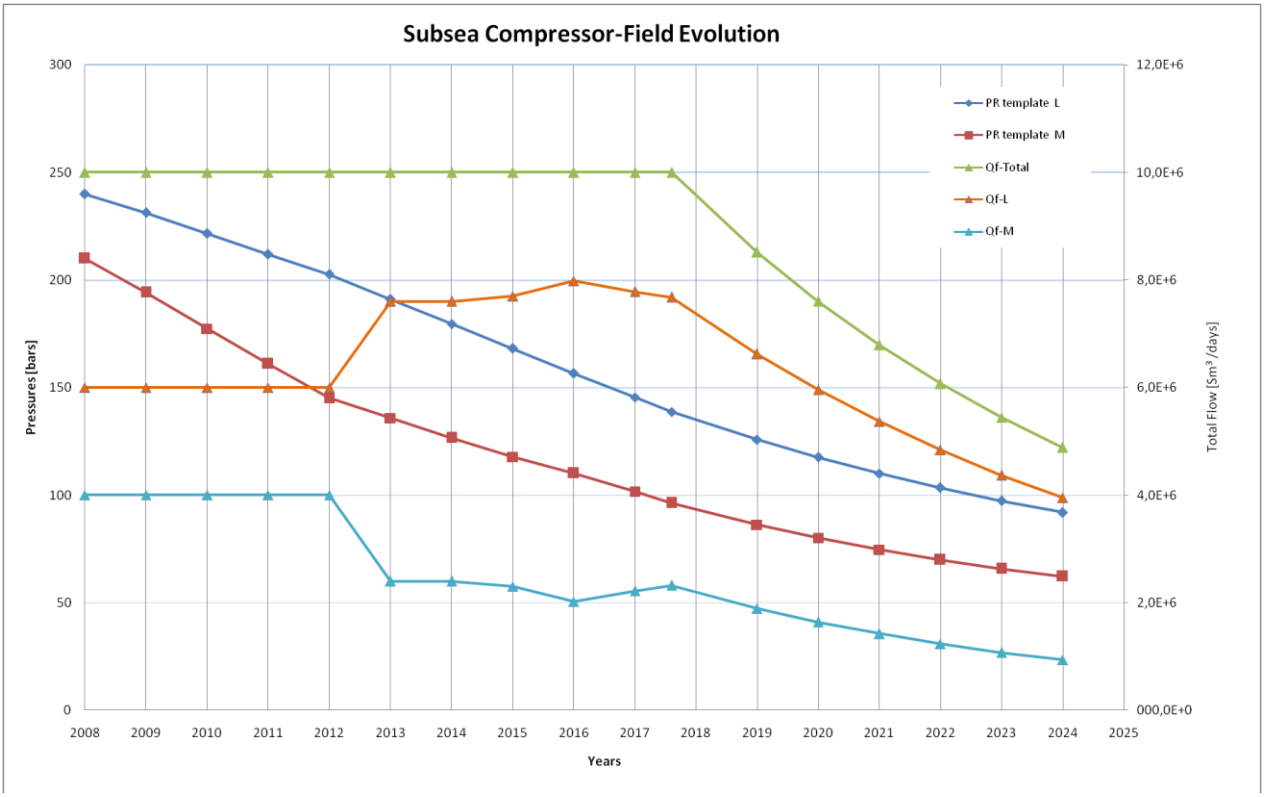

Figure 3.3.4 The Subsea Compressor field evolution. The effect of compressor installation is shown in the graphs by extended flow plateau from 2016-2017,6 (this is called as driven plateau).

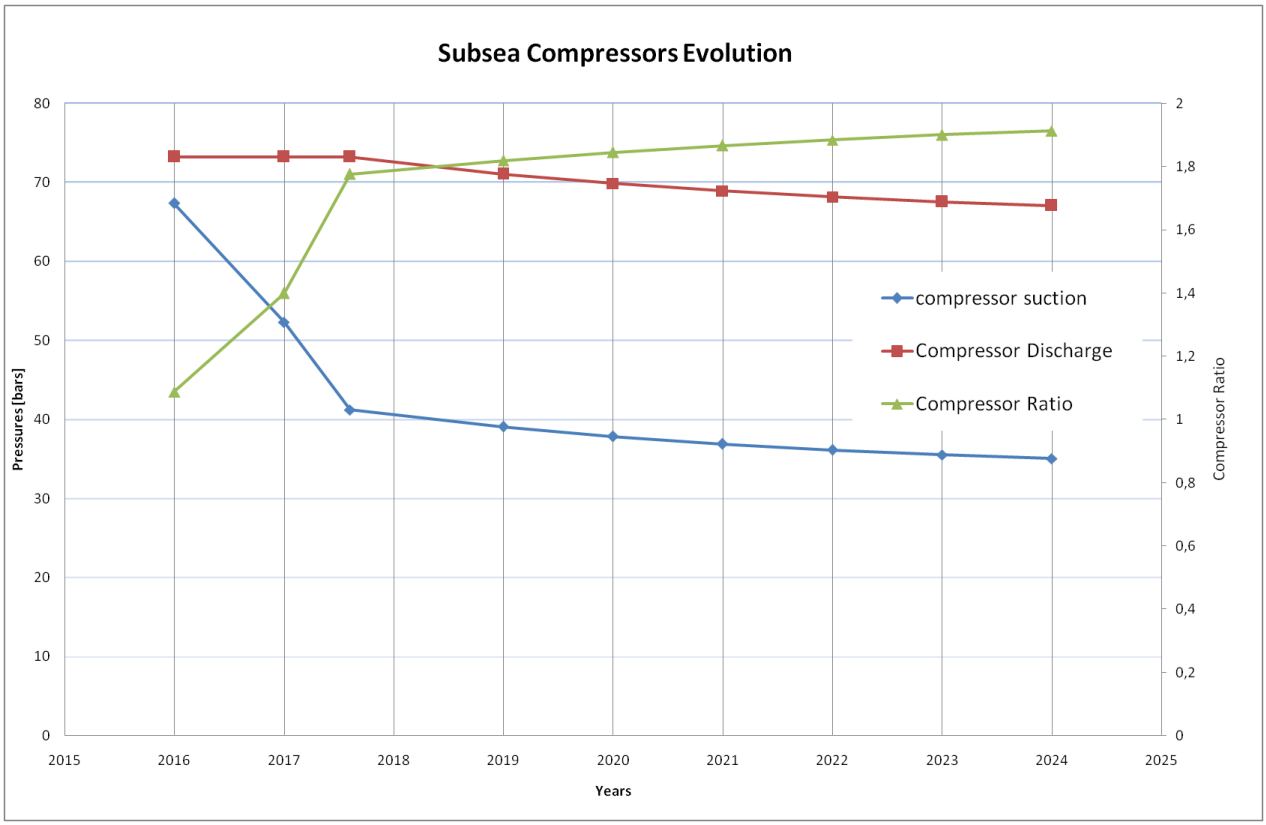

Figure3.3.5. The compressor evolution graphs shows the plot of Compressor ratio, Compressor discharge and suction pressure with time. The compressor ratio become maximum on 2017,6 (end of driven plateau) when the difference between Psuction and Pdischarge close to 32 bars.

3.3.3 Low Pressure Modification (LPM)

In this case, the impact of low pressure separator modification (LPM) to the total field rate (Q_f), life time, and economic calculations (NPV-will be discussed in other chapter of the report) of the field needs to be analyzed. Actually the LPM cases is subsea compressor, but in this case, the separator pressure on the platform is set down from 65 bars to 28 bars after driven plateau year exceeded in order to optimize the flow rate (see figure 3.3.6 and 3.3.7).

The new calculations for Q_f based on this LPM need to be conducted (see detail on Appendix F, table F.3). One critical fact with lowering the pressure of separator is that the difference between $P_{suction}$ and $P_{discharge}$ of the compressor become smaller. Thus, the compression efficiency can be increased and allows more flow (see figure 3.3.8).

Based on results of the calculation, the most optimum year to do LP modification is on 2019. The Q_f-Total on 2019 by LPM cases is 9.2 x 10^6 Sm^3/days and it gradually decrease per years and reach its minimum point (5x10^6 Sm^3/day) on 2025. Compared to the subsea case that 'only' yield 8.5x10^6 Sm^3/day on the same year and reach the minimum Q_f on 2024 respectively, it is obvious that The LPM give more benefit than subsea compressor cases (see table 3.3.2).

In the end, the outcome of applying LPM is that the recovery factor obtained from LPM cases is slightly bigger than that in subsea and topside compressor cases. The recovery factors resulted varies from 0.65 in template L and 0.76 in template M.

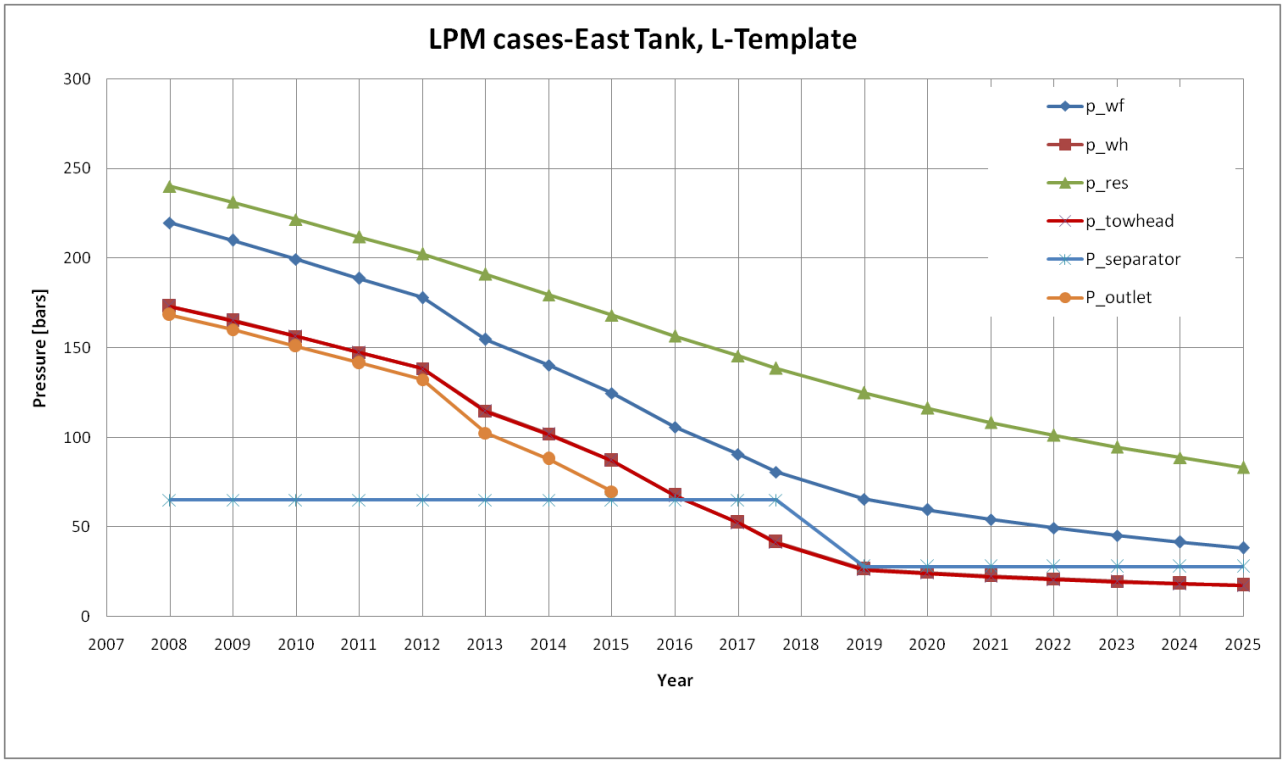

Figure 3.3.6 a (remarks on next figure)

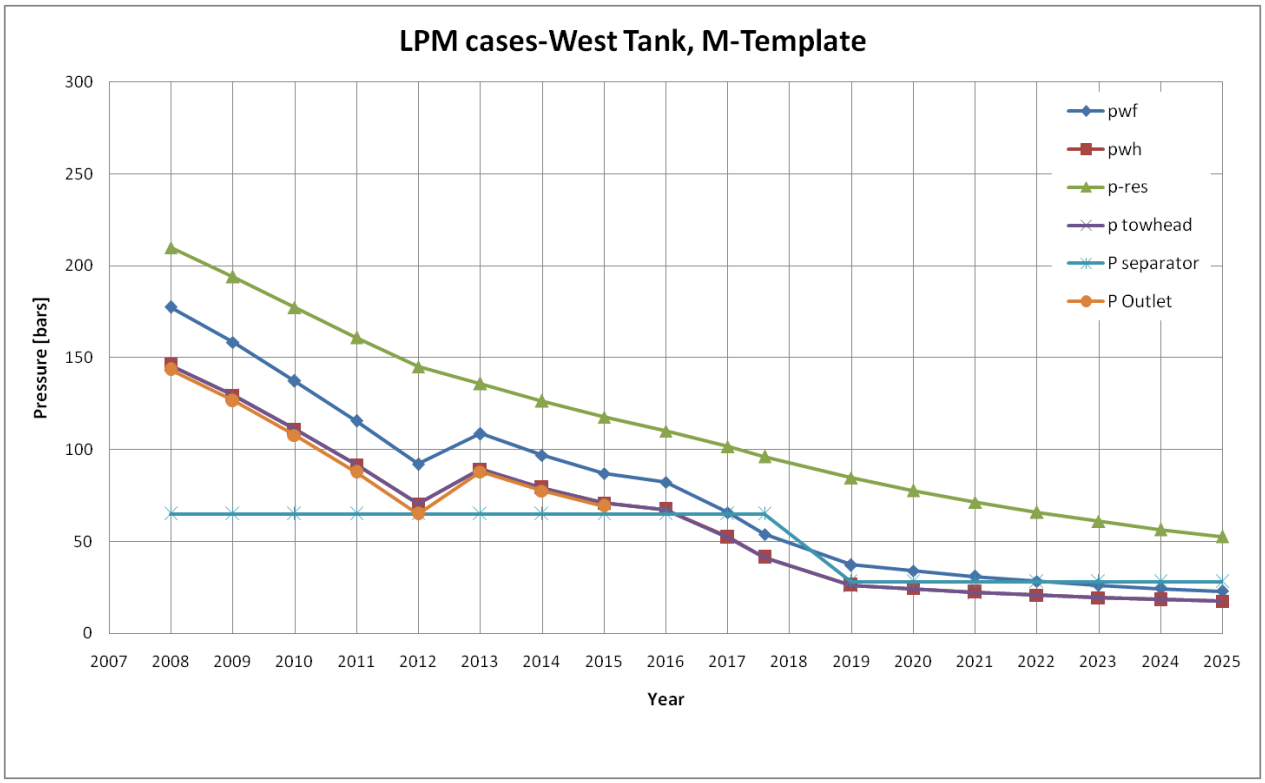

Figure 3.3.6a (top)-b (bottom). The LPM cases- The L and M template pressure plot. The figure show the pressure (bars) is decreasing with years. On LPM, the separator pressure (Pseparator on legend) is set down to 28 bars on 2019 (end of driven plateau). The effect of this modification can be seen on figure 3.3.7 and 3.3.8

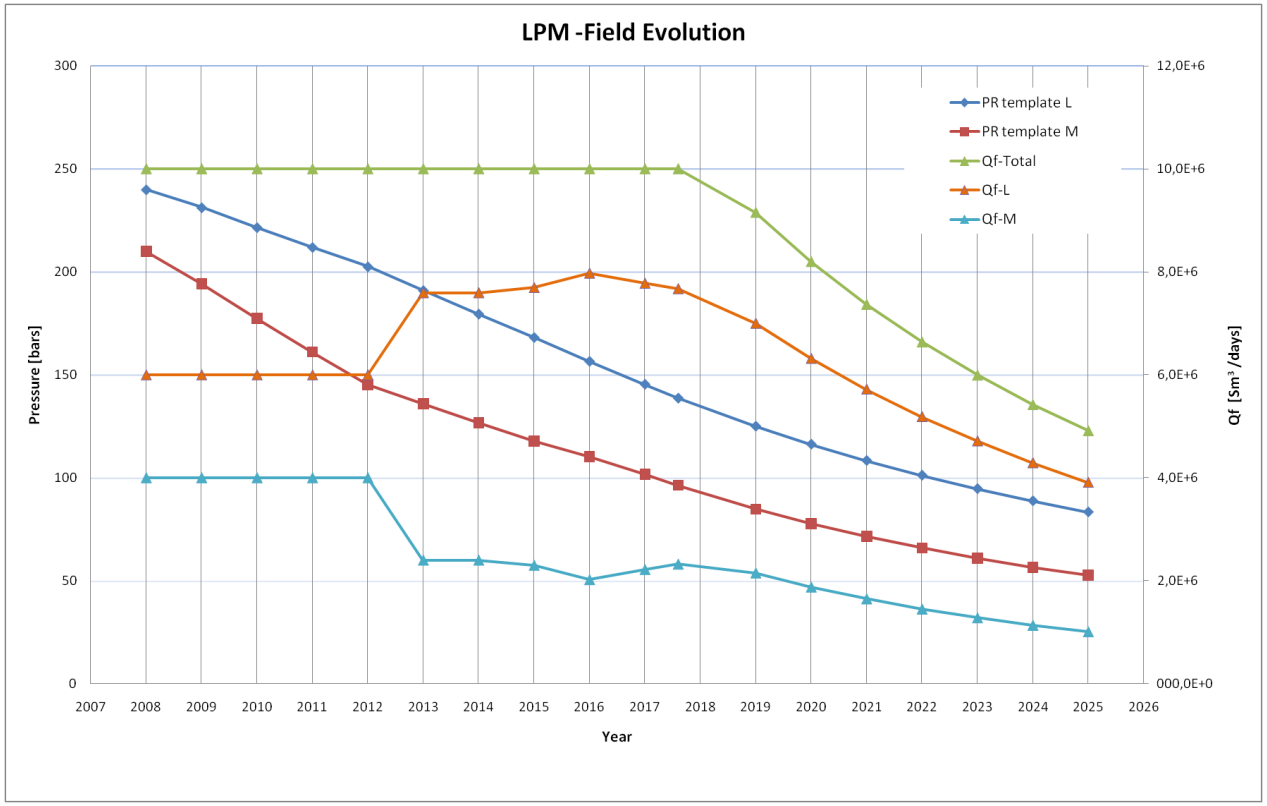

Figure 3.3.7 The LPM field evolution shows plot of Q_f Total and Q_f -L and M , reservoir pressure from each template (PR template L and M) with times (years). With applying LPM to the field, the Q_f can be optimized and also extending the lifetime of the field about 1 year more compare to any other cases.

Subsea Compressor Cases

Psep	PtowheadL	P-outL	DpChookeL	PtowheadM	P-outM	DPChookeM	2*14 Ptowhead	P suc av	errorsuc	delta p comp	rp				Qfield	Years
bara	bara						bara	bara	bara^2	bara						
65	173,12	168,32	103,32	145,95	143,43	78,43									10,0E+6	2008
65	165,18	160,15	95,15	129,46	126,62	61,62									10,0E+6	2009
65	156,26	150,93	85,93	111,07	107,74	42,74									10,0E+6	2010
65	147,29	141,62	76,62	91,73	87,67	22,67									10,0E+6	2011
65	138,34	132,29	67,29	70,43	65,05	0,05									10,0E+6	2012
65	114,59	102,48	37,48	89,41	87,93	22,93									10,0E+6	2013
65	101,76	87,90	22,90	79,20	77,53	12,53									10,0E+6	2014
65	86,99	69,77	4,77	70,88	69,16	4,16					<-- End of natural plateu				10,0E+6	2015
65	67,34			67,34			73,23	67,34	4,26E-15	5,89	1,087530845				10,0E+6	2016
65	52,32			52,32			73,23	52,32	8,58E-08	20,92	1,399792111	Δp comp fixed	error comp	Total flow	10,0E+6	2017
65	41,23			41,23			73,23	41,23	1,53E-14	32,00	1,776091324	[bara]	[bara^2]	<-- End of driven plateu	10,0E+6	2017,9
65	39,05			39,09			71,07	39,07	1,00E-03	32,00	1,819015578	32	7,85E-06	8,52E+06	8,5E+6	2019
65	37,85			37,89			69,87	37,87	8,67E-04	32,00	1,844883512	32	7,35E-07	7,60E+06	7,6E+6	2020
65	36,94			36,89			68,92	36,92	1,00E-03	32,00	1,866799491	32	1,18E-06	6,79E+06	6,8E+6	2021
65	36,18			36,15			68,15	36,16	5,73E-04	31,99	1,884532304	32	1,45E-04	6,07E+06	6,1E+6	2022
65	35,52			35,57			67,54	35,54	9,37E-04	32,00	1,900292633	32	1,43E-07	5,44E+06	5,4E+6	2023
65	35,03			35,08			67,05	35,06	9,12E-04	32,00	1,91283047	32	3,06E-07	4,88E+06	4,9E+6	2024

LPM Cases

Psep	PtowheadL	P-outL	DpChookeL	PtowheadM	P-outM	DPChookeM	2*14 Ptowhead	P suc av	errorsuc	delta p comp	rp				Qfield	Year
bara	bara						bara	bara	bara^2	bara						
65	173,12	168,32	103,32	145,95	143,43	78,43									10,0E+6	2008
65	165,18	160,15	95,15	129,46	126,62	61,62									10,0E+6	2009
65	156,26	150,93	85,93	111,07	107,74	42,74									10,0E+6	2010
65	147,29	141,62	76,62	91,73	87,67	22,67									10,0E+6	2011
65	138,34	132,29	67,29	70,43	65,05	0,05									10,0E+6	2012
65	114,59	102,48	37,48	89,41	87,93	22,93									10,0E+6	2013
65	101,76	87,90	22,90	79,20	77,53	12,53									10,0E+6	2014
65	86,99	69,77	4,77	70,88	69,16	4,16								<-- End of natural plateu	10,0E+6	2015
65	67,34			67,34			73,23	67,34	4,26E-15	5,89	1,087530845				10,0E+6	2016
65	52,32			52,32			73,23	52,32	8,58E-08	20,92	1,399792111	Δp comp fixed	error comp	Total flow	10,0E+6	2017
65	41,23			41,23			73,23	41,23	1,53E-14	32,00	1,776091324	[bara]	[bara^2]	<-- End of driven plateu	10,0E+6	2017,6
25	26,04			26,04			41,69	26,04	1,61E-06	15,65	1,600777489	15	4,16E-01	9,16E+06	9,2E+6	2019
25	24,22			24,23			39,35	24,22	2,97E-06	15,13	1,624610084	15	1,70E-02	8,20E+06	8,2E+6	2020
25	22,29			22,29			37,44	22,29	3,52E-10	15,15	1,679548722	15	2,23E-02	7,37E+06	7,4E+6	2021
25	20,73			20,73			35,85	20,73	1,64E-10	15,12	1,72920214	15	1,42E-02	6,64E+06	6,6E+6	2022
25	19,38			19,38			34,54	19,38	3,32E-10	15,16	1,782565983	15	2,66E-02	5,99E+06	6,0E+6	2023
25	18,28			18,28			33,45	18,28	2,55E-10	15,16	1,829218651	15	2,63E-02	5,42E+06	5,4E+6	2024
25	17,39			17,39			32,54	17,39	1,81E-10	15,16	1,87182543	15	2,46E-02	4,92E+06	4,9E+6	2025

Table 3.3.2 The calculation comparison table shows that The Q_f with LPM is slightly bigger than subsea compressor case during 2019-2024. The minimum Q_f values which is 5 x 10^6 Sm^3/days is also reached on different year in both calculation. In Subsea compressor case the minimum Q_f is reached on 2024 while with LPM, the minimum Q_f reach on 2025. So, It is clear that the LPM give more optimum Q_f and also extend the lifetime of the field, Thus give more benefits.

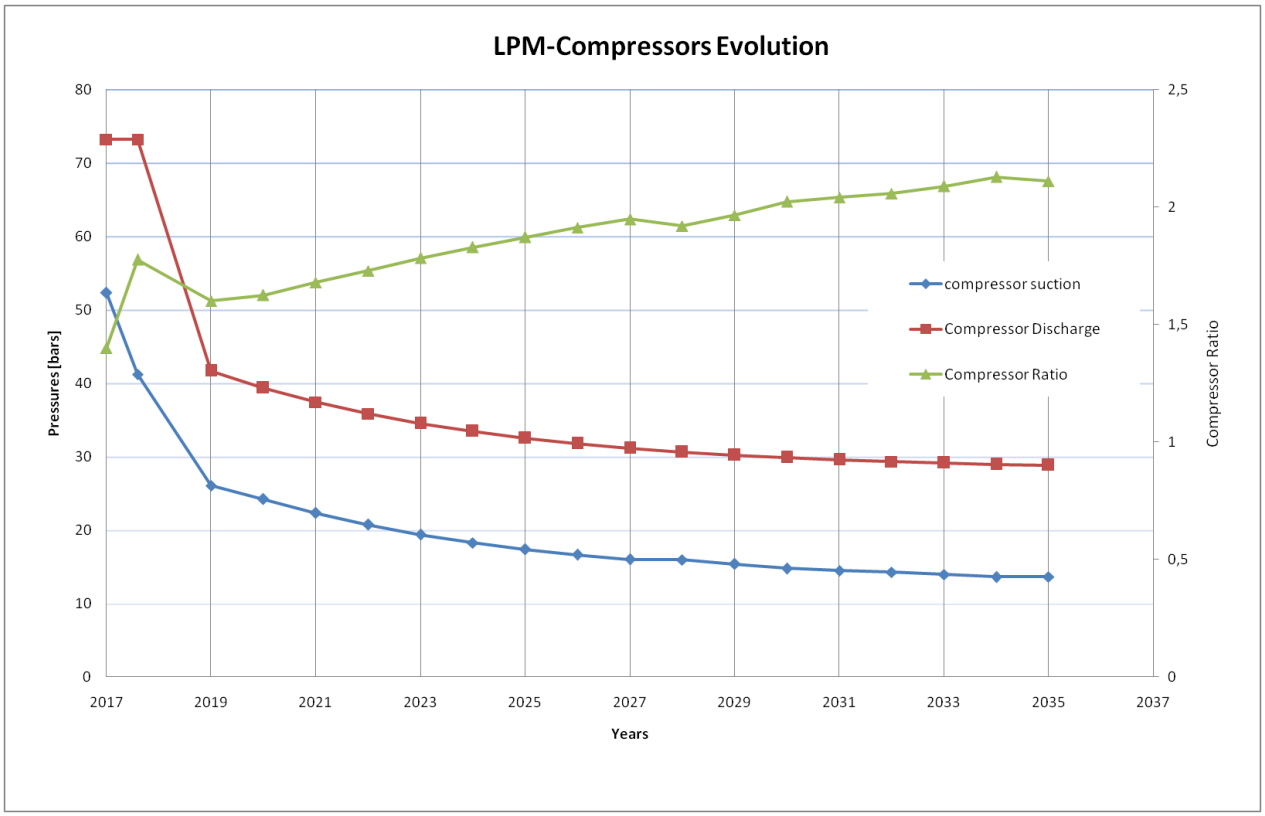

Figure 3.3.8 The Compressor Evolution with Low pressure modification. The figure demonstrates the evolution of $\Delta P_{discharge}$ which represent the separator pressure from 65 bars to 28 bars on 2019. This modification will come up with smaller difference between Psuction and Pdischarge (Δp compressor would decrease from 32 bars to 15 bars) so that the compression ratio increment will be smaller than that in subsea compressor and topside compressor case. This will allow more flow after driven plateau exceeded.

3.3.4 Topside Pre-Compressor

On this case, it is assumed that the compressor will be installed and placed on the platform, just before the separator. The new calculation model was created to get Qf Total (see detail result on appendix F on table F.2). Based on this Qf -Total calculation, one can compare the Qf -Total resulted from topside compressor system and compare it to other cases to analyze which of those would give more benefits based on NPV (will be discussed in section 3.5).

With installing the compressor system on the topside, the pressure input for the separator (P suction) will be smaller than the P suction on the subsea and LPM cases. This is caused by the longer distances needed (±14 km) to transport the gas from wellhead to compressor system, thus more pressure lost. The Gas need to flow through the 12" pipe -166m long from each template to towhead and then continue to flow to compressor within 14 "pipe -14 km long (see figure3.3.9). The cases actually gives more disadvantages than subsea and LPM cases because of the lesser driven plateau duration on topside compressor compared to LPM and subsea compressor system. The driven plateau on subsea and LPM cases will lasting for 2.6 years while on topside compressor system cases it is only 0.9 year (see figure 3.3.10 and 3.3.11). Not only reduce the driven plateau duration but the topside compressor will also reduce the Qf Total that resulted in the later stage of the flow after driven plateau exceeded (see figure 3.3.11).

It can be observed that the subsea compressor and LPM would give more benefit than the topside compressor system. On the other part of the report, the qualitative potential risk assessments for both compressor system location were conducted to observe and analyze the advantages and disadvantages between both cases.

The recover factor obtained from this cases vary from 0.6 (template L) and 0.72 (template M).

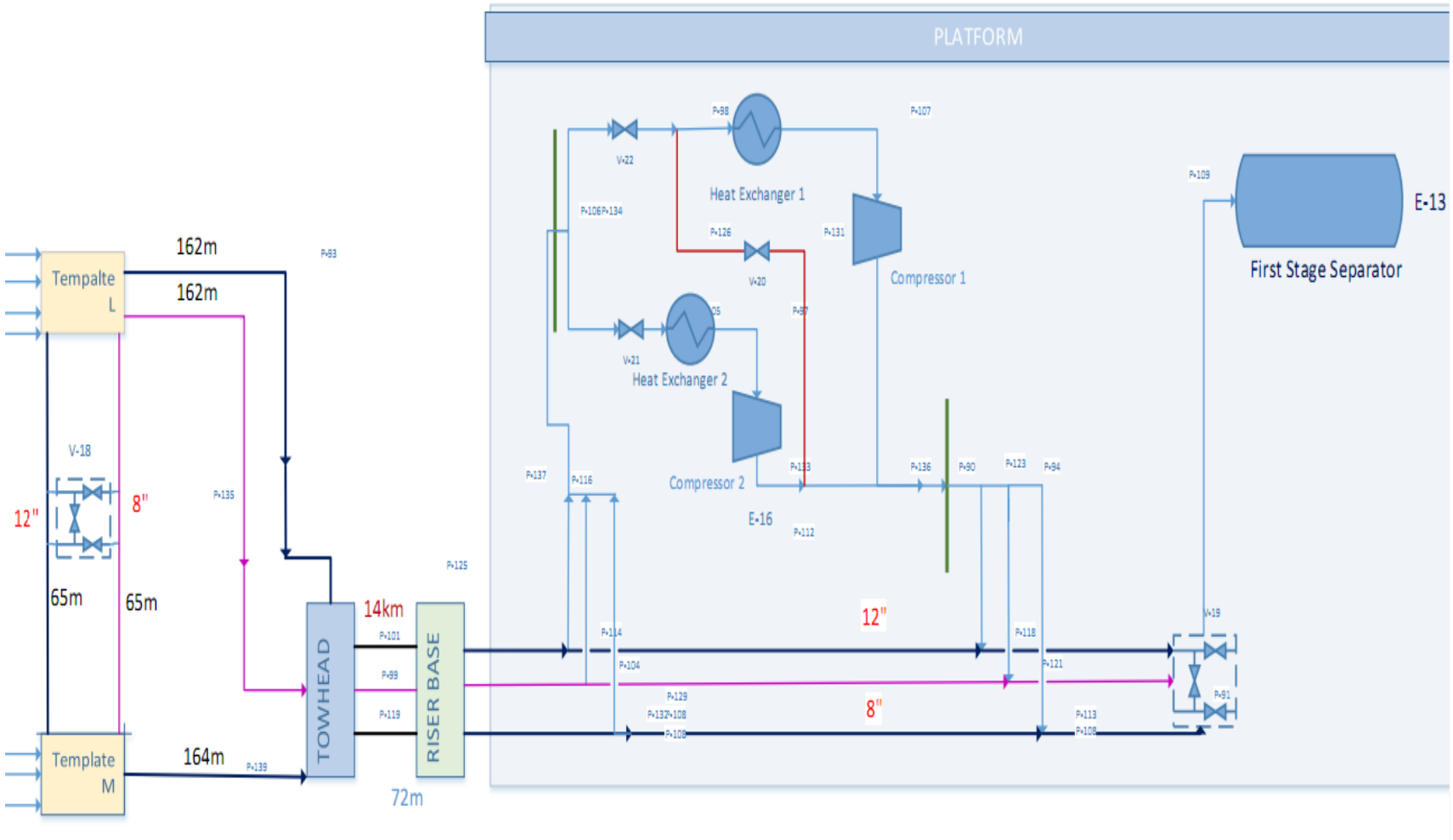

Figure 3.3.9The topside flow diagram. On topside cases, The compressor will be installed on platform, next to separator. The effect of locating the compressor in platform will impact negatively to the Q_f Total, because longer distance is needed for gas to flow from wellhead to compressor than that on subsea and LPM cases. Thus, more pressure losses that trigger the reduction of flow on topside cases.

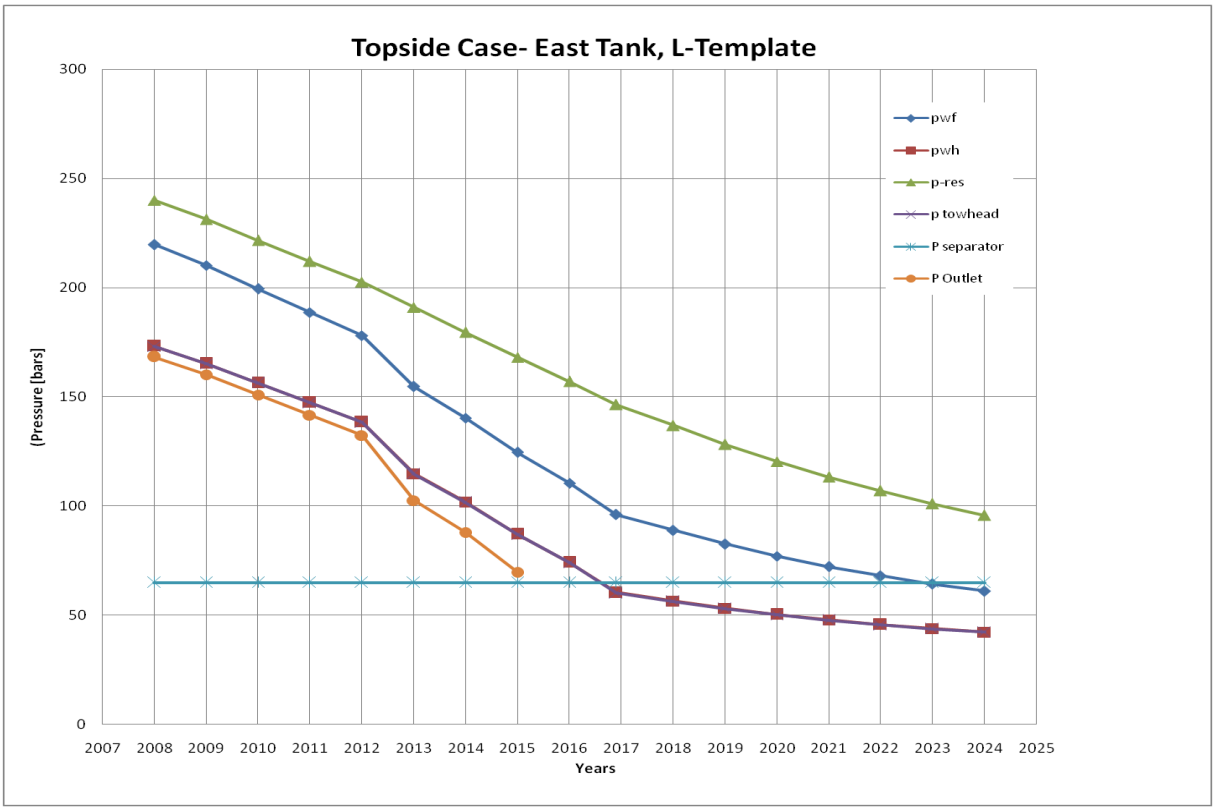

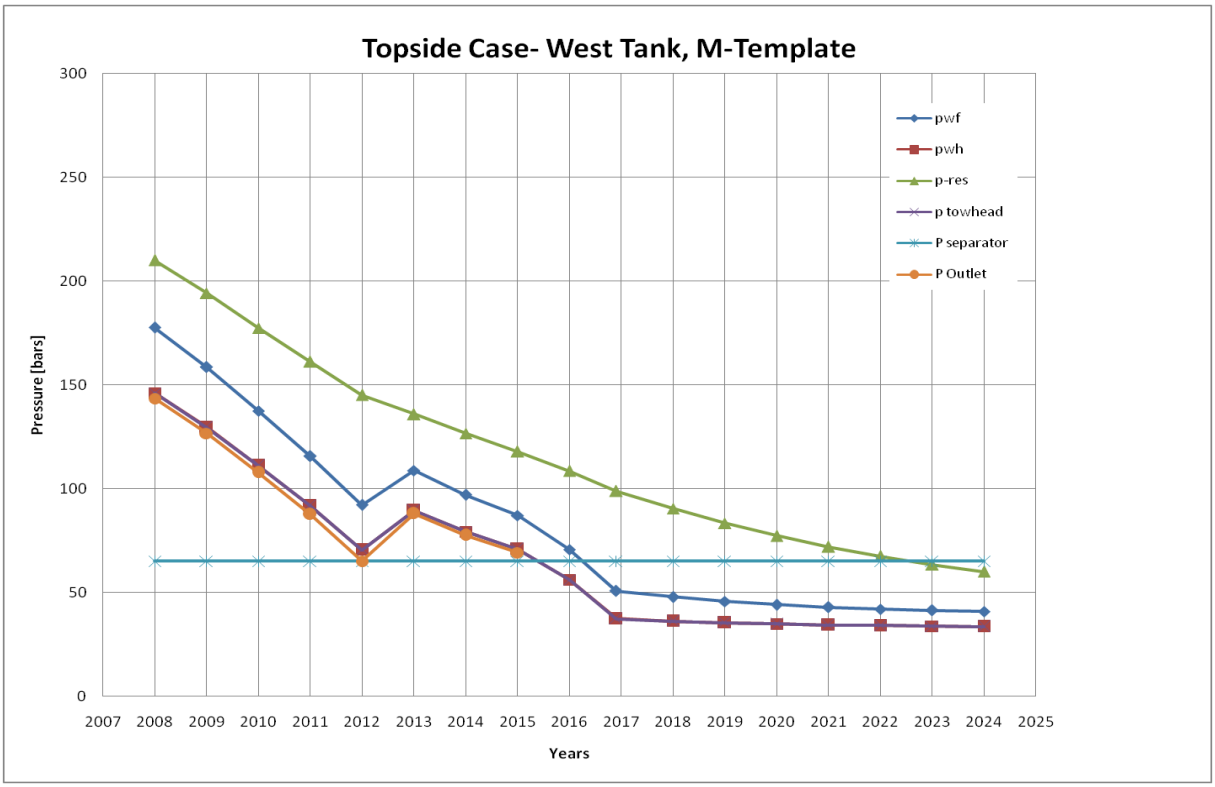

Figure 3.3.10a (top)- b(bottom) The topside compressor case's pressure plot (bars) through times (years) for both East Tank-L Template and West Tank-M Template. The figure shows that from 2008-2015, the gas will flow with natural flow (Poutlet>Pseparator) and in 2016-2016.9 when P outlet is smaller than Pseparator, the gas will flow by driven flow, lastly the flow reduced until it reach minimum Q_f Total at 2024.

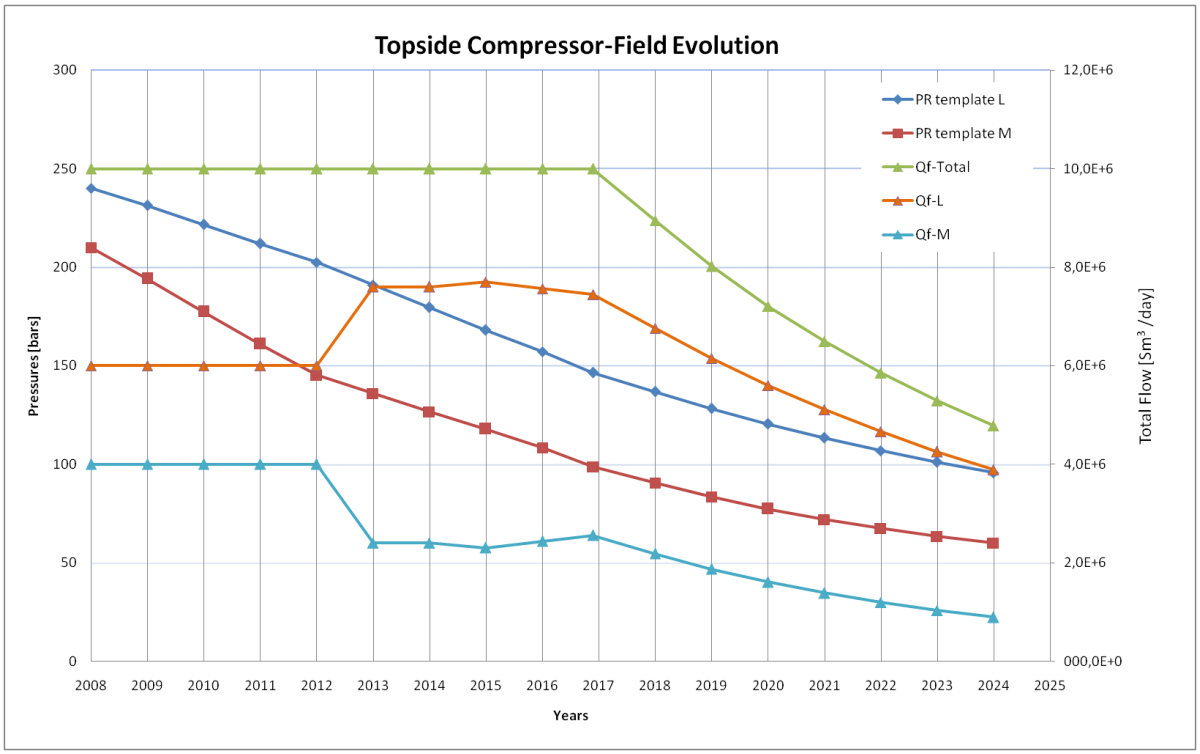

Figure 3.3.11The topside compressor field evolution. The figure shows on topside compressor cases, the field will continuously flowing the gas with constant plateau from 2008- 2016.9 before it reach the minimum Qf on 2024.The topside compressor will give the lesser duration of driven plateau which is only lasting for 0.9 years compared to that on subsea and LPM cases.

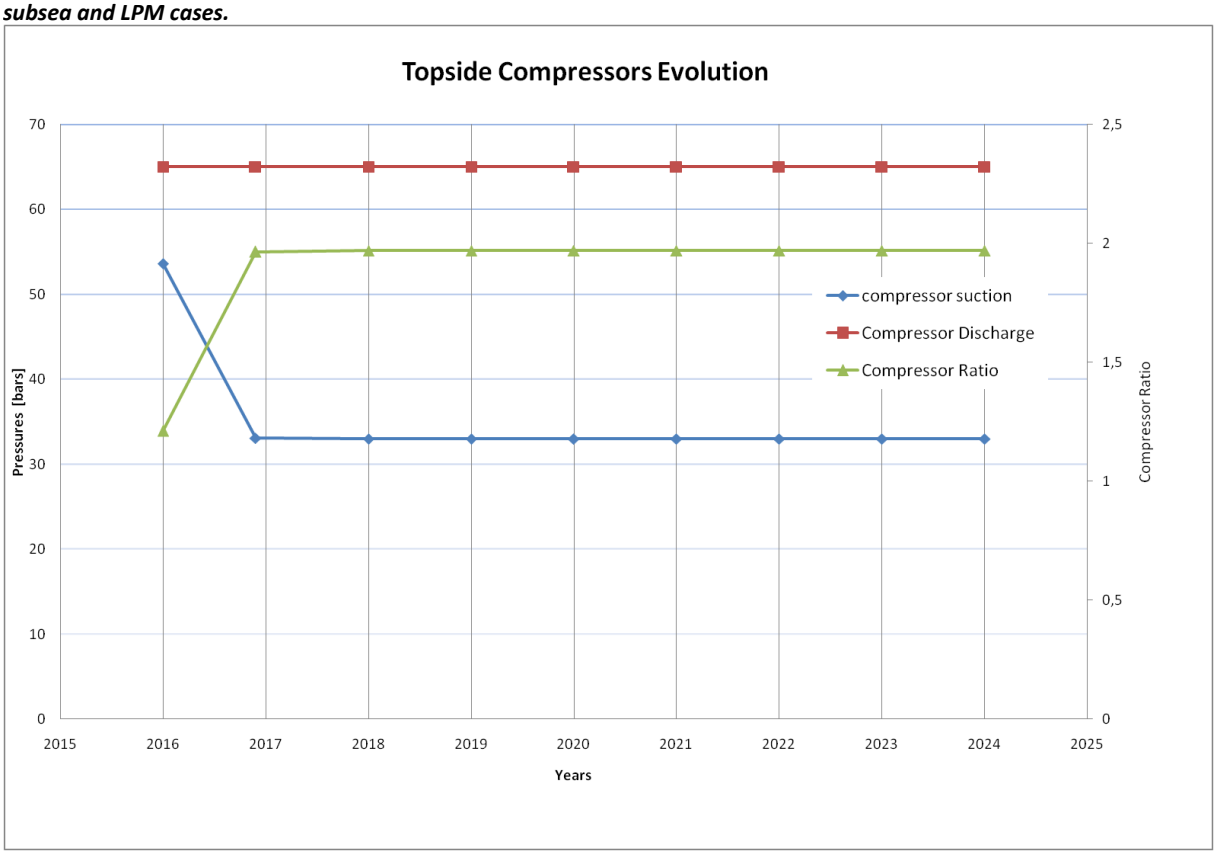

Figure 3.3.12The topside compressor evolution graphs. The figure shows that the compressor start to operate on 2016 in order to keep the Q_f Total plateau ($10x10^6$ Sm^3/day) . In 2016.9, the compressor reaches its maximum ratio because the pressure difference between compressor suction and discharge will be close to the 32 bars (maximum dp compressor).

3.3.5 Summary and Conclusion

For comparing each of cases above, the table (see table 3.3.3) and plots were made to show the results contrast between the cases (see figure 3.3.13 and 3.3.14).

No	Case	End of Natural Plateau	Compressor Installation	End of Driven Plateau	Min.Qf Year	Cum.Qf (Sm3/day)	Rec Factor	
							Template L	Template M
1	**Reference**	2014	-	-	2020	140,4E+6	0,44	0,56
2	**Subsea Compressor**	2015	2016	2017,6	2024	149,3E+6	0,61	0,71
3	**Low Pressure Modification (LPM)**	2015	2016	2017,6	2025	157,7E+6	0,65	0,76
4	**Topside Compressor**	2015	2016	2016,9	2024	146,6E+6	0,60	0,72

Tabel3.3.3 The table shows the different result between cases. It is obvious that the Low Pressure Modification will be the most prominent cases to give more benefit in optimizing the gas production on Gullfaks C field.

Based on the table 3.3.3 and plot (figure 3.3.13 and 3.3.14), It can be conclude that the low pressure modification (LPM) is the best cases to optimize the production rate of Gullfaks C field, with giving 0.65-0.72 recovery factor and extending the flow plateau from 2016-2017.6 (2.6 years).

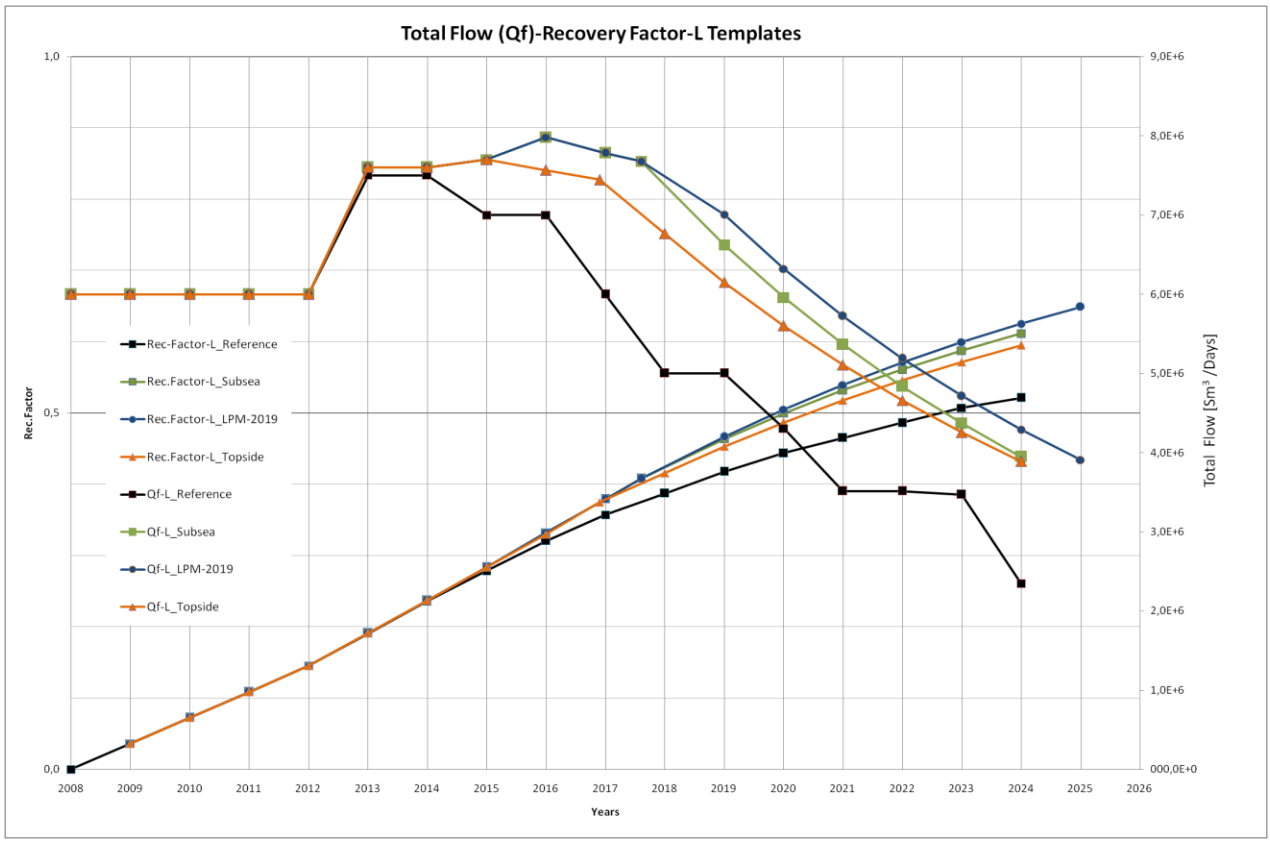

Figure 3.3.13The Q_f and Recover factor for template L in different cases. The LPM methods give the highest Q_f and Recovery rate.

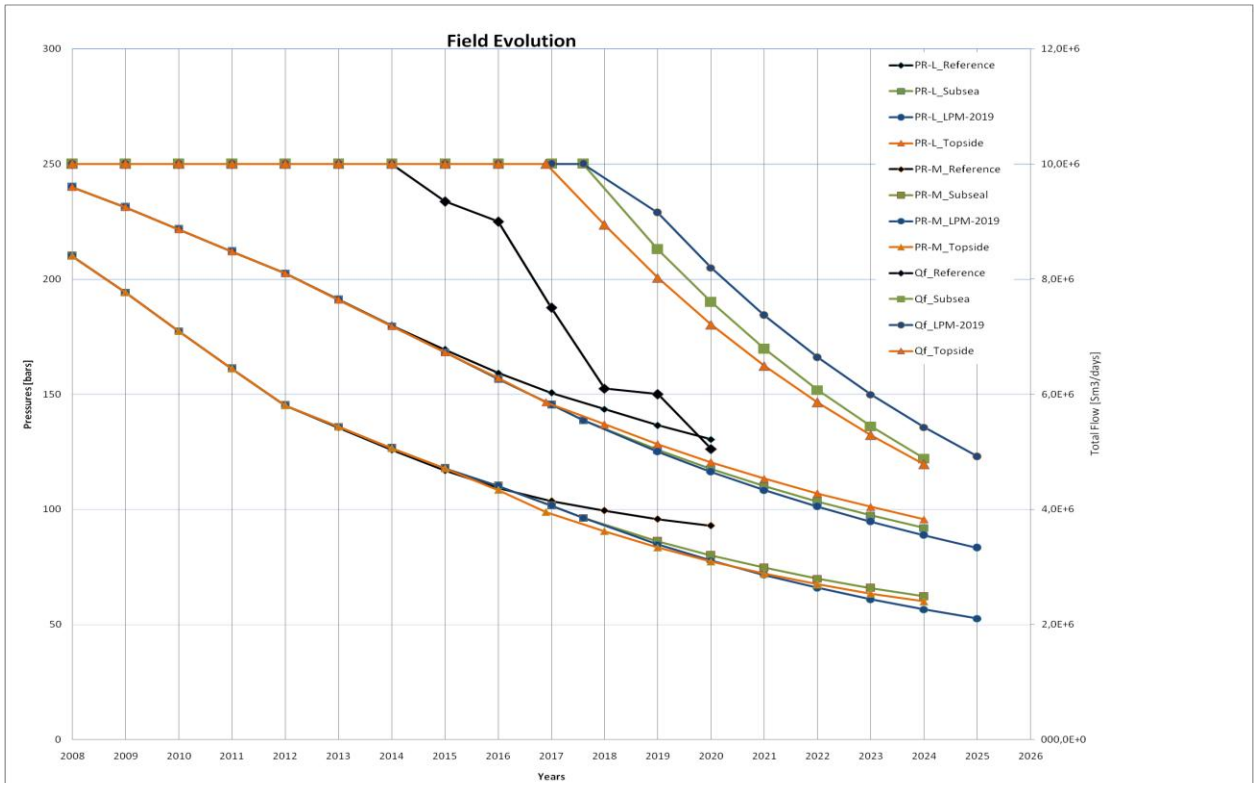

Figure 3.3.14 The Qf and Reservoir Pressure Plot. The figure shows the comparison between Qf and PR in different cases. It can be noticed that the LPM cases (dark blue) would give higher Qf than any other cases.

3.4. Liquid Accumulation in Gas Wells

Liquid accumulation in a gas well can come from several sources. Liquid might be present with the gas in the reservoir, or might condensate out of the gas phase as the pressure decreases.[11] Preventing all liquids from leaving the reservoir together with the gas is almost impossible, so the usual focus is placed upon making sure that they do not accumulate in the well or later in the piping. This is done by making sure that the gas velocity is kept higher than the critical velocity, v_c. Contrary to what one might expect, the amount of liquid present in the stream is not that important for most normal cases;[11] this makes the gas velocity the key variable to control.

There exist two physical models describing how liquid is transported out of the well with the gas flow. The film model, which assumes that a liquid film forms at the well interface and the droplet model, which assumes that liquid is present as small droplets in the moving gas phase.[4] For this project only variations of the droplet model have been considered. The theory behind the droplet model is described in Appendix C.

3.4.1. Graphs and Discussion

The graphs in this section compare the predicted flow out of a well with the critical flow at that specific time. If the predicted flow, Q_{wh}, is below the critical flow, Q_c, liquid accumulation will occur. To test for the scenario involving the smallest flow rates, the plots assume compressor installation and LP modification for the predicted critical flow. As this gives significantly lower flow rates through the wells, no liquid accumulation for this scenario guarantees that no liquid accumulation will occur for any of the other cases. For the calculations the temperature in the wellhead was assumed to be equal to the temperature in the reservoir. The wellhead is the safest place to calculate for liquid accumulation as it the lower pressure increases gas slippage.

When using the droplet model to calculate if there is risk of liquid accumulation it is common to only calculate the risk of water accumulation. This is because oil generally is a lighter phase, and thus easier to transport to the surface. To confirm this assumption the critical flow rate was found for both water and oil using the Coleman model. The result for an L-template well is shown in Fig. 3.4.1 and indicates, as predicted, that the critical flow rate to keep water from accumulating is greater than the one necessary to keep oil from accumulating. Based on this, only critical flow rates for water are calculated.

There exist several different droplet model variations, giving different predicted critical flows. For an indication of how the different models predictions compare to each other, see Fig. 3.4.2.

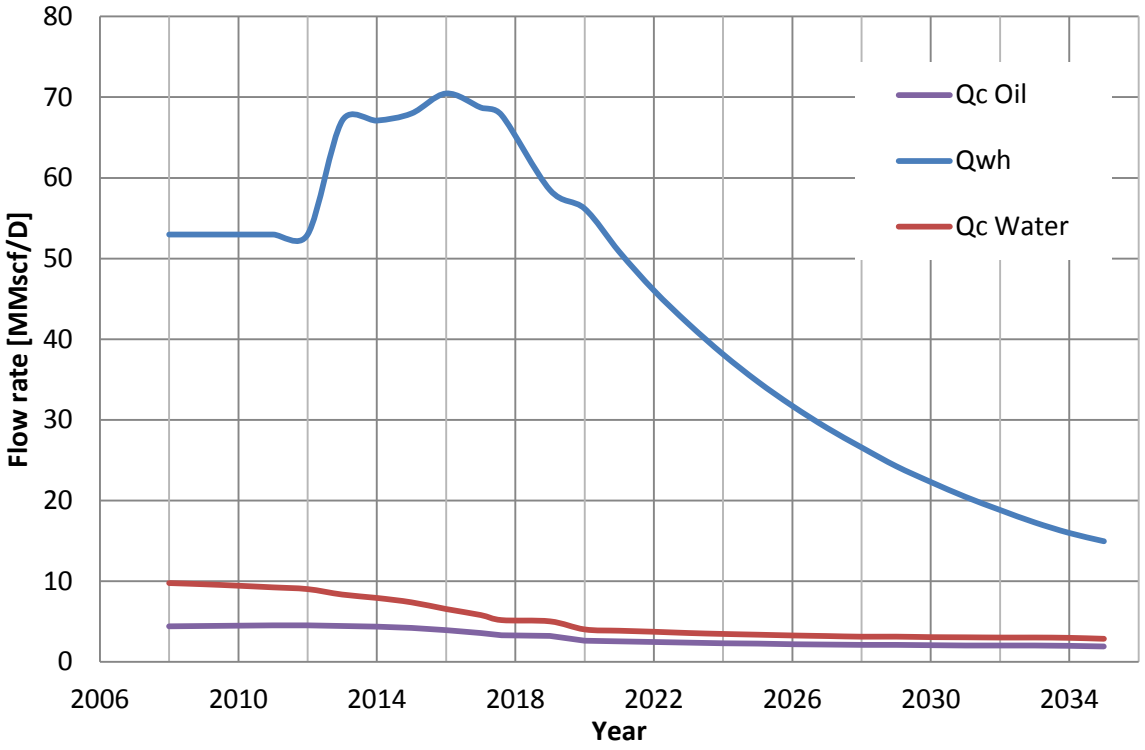

Figure 3.4.1: Critical flow rate for oil and water plotted with the predicted flow rate for a well in the L-template.

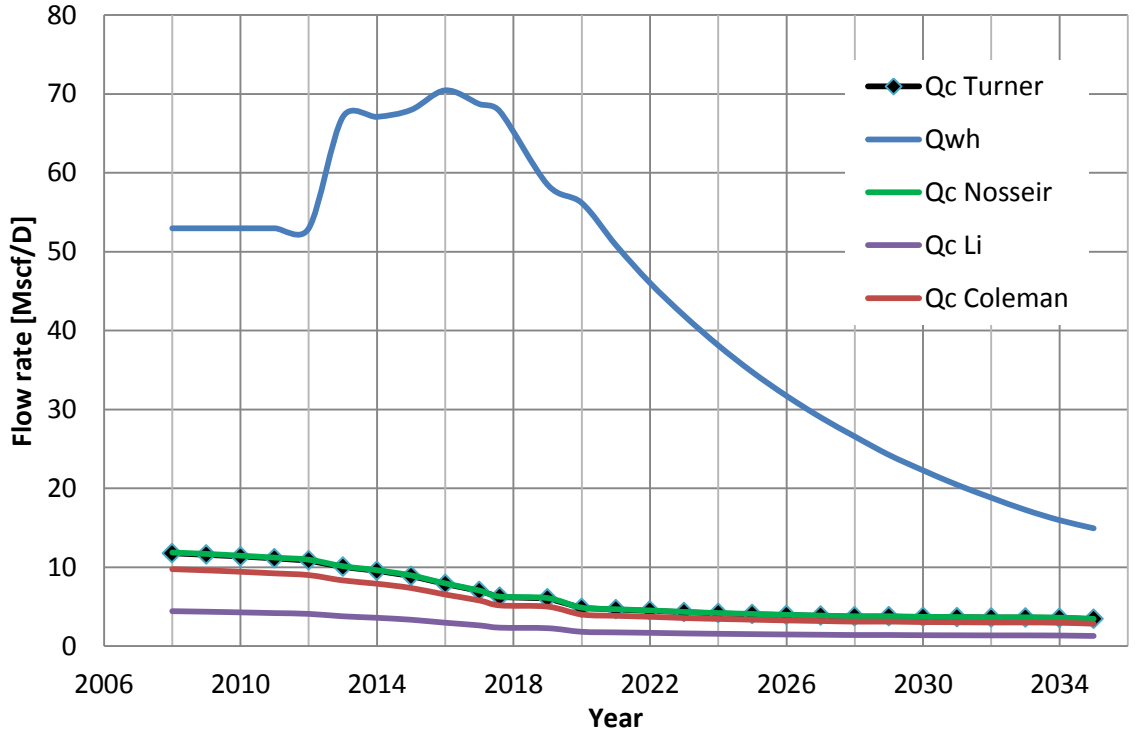

Figure 3.4.2: Predicted flow out of an L-template well, plotted with the calculated critical flows. The critical flows were found using four different droplet models: Adjusted Turner, Coleman, Li and Nosseir.

As seen from Fig. 3.4.2, the Turner and Nosseir equation give almost identical critical rates while the Coleman and Li equations give slightly lower results. The Coleman and Li equations therefore allows for a lower actual flow rate before liquid accumulation. The Coleman, Li and Nosseir equations are all based on the Turner equation, and have been shown to improve on the results of the adjusted Turner given specific flow conditions. However no model has as of yet been developed specifically for large diameter wells such as the ones in use for the Gullfaks South templates. Nosseir developed an alternative model to the Turner equation for highly turbulent flows, defined as flows with Reynolds number, $N_{Re} > 2\times10^5$. Calculating the Reynolds number for our flow showed highly turbulent flow for all years of production, indicating that the Nosseir equation might be our best bet among the equations. The Nosseir equation also gives a high critical rate compared to the other models. Using it as a basis to some degree gives a "worst case" scenario. Fig. 3.4.3 shows the resulting flow rate comparison for a well in the M- template. As seen from the figure the liquid drop model gives no liquid accumulation. However, the models are not exact and taking insecurities into account the proximity of the two lines indicates a risk of liquid accumulation for the last years of production.

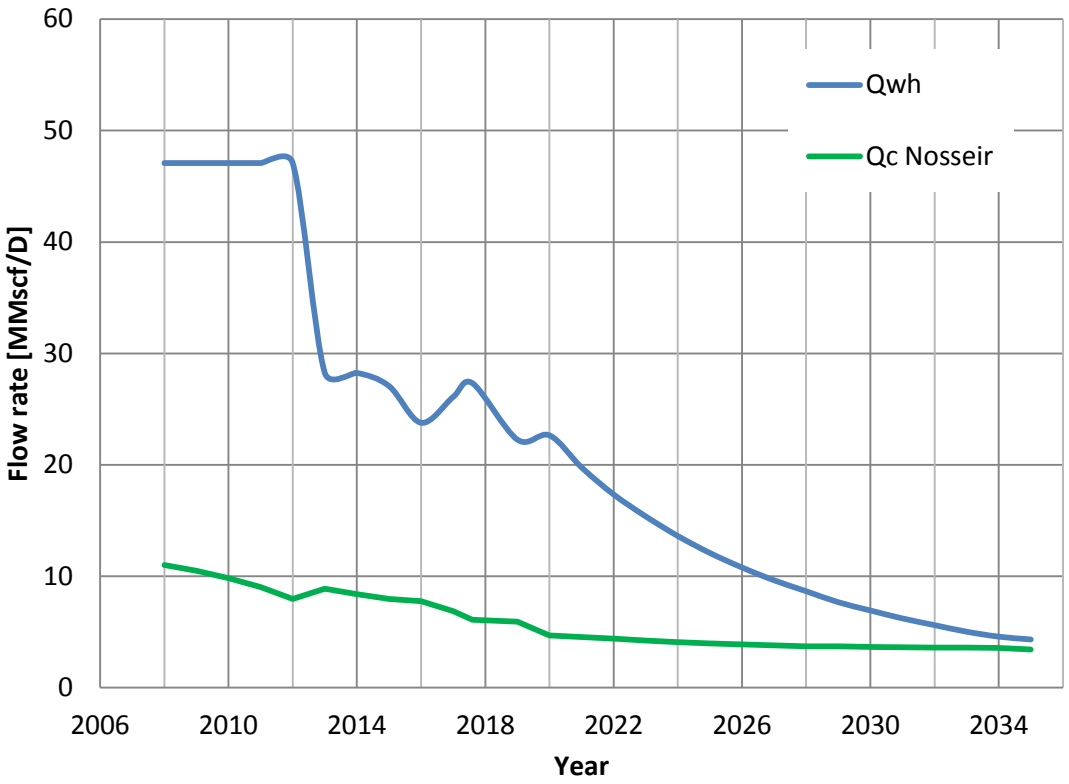

Figure 3.4.3: Predicted flow out of an M-template well, plotted with the critical flow found from the Nosseir model.

Even though the Fig.3.4.3 indicates no liquid accumulation it should be noted that none of the droplet models have been tested for wells with internal diameters close to 6''. In general fluid models do not scale well, raising some concern as to the accuracy of the results. In addition to this, it has been

assumed that the flow from each well in a template is identical. This simplification is not realistic, and gives higher minimum flows than if the flow differed from well to well. With a significant difference between the different wells, the wells with smaller flow rates might have liquid accumulation. Fig. 3.4.4 was made to test how different flow rates for each well might affect the result for a well in the M-template. The flow rate from the plotted well is assumed to be half of the average flow rate to the M-template, giving liquid accumulation in the well from 2029.

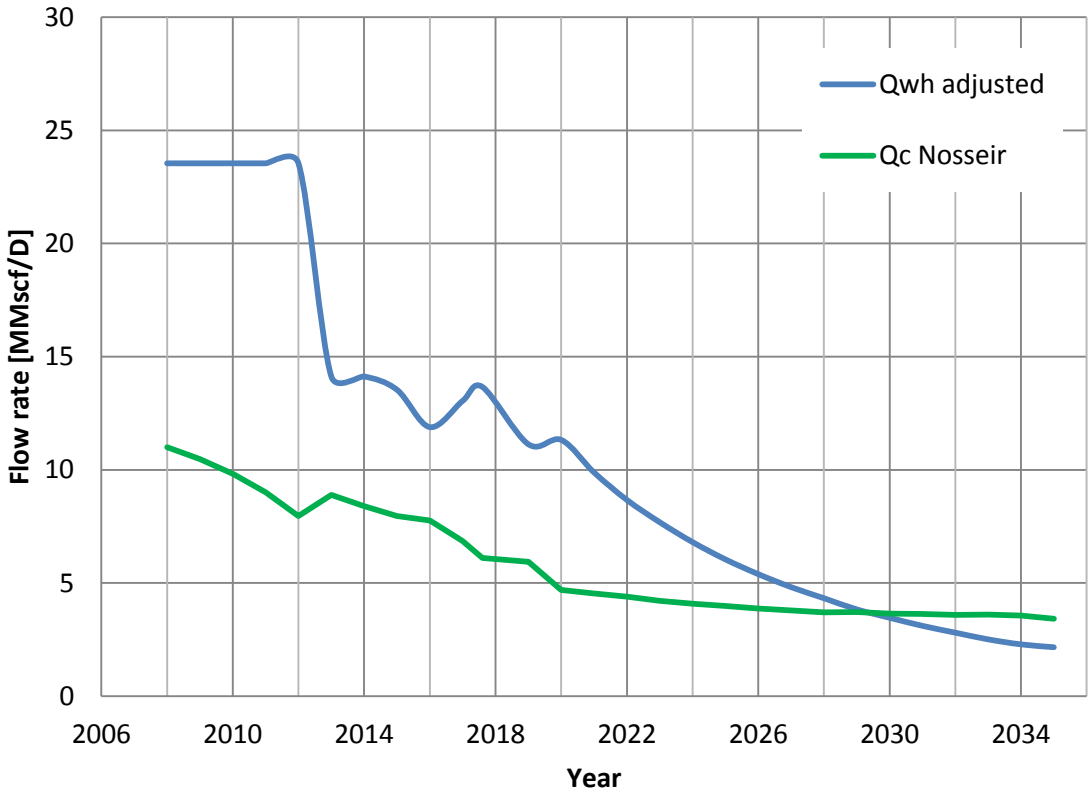

Figure 3.4.4: Adjusted predicted flow out of an M-template well, plotted with the critical flow found from the Nosseir model.

3.4.2. Solutions

If liquid accumulation does occur, there exist several technological possibilities to minimize its negative effects. Here, only a short list mentioning some of the common alternatives is included. For a more thorough introduction to the subject, see Dotson[11] and Lea et al. [12] Usually, one or several of the following methods can be applied to solve a liquid loading problem:

1. Resizing production strings to eliminate liquid loading.
2. Compression is used to lower the tubing pressure and increase gas velocity, but the economic effect should be taken into account.

3. Plunger lift is a premier method of operating a gas well with liquids. It uses a free-traveling plunger to assist the gas in carrying liquid upward without excessive liquid fallback. This method is preferred over smaller tubing when the rates decrease as it does not require refitting.
4. Beam-pump systems are a common method of dewatering gas wells. They are only valid when wells do not have adequate pressure and GLR to allow use of other methods.
5. Hydraulically powered down hole pumps are manipulated by a stream of high-pressure water or other fuel supplied by a power-fluid pump at the surface. There are some advantages to this method, including easy installation, high rate productions and low operating costs. Unfortunately, it is unlikely to obtain producing bottom hole pressures and the startup costs are significant.
6. Gas lift introduces extra gas into the tubing to lighten the flow gradient and can increase the fluid velocity above critical. This method is available if high-pressure gas is viable.
7. Injecting the water into a zone below the gas zone is feasible, but demands that a possible injection zone is present.

Many other approaches, such as using a residence cable, various controller or inserts, have been demonstrated over the past years but the major concepts are identified in the list above.

3.5. Economic Analysis

For the quantitative analysis of economic part resulting from the technical parameters (on section 3.3), we are interested in the total revenues, cumulative net present values and relative increments compared with the reference case of three different cases since these two terms reflect the economic effect intuitively and comprehensively. For the detail result, the calculation sheet for each cases can be found on Appendix E. The figures 3.5.1 representing the total revenues, cumulative net present values and increments compared with the reference case are shown as follows. The parameters here we plan to use are the same as those in case A and we take into account the tax rate up to 78% in each case.

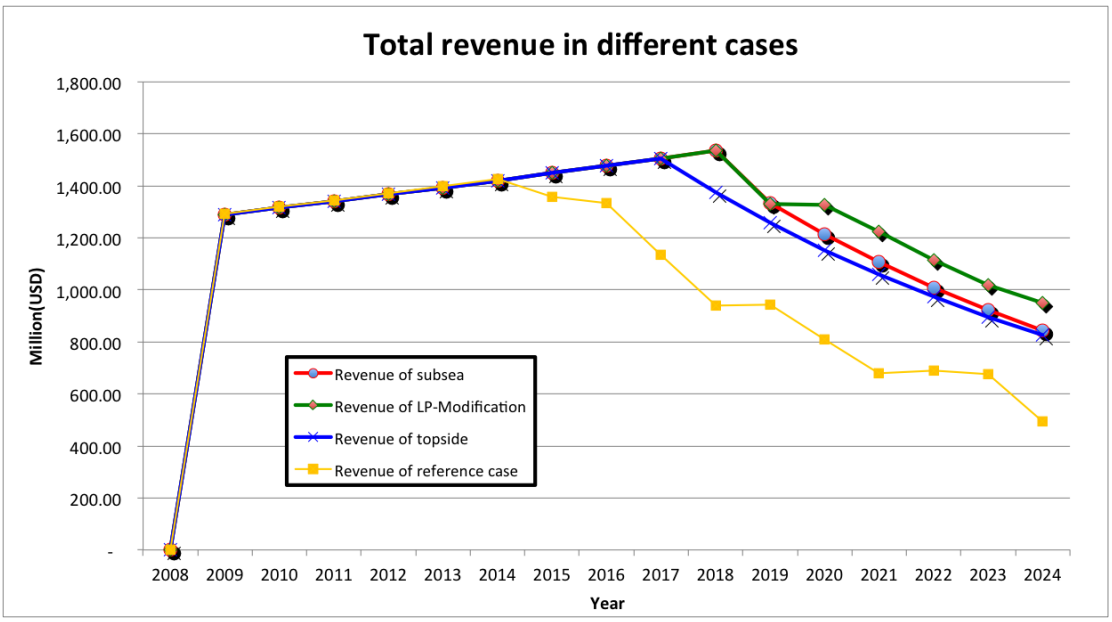

Figure 3.5.1: The total revenues in four different cases including the reference case

According to Fig. 3.5.1, we observe that at the beginning time interval between 2008 and 2014 the total revenues are completely identical due to the same parametric settings (e.g. Qf and economic terms etc.).Meanwhile, the revenue of subsea, LPM and topside start to depict the downward trend later than 2017 whereas the reference case becomes going down immediately at the end of 2014. The turning point in each case implies the time at which the total flow of each case is going to decrease. Furthermore, it is the total revenue of LPM staying on the top that means we will have more income than any other cases if applying the LPM.

From Fig. 3.5.2, we can conclude that there is no reason to reject the priority of choosing LPM as our potential method though the others cost less expenditure than LPM.

With respect to the reference, we calculated the relative increments in each case. From Fig. 3, the break event point is approximately between 2016 and 2017, which implies the extra profits began to be obtained. After this time at which the compressors were installed, the LPM becomes the optimal choice and not surprisingly, this fact is consistent with the results we analyzed in Section 3.3.

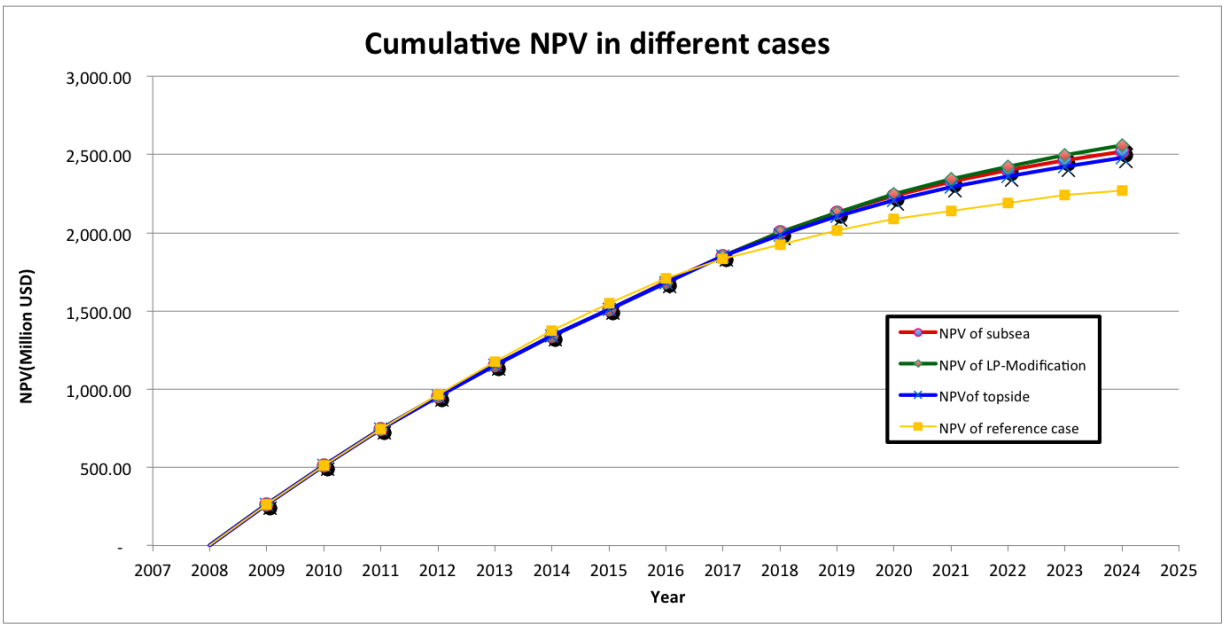

Figure 3.5.2: The cumulative NPV of producing from the reservoir for the three different modifications and the reference case.

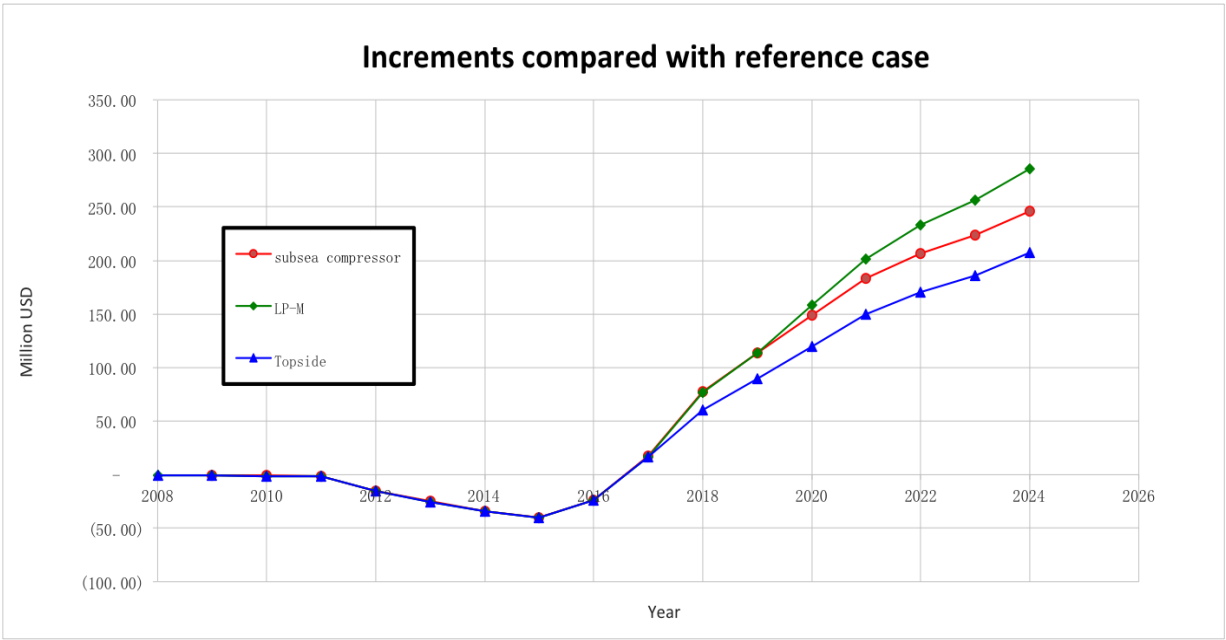

Figure 3.5.3: The actual NPV of each project.

3.6. Qualitative Risk Analysis

Based on DNV's guidebook "*Risk Management in Marine and Subsea Operation",* there are 7 key assessment parameters that need to be considered. These parameters are shown in Table 3.6.1.

Table 3.6.1: The Important Assessment Parameters for Risk Analysis.[13]

Assessment Parameter	*Keywords for assessment*
Personnel exposure	- Qualification and experience of personnel - Organisation - Required presence - Shift arrangements - Deputy and backup arrangements
Overall project particulars	- Delay - Replacement time/cost - Repair possibilities - No. of interfaces and contractors or subcontractors - Project development period
Existing field infrastructure	- Infrastructure - surface - Infrastructure - subsea
Handled object	- Value - Structural Strength/Robustness
Marine operation method	- Novelty and feasibility - Robustness - Type of operations - Previous experience - Installability
Equipment used	- Margins/robustness - Condition/Maintenance - Previous experience - Suitability - Experience with operators or contractors (track record)
Operational aspects	- Cost of mobilised equipment and spread - Language barriers/hindrance - Season/Environmental conditions - Local marine traffic - Proximity to shore

These 7 assessment parameters are used in accordance to personal safety, environment, assets damage, business interruption, and reputation. By comparing these parameters for the subsea compression and the topside compression, we can determine how those two alternatives compare from a safety standpoint. The qualitative risk analysis can be useful as a compliment of quantitative analysis (based on total flow and economical calculation). If both of them are align the decision is already given.

As the systems that are involved in both subsea compression and topside compression are quite complex it is hard to judge the assessment level accurately.

Another problem with qualitative risk analysis is that there is no predefined way to do qualitative risk assessment that accurately represent for every case. Our qualitative risk analysis is therefore based on our own evaluation of risk and is only applicable as comparison between the two given cases. The different risk parameters might be evaluated differently if performed by a different team or if the project took place at some other place in the world.

The step-by-step procedure for the qualitative risk assessment is shown below:

1. Decide the level of severity of each assessment parameter in accordance to personal safety, environment, assets damage, business interruption, and reputation. For this assessment, one had decided to choose L (low), M (medium), H (high) as 3 types of severity where L represents 1 value and H represents 3 values.
2. Refer to the Statoil company value as fundamentals to fill in the priority between personal safety, environment, assets, business, and reputation. The personal safety, environment and business are the most considered value in Statoil, so they will take more weight in the summation of each risk assessment. The weighting value for each assessment parameter =(level of severity in Personal Safety x 0.3)+(level of severity in Environment x 0.25)+(level of severity in Business Interruption x 0.25)+ (level of severity in Reputation x 0.20)
3. Make a recommend risk category as a summary of the each assessment parameter and also sum up all of the weighted value in each assessment parameters to compare between the cases (subsea and topside cases)

The result of the assessments in Table 3.6.2 show casing the difference between the two different cases.

Table 3.6.2: The Qualitative Risk Assessment for Topside and Subsea Compressor Installation.

No	**SUBSEA** Assesment Parameter	30% Personal Safety	25% Environment	10% Assets Damage	25% Business Interuption	20% Reputation	Weighting
1	Personal Exposure	L	H	M	L	H	1
2	Overall Project Particular	L	H	M	H	H	3
3	Existing Field Infrastructure	L	H	L	L	M	1
4	Handled Object	L	H	H	M	L	2
5	Operation Aspect	M	H	H	M	L	3
6	Equipment Used	H	H	H	M	L	3
	Recommend Risk Category	L	H	H	M	L	13

No	**TOPSIDE** Assesment Parameter	30% Personal Safety	25% Environment	10% Assets Damage	25% Business Interuption	20% Reputation	Weighting
1	Personal Exposure	H	M	H	H	H	3
2	Overall Project Particular	H	M	H	M	H	3
3	Existing Field Infrastructure	L	L	H	M	L	1
4	Handled Object	H	M	M	M	L	2
5	Operation Aspect	H	M	M	H	L	3
6	Equipment Used	H	L	M	H	L	3
	Recommend Risk Category	H	M	M	H	L	15

Based on risk assessment analysis table (see Table 3.6.2), some facts that can be observed:

The topside compressors would cause more risks in personal safety than the subsea compressor system, since the compressors would have to be placed on the platform, which means that human injuries are always a possibility if something goes wrong. It will also involve manual labor to do maintenance work and small repairs, which can drive to low level of injuries until fatality of the crews.

The subsea compressor would cause more risks for the environment than the topside; Since the ROV of the subsea compressor will be planted on the subsea which is directly in contact with the sea/environment, so any malfunction of the system can be seriously affected the environment.

The topside compressor system would have a higher chance of causing business interruption than the subsea compressor system. This is because any error that could have led to personal injury would have to be investigated more thoroughly. Also the negative PR-impact of human injuries should not be underestimated, although this is also the case for environmental damage.

3.7. Sensitivity Analysis

Sensitivity analysis is a tool which helps to estimate which parameters can most significantly influence project value. A spider diagram and a tornado diagram were used to show how changing certain parameters affected the base case.

Fig. 3.7.1 shows the impact changing each parameter has on the NPV of the project. The percentage variation in NPV is displayed on the y-axis, while the percentage variation in different parameters is shown on the x-axis. Since the steeper line illustrates more sensitivity, this figure shows that the factor that has the highest influence on the NPV is the gas price followed by the Capex, Opex and oil price. Corresponding to the considerably less amount of oil production compared with gas, it makes sense that oil price shows extremely less sensitivity with NPV. Based on the assignment given by Statoil, we make comparison Capex +/-30 with Opex +/-30%, oil price +/-30%, gas price +/-5%, in order to make better assessment with other parameters.

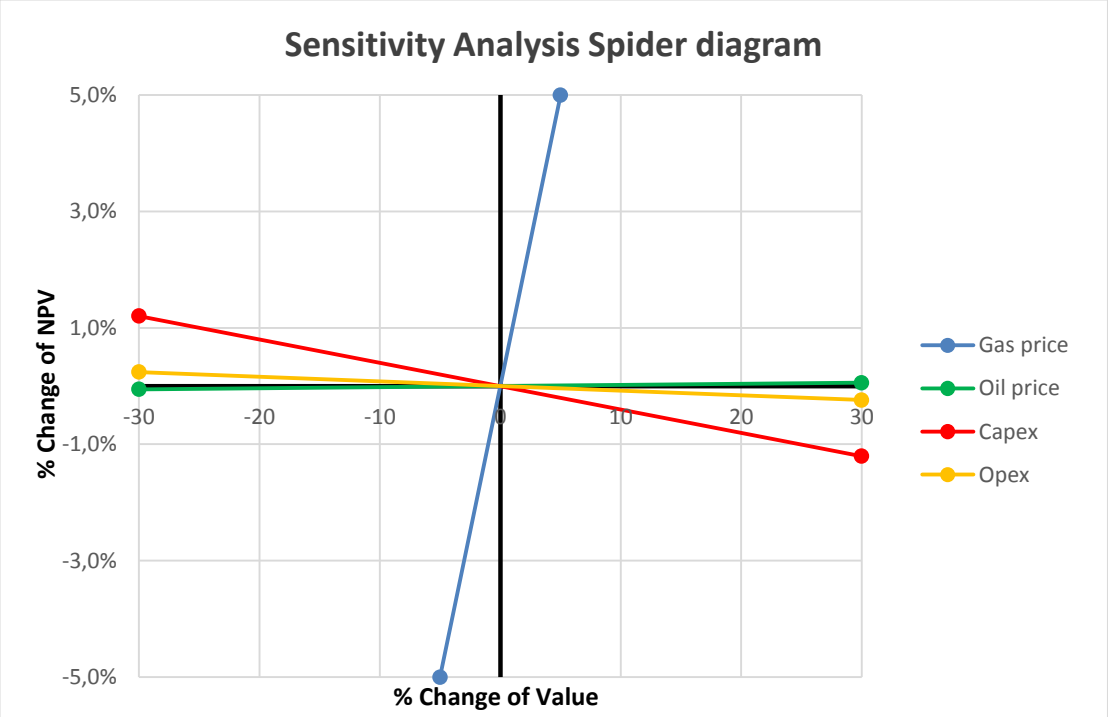

Figure 3.7.1 Sensitivity analysis shown on a Spider diagram

Fig. 3.7.2 show how each individual input affects the NPV. The different cases are ranked by their importance. This is useful for sorting those parameters of considerable influence from those whose effect on the project value is not significant. The benefit of this approach is that it can accommodate any shape of distribution for the input parameter, rather than single changes in the input. Based on our choice in assignment part B, we compare three different cases in our sensitivity analysis.

The first case shows the NPV effect of decreasing or increasing the CAPEX of the subsea compressor 30%. According to excel calculations, this brings about approximately -/+1.2% of cumulative NPV in the end of 2024, which proves to be a more important variable parameter than the others. In the second case we assume that the subsea compressor increases the downtime by 10 or 15%, which means the production time decreasing. By changing the amount of production days per year, the total daily flow show a slightly higher compared with the base case, as illustrated in the Table3.7.1. However, the total yearly flow decreased due to the more sensitivity, giving an NPV decrease of 0.46% and 0.61% by increasing the downtime by 10% and 15% respectively.

Original		DT 10%		DT 15%	
Year	Qf	Year	Qf	Year	Qf
2015.0	10.0E+6	2015.2	10.0E+6	2015	10.0E+6
2016.0	10.0E+6	2016.0	10.0E+6	2016	10.0E+6
2017.0	10.0E+6	2017.0	10.0E+6	2017	10.0E+6
2017.6	10.0E+6	2017.7	10.0E+6	2017.6	10.0E+6
2019.0	8.5E+6	2019.0	8.6E+6	2019	8.7E+6
2020.0	7.6E+6	2020.0	7.7E+6	2020	7.8E+6
2021.0	6.8E+6	2021.0	6.9E+6	2021	6.9E+6
2022.0	6.1E+6	2022.0	6.2E+6	2022	6.2E+6
2023.0	5.4E+6	2023.0	5.5E+6	2023	5.5E+6
2024.0	4.9E+6	2024.0	4.9E+6	2024	5.0E+6

Table3.7.1 Total daily flow after subsea compressor installation in three different cases

If we assume that the subsea compressor starts 1 year later, it brings about a significant decrease of the total flow Q_f to 9.1E+6 Sm^3/d in 2016 until the end of driven plateau 1.7 year later. Meanwhile the original case maintains a total flow of 10E+6 Sm^3/d during the 2.6 year period. The delayed installation impacts the NPV negatively, decreasing it by 0.46%, a loss of 320 million NOK. Then this tornado diagram shows the degree of sensitivity compared with these three different cases.

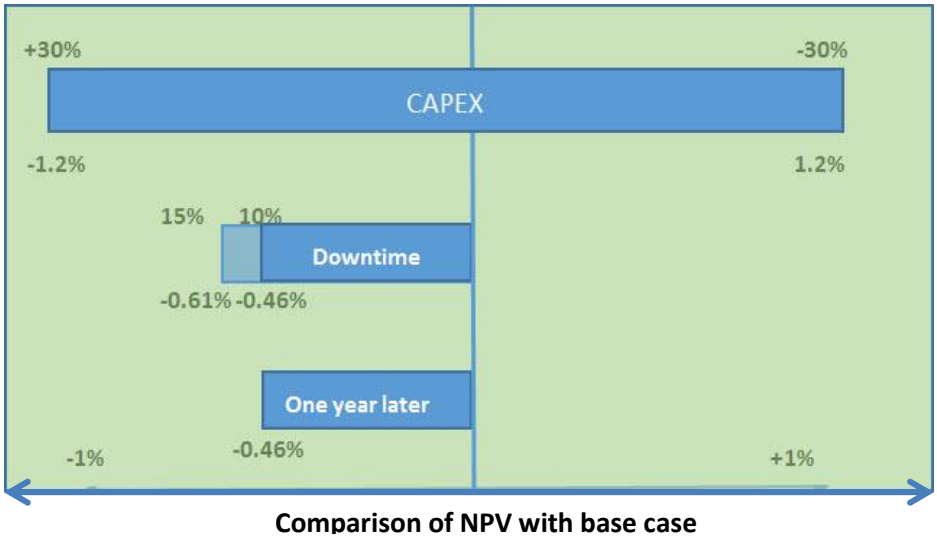

Figure 3.7.2Sensitivity analysis shown on a Tornado diagram

References

1. A. Hesjedal and P. Eltvik, (Statoil, 2006).
2. Statoil, in *EIT meeting* (Trondheim, 2013).
3. in *Aspen HYSYS* (aspentech, 2012).
4. R. G. Turner, M. G. Hubbard and A. E. Dunkler, Journal of Petroleum Technology (4), 1475-1480 (1969).
5. C. H. Whitson, M. R. Brulé and Society of Petroleum Engineers (U.S.), *Phase behavior*. (Henry L. Doherty Memorial Fund of AIME, Society of Petroleum Engineers, Richardson, Tex., 2000).
6. J. A. Trangenstein and J. B. Bell, Siam Journal on Applied Mathematics **49** (3), 749-783 (1989).
7. L. C. Young and R. E. Stephenson, Society of Petroleum Engineers Journal **23** (5), 727-742 (1983).
8. . (2000).
9. H. B. Bradley, F. W. Gipson and Society of Petroleum Engineers (U.S.), *Petroleum engineering handbook*. (Society of Petroleum Engineers, Richardson, TX, U.S.A., 1987).
10. L. P. Dake, *Fundamentals of reservoir engineering*. (Elsevier Scientific Pub. Co. ;

distributors for the U.S. and Canada Elsevier North-Holland, Amsterdam ; New York

New York, 1978).
11. B. Dotson, in *Seminar at the University of Oklahoma* (BP, Oklahoma, 2009).
12. J. F. Lea and H. V. Nickens, Journal of Petroleum Technology **56** (4), 30-+ (2004).
13. DNV, *Risk Management in Marine and Subsea Operation Hand Book*. (2003).
14. J. O. Hinze, A.I.Ch.E. J. **1**, 289-295 (1955).
15. C. University.
16. S. B. Coleman, H. B. Clay, D. G. Mccurdy and H. L. Norris, Journal of Petroleum Technology **43** (3), 329-333 (1991).
17. M. A. Nosseir, T. A. Darwish, M. H. Sayyouh and M. E. Sallaly, Journal of Petroleum Technology, 241-246 (2000).
18. M. Li, S. L. Li and L. T. Sun, SPE Production & Facilities, 42-46 (2002).

Appendix A. Formulas used for dry gas model

Mass Balance Equation

$$p_R = p_i \left(\frac{z_R}{z_i} \right) \left(1 - \frac{Gp}{G} \right) \tag{A.1}$$

Inflow Equation

$$q_{gsc} = C_R \left(p_R^2 - p_{wf}^2 \right)^n \tag{A.2}$$

Tubing Equation

$$q_{gsc} = C_T \left(\frac{p_{in}^2}{e^s} - p_{out}^2 \right)^{0.5} \tag{A.3}$$

Horizontal Pipeline and Flowline Equation

$$q_{sc} = C_{FL} (p_{in}^2 - p_{out}^2)^{0.5} \tag{A.4}$$

Z factor

$$\underline{Z\,factor:\ \ Z=f(P_R, T_R, \gamma_g)} \tag{A5}$$

Appendix B. Compressor Map

Compressor maps were made to test if the installed compression system actually can deliver the 32 bars that was assumed in the two previous sections.

For case 2, 2016-2024 are the years we are going to use subsea compression to maintain pressure. The compressor map is the graph of Power consumption which is P_{ow} versus inlet flow rate which is Q_{in}. By creating a compressor map for each year we can make sure that the compressor has ability to work with the assumed inlet and outlet pressure. Inlet and outlet pressures are taken from the dry gas basis excel sheet, shown in Appendix E.

The red point in each graph illustrates the operating point of the compressor system and should not exceed the compressors range. Each blue line indicates a certain rotational speed inside the compressor, given in rotations per minute.

For 2016 we can clearly observe that compressor does not require maximum power. From this year the power consumption increases until reaching a maximum point in 2017.7. Until late 2017 the production rate is fixed at 10.000.000Sm^3/D. The after decreasing the rate we can see that the compressor will be able work till the end of the plateau.

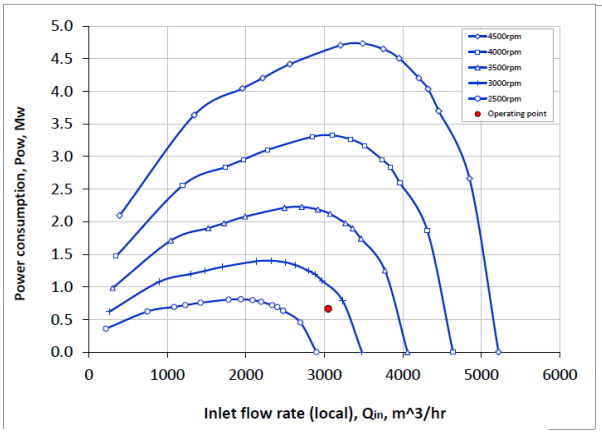

Figure B.1: Compressor map for year 2016

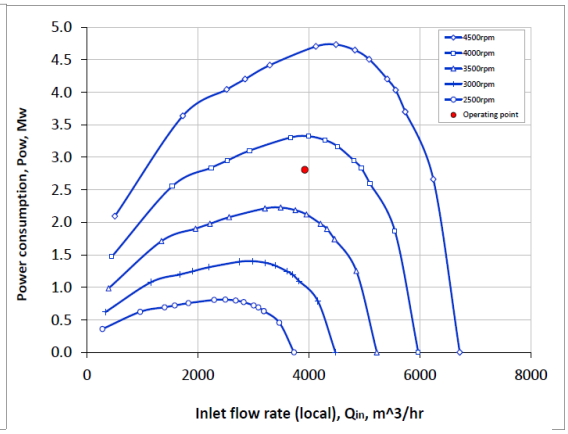

Figure B.2: Compressor map for year 2017

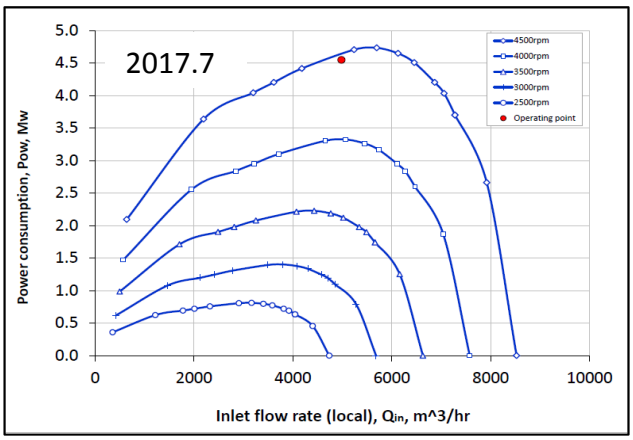

Figure B.4: Compressor map for year 2017.7

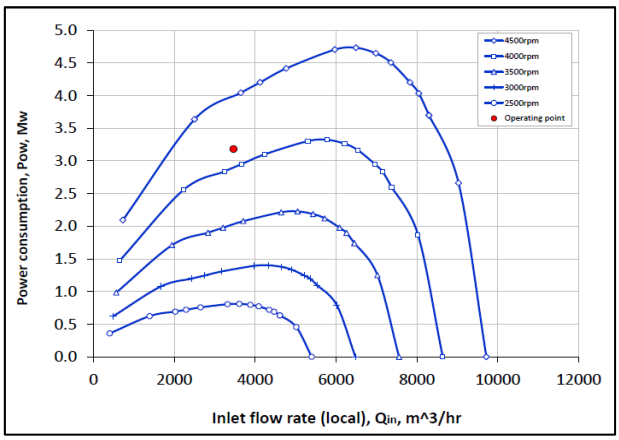

Figure B.5: Compressor map for year 2018

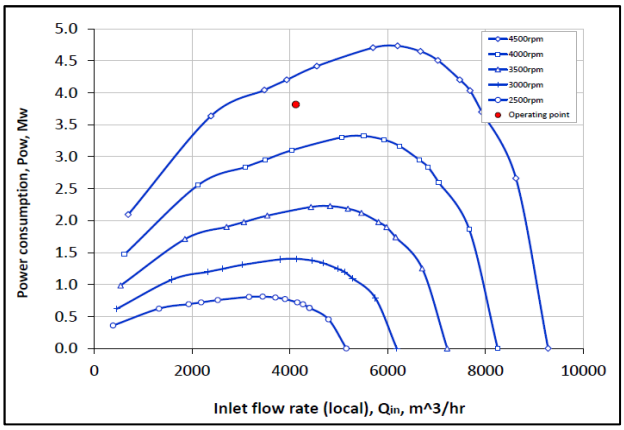

Figure B.6: Compressor map for year 2019

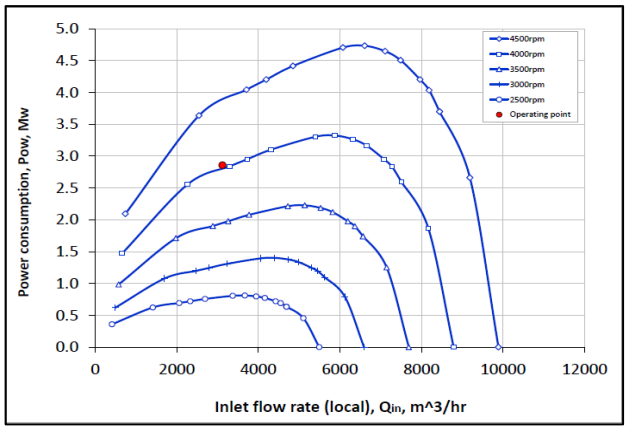

Figure B.7: Compressor map for year 2020

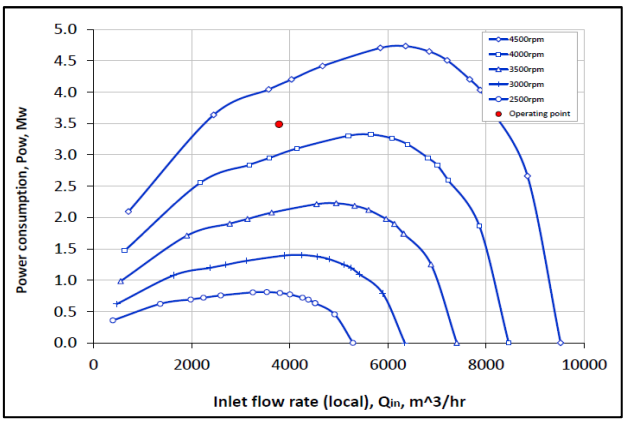

Figure B.8: Compressor map for year 2021

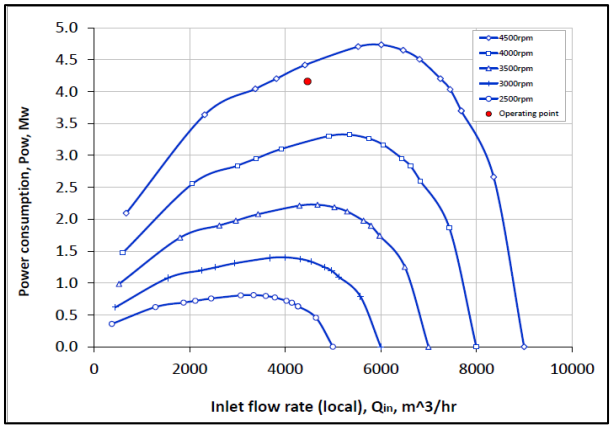

Figure B.9: Compressor map for year 2022

Appendix C. Modified Black Oil Parameters

The black oil parameters

While formulas were used to actually find most of the parameters shown in Table 3.2.1, some of the parameters were found directly from Hysys. Those that were taken directly from Hysys was: The viscosity of the oil at reservoir conditions, μ_o, and the gas, μ_g, as well as the densities at standard conditions of the oil from the oil phase, ρ_{oo}, the oil from the gas phase, ρ_{og}, the gas from the oil phase, ρ_{go}, and the gas from the gas phase, ρ_{gg}. The densities were used to find the surface gravities of the oil and gas phase, γ_o^* and γ_g^* using Eq. B.3.[5]

$$\gamma_{go} = \frac{\rho_{go}}{\rho_w} \qquad \gamma_{oo} = \frac{\rho_{oo}}{\rho_w} \qquad \gamma_{og} = \frac{\rho_{og}}{\rho_w} \qquad \gamma_{go} = \frac{\rho_{go}}{\rho_w} \tag{B.1}$$

$$\gamma_o^* = \frac{\gamma_{og}}{\gamma_{oo}} \qquad \gamma_g^* = \frac{\gamma_{go}}{\gamma_{gg}} \tag{B.2}$$

Inserting Eq. B.1 into Eq. B.2 the density of water falls out of the equations and we are left with Eq. B.3:

$$\gamma_o^* = \frac{\rho_{og}}{\rho_{oo}} \qquad \gamma_g^* = \frac{\rho_{go}}{\rho_{gg}} \tag{B.3}$$

In addition to the parameters already mentioned, several volumetric flows were used in calculations. The total flow of gas from gas, the flow of gas from oil, the flow oil from gas and the flow of oil from oil at standard conditions were all collected from Hysys. These four parameters, q_{gg}, q_{go}, q_{og} and q_{oo} respectively, were used in combination with the flows at reservoir conditions of oil, q_o and gas, q_g to find the remaining parameters in the BO-tables as shown in Eqs. B.4-B.7.[5]

$$B_o = \frac{q_o}{q_{oo}} \tag{B.4}$$

B_o is known as the oil formation volume factor, and describes how much surface oil is formed from the oil phase at reservoir conditions. It is always higher or equal to one, and tends to increase with reservoir pressure.[5]

$$R_s = \frac{q_{go}}{q_{oo}} \tag{B.5}$$

R_s is known as the solution gas/oil ratio and shows how much gas and how much oil is produced from that which is the oil phase at reservoir conditions. R_s increases with high pressures in the reservoir.

$$B_{gd} = \frac{q_g}{q_{gg}} \tag{B.6}$$

B_{gd} is known as the dry-gas formation volume factor. It describes how much a unit of gas at standard conditions take up at reservoir conditions.[10]

$$r_s = \frac{q_{og}}{q_{gg}} \tag{B.7}$$

Here r_s show how much gas and how much oil is produced from that which is the gas phase at reservoir conditions. Typically this value will be way smaller than 1, even at very high reservoir pressures.

Formulas and Steps that are used in IPT-MATBAL

All steps that followed during the calculations for Gulfaks reservoir by using the excel file IPT-MATBAL which was provided to us by the Ph.D. students.

"The basis of calculation is 1bbl reservoir bulk volume. The conservation-of-mass equations for single-cell material balance yields the following difference equations for reservoir-oil and –gas phases during the time step $\Delta t_k = t_k - t_{k-1}$ with a change in average pressure from $(\bar{P}_R)_{k-1}$ to $(\bar{P}_R)_k$.

In the calculation for Gulfaks condensate reservoir 1 year is taken as a time step. Then,

$$(A_0)_k - (A_0)_{k-1} + \Delta N_p = 0 \text{ and } (A_g)_k - (A_g)_{k-1} + \Delta G_p = 0 \tag{B.8),(B.9}$$

Where ΔN_p and ΔG_p = incremental quantities of total surface oil and total surface gas, respectively, produced during the timestep;

$$A_0 = \emptyset \left[\frac{S_0}{B_0} + \frac{5.615(1-S_w-S_o)r_s\gamma_o^*}{B_{gd}}\right] \tag{B.10}$$

$$A_g = \emptyset \left[\frac{S_0 R_s \gamma_g^*}{B_0} + \frac{5.615(1-S_w-S_o)}{B_{gd}}\right] \tag{B.11}$$

ΔN_p and A_0 are in STB/bbl, $\Delta G_p$and $A_g$are in scf/bbl, $\Delta G_p$and $A_g$are in scf/bbl, R_s is in scf/STB, r_s is in STB/scf, and B_{gd} is in ft^3/ scf. Other quantities used in the material-balance procedure are

$$E_0 = 1 + 5.615 r_s \gamma_o^* \frac{k_{rg}\mu_o B_o}{k_{ro}\mu_g B_{gd}} \tag{B.12}$$

$$E_g = R_s \gamma_g^* + 5.615 r_s \frac{k_{rg}\mu_o B_o}{k_{ro}\mu_g B_{gd}} \tag{B.13}$$

$$R_p = \frac{\Delta G_p}{\Delta N_p} \quad \text{(B.14)}$$

$$\frac{k_{rg}}{k_{ro}} = f(S_o) \quad \text{(B.15)}$$

Application of these relations for gas-condensate reservoirs is outlined step by step.

1. Specify $(\Delta G_p)_k$, total surface gas produced in scf/bbl of bulk volume.
2. Assume $(\bar{P}_R)_k$ and calculate PVT properties and porosity:
3. Calculate oil saturation $(S_o)_k$:

$$(S_o)_k = \frac{(A_g)_{k-1} + (\Delta G_p)_k - [\emptyset(1-S_w)/B_{gd}]}{\left[\emptyset\left(R_s\gamma^{\frac{*}{g}}/B_o - \frac{1}{B_{gd}}\right)\right]_k} \quad \text{(B16)}$$

4. Calculate $(k_{rg}/k_{ro})_k$ from$(S_o)_k$.
5. Calculate$(A_0)_k$, $(A_g)_k$, $(E_0)_k$ and $(E_g)_k$.
6. Calculate ΔN_{po}, incremental surface oil produced from reservoir oil, where $\Delta N_{po} = \Delta G_p/\bar{E}_g$ and

$$\bar{E}_g = 0.5\left[(E_g)_k + (E_g)_{k+1}\right] \quad \text{(B.17)}$$

7. Calculate ΔN_p, incremental total surface oil produced, where $\Delta N_{po} = \Delta N_p/\bar{E}_o$ and $\bar{E}_o =$

$$0.5[(E_o)_k + (E_o)_{k+1}] \quad \text{(B.18)}$$

8. Calculate the material balance error,

$$\varepsilon = (A_g)_k - (A_g)_{k-1} + \Delta G_p \quad \text{(B.19)}$$

9. If the error is not sufficiently small different pressure should be assumed."[8]

Figures C1,C2 and C3 is the snapshots from the calculation is done in IPT-MATBAL which is made in Microsoft Excel, it is divided into three parts to make it readable. It is only for Template L and the method of calculation for Template M is the same.

First of all, given data and formulas above inserted to the excel sheet and calculated. To fix the material balance error Solver Add-in is used. Then, all graphs which is mentioned in 3.2 Modified Black Oil Model is plotted from this excel sheet.

Snapshots from the IPT-MATBAL

Effective production days/year		328	
Initial pressure	p_i	240	[bar]
Reservoir temperature	Tr	128	[°C]
Initial water saturation	S_{wi}	0.05	fraction
Initial gas in place	G	54.2E+9	[Sm^3]
Reservoir Bulk Volume	Vb	1.8E+9	[m^3]
Porosity	ϕ	0.17	
Data for relative permeability model			
Corey exponent for oil	no	5.02	
Residual oil saturation	Sro	0.00	
Maximum oil saturation	Smo	0.95	
Relative permeability at Smo	Kromax	1.00	
Corey exponent for gas ng	ng	1.56	
Maximum gas saturation	Smg	0.95	
Gas relative permeability for Smg	Krgmax	0.90	
Critical gas saturation	Sgc	0.00	

Table C1: Given data

DRY GAS MB SOLUTION

time	p_R	r_s	qf	qcond
[years]	[bara]	[Sm^3/Sm^3]	[Sm3/D]	[Sm^3/d]
0	240.00		6.00E+06	
1	231.29	8.88E-05	6.00E+06	533
2	221.59	8.04E-05	6.00E+06	483
3	211.98	7.22E-05	6.00E+06	433
4	202.54	6.48E-05	6.00E+06	389
5	191.01	5.73E-05	7.60E+06	436
6	179.54	4.99E-05	7.60E+06	379
7	168.15	4.33E-05	7.70E+06	334
8	156.56	3.76E-05	7.98E+06	300
9	145.40	3.26E-05	7.78E+06	254
9.6195821	138.98	2.92E-05	7.33E+06	214
11	126.09	2.60E-05	6.61E+06	172
12	117.86	2.30E-05	5.94E+06	137
13	110.45	2.11E-05	5.35E+06	113
14	103.78	1.97E-05	4.82E+06	95
15	97.77	1.85E-05	4.35E+06	80
16	92.34	1.76E-05	3.93E+06	69

Table C.2: Calculation for the condensate

East TankL-Template Fault Block 13 Brent Formation

Solve automatically:*

From year 1

To year 16

SOLVE!

*NOTE: for the automatic solver to work, the current cell positions (rows starting point and column position) must not change

time	qf	ΔGp	Gp	RF	ΔGp''	p_R	B_o	B_g	R_s	r_s	μ_o	μ_g	γ_o^*	γ_g^*	So	Sg	ϕ	A_o	A_g	E_o	E_g	krg	kro	ΔN_{po}	ΔN_p	ε− error	qcond	qcond	OGR
[years]	[Sm3/D]	[Sm3]	[Sm3]	[-]	[Sm^3/m^3]	[bara]	[m^3/Sm^3]	[m^3/Sm^3]	[Sm^3/Sm^3]	[Sm^3/Sm^3]	[cp]	[cp]	[-]	[-]	[-]	[-]	[-]	[Sm^3/m^3]	[Sm^3/m^3]	[-]	[Sm^3/Sm^3]	[-]	[-]	[Sm^3/m^3]	[Sm^3/m^3]	[-]	[Sm^3/d]	[STB/d]	[STB/MMscf]
0	6.00E+06		0	0.00		240.00	1.63	5.42E-03	170	9.27E-05	0.22	0.023	0.989	1.081	0	0.950	0.17	2.74E-03	2.98E+01	2.61E+31	2.84E+35	9.04E-01	0.00E+00						
1	6.00E+06	1.97E+09	1.97E+09	0.04	1.083	230.89	1.61	5.61E-03	161	8.45E-05	0.2275	0.023	0.989	1.085	0.002	0.948	0.17	2.64E-03	2.87E+01	3.28E+12	3.92E+16	9.01E-01	6.55E-14	7.62E-36	9.93E-05	1.10E-23	5.50E+02	3.46E+03	16.340
2	6.00E+06	1.97E+09	3.94E+09	0.07	1.083	221.08	1.58	5.83E-03	151	7.56E-05	0.2357	0.022	0.989	1.088	0.004	0.946	0.17	2.55E-03	2.77E+01	9.13E+10	1.22E+15	8.98E-01	2.11E-12	5.35E-17	9.02E-05	5.40E-25	5.00E+02	3.14E+03	14.836
3	6.00E+06	1.97E+09	5.9E+09	0.11	1.083	212.23	1.55	6.06E-03	142	6.86E-05	0.2432	0.022	0.989	1.091	0.006	0.944	0.17	2.47E-03	2.66E+01	1.77E+10	2.60E+14	8.95E-01	9.85E-12	1.46E-15	7.96E-05	8.74E-23	4.41E+02	2.78E+03	13.100
4	6.00E+06	1.97E+09	7.87E+09	0.15	1.083	202.86	1.52	6.32E-03	133	6.14E-05	0.2513	0.021	0.990	1.095	0.008	0.942	0.17	2.39E-03	2.55E+01	5.08E+09	8.37E+13	8.93E-01	3.05E-11	6.29E-15	7.16E-05	3.19E-23	3.97E+02	2.50E+03	11.783
5	7.60E+06	2.49E+09	1.04E+10	0.19	1.371	191.82	1.49	6.67E-03	123	5.40E-05	0.2611	0.021	0.990	1.100	0.009	0.941	0.17	2.31E-03	2.41E+01	1.87E+09	3.51E+13	8.91E-01	7.19E-11	2.31E-14	8.04E-05	2.50E-23	4.45E+02	2.80E+03	10.438
6	7.60E+06	2.49E+09	1.29E+10	0.24	1.371	180.09	1.46	7.07E-03	113	4.65E-05	0.2716	0.020	0.990	1.105	0.010	0.940	0.17	2.24E-03	2.27E+01	8.24E+08	1.79E+13	8.89E-01	1.39E-10	5.18E-14	6.99E-05	2.47E-23	3.87E+02	2.44E+03	9.074
7	7.70E+06	2.53E+09	1.54E+10	0.28	1.390	169.57	1.44	7.53E-03	104	4.11E-05	0.2815	0.020	0.990	1.109	0.011	0.939	0.17	2.18E-03	2.14E+01	4.92E+08	1.21E+13	8.88E-01	2.02E-10	9.27E-14	6.10E-05	2.26E-23	3.38E+02	2.13E+03	7.819
8	7.98E+06	2.62E+09	1.8E+10	0.33	1.440	157.82	1.41	8.07E-03	95	3.53E-05	0.2926	0.019	0.990	1.115	0.012	0.938	0.17	2.13E-03	1.99E+01	3.00E+08	8.56E+12	8.87E-01	2.77E-10	1.40E-13	5.52E-05	2.52E-25	3.06E+02	1.92E+03	6.828
9	7.78E+06	2.55E+09	2.06E+10	0.38	1.405	147.16	1.38	8.68E-03	87	3.11E-05	0.3032	0.019	0.990	1.120	0.012	0.938	0.17	2.08E-03	1.85E+01	2.13E+08	6.93E+12	8.86E-01	3.31E-10	1.81E-13	4.65E-05	4.95E-24	2.58E+02	1.62E+03	5.897
9.61958	7.33E+06	1.49E+09	2.2E+10	0.41	0.820	140.16	1.36	9.08E-03	81	2.83E-05	0.3102	0.018	0.990	1.124	0.013	0.937	0.17	2.06E-03	1.77E+01	1.73E+08	6.16E+12	8.86E-01	3.66E-10	1.25E-13	2.42E-05	1.82E-22	2.16E+02	1.36E+03	5.252
11	6.6E+6	3E+09	2.5E+10	0.46	1.648	128.17	1.34	1.00E-02	73	2.48E-05	0.323	0.018	0.989	1.130	0.013	0.937	0.17	2.01E-03	1.60E+01	1.31E+08	5.37E+12	8.85E-01	3.98E-10	2.86E-13	4.35E-05	2.07E-22	1.74E+02	1.10E+03	4.698
12	5.9E+6	1.95E+09	2.7E+10	0.50	1.072	119.29	1.32	1.07E-02	66	2.22E-05	0.3325	0.018	0.989	1.135	0.013	0.937	0.17	1.99E-03	1.50E+01	1.09E+08	4.95E+12	8.85E-01	4.15E-10	2.08E-13	2.49E-05	2.15E-22	1.38E+02	8.69E+02	4.143
13	5.3E+6	1.75E+09	2.87E+10	0.53	0.965	112.63	1.30	1.15E-02	62	2.08E-05	0.3403	0.017	0.988	1.138	0.013	0.937	0.17	1.97E-03	1.40E+01	9.72E+07	4.73E+12	8.85E-01	4.17E-10	1.99E-13	2.05E-05	5.47E-23	1.14E+02	7.15E+02	3.788
14	4.8E+6	1.58E+09	3.03E+10	0.56	0.870	105.80	1.29	1.22E-02	57	1.94E-05	0.3483	0.017	0.987	1.142	0.013	0.937	0.17	1.95E-03	1.31E+01	8.71E+07	4.55E+12	8.85E-01	4.17E-10	1.88E-13	1.73E-05	5.52E-22	9.58E+01	6.03E+02	3.539
15	4.4E+6	1.43E+09	3.18E+10	0.59	0.785	99.22	1.27	1.30E-02	53	1.81E-05	0.3561	0.017	0.986	1.145	0.013	0.937	0.17	1.94E-03	1.24E+01	7.88E+07	4.41E+12	8.85E-01	4.15E-10	1.75E-13	1.45E-05	1.85E-22	8.06E+01	5.07E+02	3.298
16	3.9E+6	1.29E+09	3.3E+10	0.61	0.710	94.52	1.26	1.38E-02	50	1.75E-05	0.3623	0.017	0.985	1.147	0.013	0.937	0.17	1.92E-03	1.16E+01	7.42E+07	4.30E+12	8.85E-01	4.08E-10	1.63E-13	1.25E-05	2.45E-22	6.91E+01	4.34E+02	3.127

Table C.3: All parameters and the button for the solver.

Appendix D. Liquid Accumulation

As mentioned in section 3.4, liquid loading can be described using two different models, the droplet model and the film model. Both of these models were discussed in R. G. Turner's master thesis, where he found that the droplet model yielded superior results. The film model assumes that the liquid phase will form a film on the well interface, while the droplet model assumes that liquid will be present as droplets in the continuous gas phase. Liquid accumulation occurs when the liquid is no longer transported out of the well along with the gas. This will often lead to backpressure and decreased production from the well. I some cases however, the liquid might flow from the bottom of the well to a part of the reservoir with lower pressure, making liquid accumulation a nonissue. For this case however we do not know enough about the reservoir to assume this and as such has to investigate whether liquid accumulation would occur at all. Both the film and droplet models were originally investigated by Turner, which found that the droplet model correlated better with his experimental data. It also has the advantage of explaining why the amount of liquid present in the gas stream seems to have little effect on the liquid loading. To the best of our knowledge no improvements have been made on the film model since, while several new variations of the droplet model have been proposed. Therefore, four different variations of the droplet model have been selected for our calculations. These are Li's equation, Nosseir's equation, Coleman's equation and Turner's modified equation.

The Droplet Models

The first droplet model as described by Turner is based on a force balance on a droplet in a vertical well. The droplet is affected by two forces, the drag force from the surrounding gas pushing it up and the gravitational force pushing it down. This is shown in Fig. C.1.

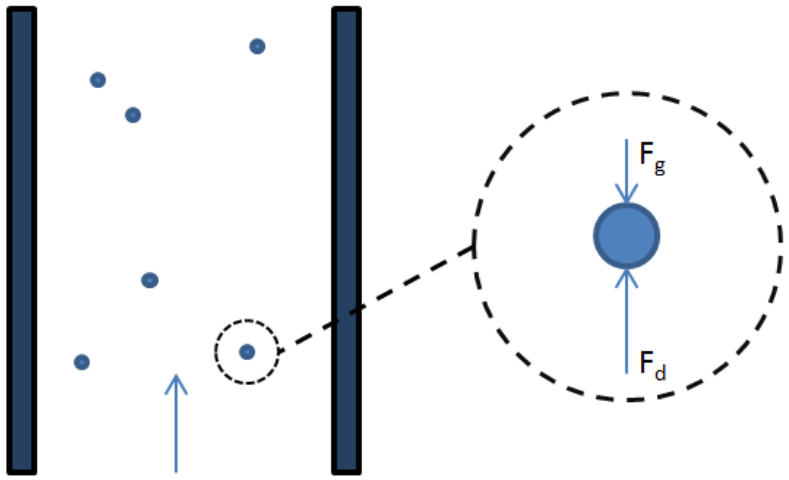

Figure C.1: Force balance on a liquid droplet in a vertical well filled with a continuous gas phase.

The flow out of the reservoir decreases with the pressure in the reservoir. As the velocity of the surrounding gas phase decreases so does the drag force, ultimately making the gravitational force dominant. The gas velocity that makes the gravitational force, F_g, and the drag force, F_d, equally large is defined as the critical velocity, v_c. If the actual gas velocity falls below this value, the liquid droplets will not exit the well along with the gas but instead accumulate in the well.

Finding Turners equation

Turners equation finds the critical velocity by using $F_g = F_d$, and Eqs. C.1-2.

$$F_g = mg \tag{C.1}$$

$$F_d = \frac{1}{2}\rho_G v^2 C_d A \tag{C.2}$$

Where m is the mass of the liquid droplet, g is the gravitational acceleration, ρ_G is the density of the gas phase, C_d is the drag force and A is the drag area. Putting the velocity at one side of the equation give Eq. C.3:

$$v_c = \left(\frac{2mg}{\rho_G C_d A} \right)^{0.5} \tag{C.3}$$

After this we replace the mass of the droplet by the relative density times the volume as seen in Eq. C.4, and express the volume and the drag area as functions of the diameter. The drag area, A, is assumed equal to the cross sectional area of the droplet, by also inserting earth's gravitational acceleration equal to 9.81 this gave Eq. C.5:

$$m = \rho_r V = \left(\rho_L - \rho_G\right)\frac{3}{4}\cdot\frac{d}{8}^3 \tag{C.4}$$

$$v_c = \left(7.358\frac{\left(\rho_L - \rho_G\right)d}{\rho_G C_d} \right)^{0.5} \tag{C.5}$$

The maximum diameter of the liquid droplet in the gas phase depends on the interfacial tension of the gas and the surface tension between the two phases. Hinze[14] found that these can be related through the Weber number. The Weber number is defined in Eq. C.6:

$$N_{We} = \frac{\rho_G v^2 d}{\sigma} = 30 \tag{C.6}$$

Solving Eq. C.6 with respect to diameter and inserting this equation into C.5 gives Eq. C.7:

$$v_c = 3.854\left(\frac{\sigma\left(\rho_L - \rho_G\right)}{{\rho_G}^2 C_d} \right)^{0.25} \tag{C.7}$$

The drag coefficient is found by assuming critical flow, that is a Reynolds number, Re, between 1000 and 200 000, and interpolate using Fig C.2.

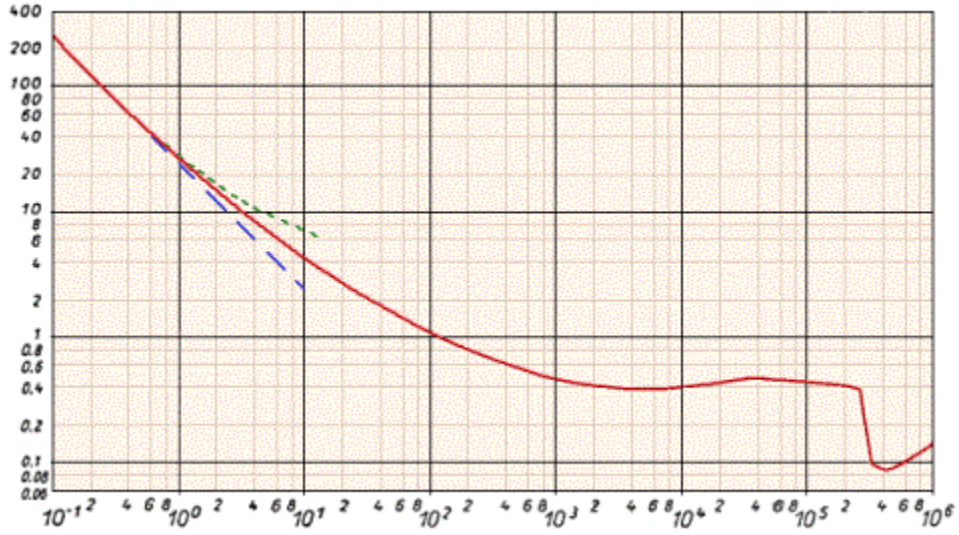

Figure C.2: Drag coefficient as a function of Reynolds number.[15]

From this Turner assumed the drag coefficient to always be equal to 0.44 which, after changing the surface tensions units from kg/m3 to dyne/cm3 gives the Eq. C.8.

$$v_c = 1.59\left(\frac{\sigma(\rho_L - \rho_G)}{\rho_G^{\,2}}\right)^{0.25} \tag{C.8}$$

This is known as Turner's unadjusted equation, or the Coleman equation. In order to make his formula fit his experimental data better Turner increased the constant on the outside by 20%. This change is shown in Eq. C.9 and is known as the adjusted Turner equation or just the Turner equation for short.

$$v_c = 1.92\left(\frac{\sigma(\rho_L - \rho_G)}{\rho_G^{\,2}}\right)^{0.25} \tag{C.9}$$

Other Droplet Models

The Coleman equation, shown in Eq. C.8, was reintroduced by Coleman et al. in 1991 after he found that the unadjusted formula correlated better with his experimental data.[16]

Nosseir et al. proposed that this was because Coleman's dataset all had critical flow,[17] making the assumption that the drag coefficient was 0.44 reasonable. Meanwhile, Turner's dataset included several data with Reynolds numbers higher than 200 000. Nosseir divided Turner's dataset into two different groups, one for those with turbulent flow, and another for those with Reynolds number above 200 000.

This flow he defined as super turbulent flow, for which he assumed a drag coefficient of 0.2 by interpolating using a drag coefficient chart such as C.2. This splitting of datasets increased the accuracy of the predictions for both groups and explained why Coleman and Turner had gotten different results previously. Nosseir's equation for super critical flow is shown in Eq. C.10.

$$v_c = 1.938\left(\frac{\sigma(\rho_L - \rho_G)}{\rho_G^{\,2}}\right)^{0.25} \tag{C.10}$$

Li et al proposed that the Turner equation had underestimated the surface area of the droplet, as the actual droplets would not be perfect spheres.[18] Li based this on the assumption that the two opposing forces on each side of the droplet would force it to flatten. Using a different drag area for the droplet Li found that the accuracy for their dataset was better than that provided by the Turner equation. Li's equation is shown in Eq. C.11.

$$v_c = 0.724\left(\frac{\sigma(\rho_L - \rho_G)}{\rho_G^{\,2}}\right)^{0.25} \tag{C.11}$$

Using the Droplet Models

Eqs. C.8-11 shows different expressions for the critical velocity. To get the actual velocity we have to relate the velocity at a point in the pipe to the standard volumetric flow out of the reservoir, which is what we know. This was done by Eq. C.12.[4] In the excel sheet called "Liquid Accumulation" and in section 3.4.1 we chose to use this formula to calculate a critical volumetric flow rate, Q_c, to compare with the known flow rate in the well, Q_w. Both of the volumetric flow rates are at standard conditions.

$$Q = \frac{3.06\,pvA}{TZ} \tag{C.12}$$

Where Q is the volumetric flow rate in $MMsft^3/D$, T is the temperature in Rankine, p is the pressure in psia, v is the velocity in ft/s, A is the cross-sectional area of the pipe in ft^2 and Z is the compressibility factor.

To actually find the different critical velocities we need to find three parameters, density of the gas phase, density of the liquid phase and the surface tension. The densities where found by inserting the well head pressures for each year of production and the respective reservoir temperature into Hysys. This gave densities for each year of production. The surface tensions for oil and water were estimated using the empirical formulas shown in Eqs. C.13-14.

$$\sigma_{OG} = 1.79 \times 10^{-6}(\rho_O - \rho_G) \tag{C.13}$$

$$\sigma_{WG} = 15 + 0.91(\rho_W - \rho_G) \tag{C.14}$$

Where σ_{OG} and σ_{WG} is the surface tension in dyne/cm^2 for oil and gas, and water and gas, respectively. ρ_O, ρ_W and ρ_G is the density of the oil, water and gas phase in lb/ft^3.

To find out if Nosseir's equation for supercritical flow was applicable we had to calculate the Reynolds number. This was done using Eq. C.15.

$$\mathrm{Re} = \frac{vL}{\nu} = \frac{\rho v L}{\mu} \tag{C.15}$$

Where the kinematic viscosity, v, was found from Hysys and L was assumed equal to the diameter of the pipe. The diameter of the pipe at the wellhead was assumed equal to 7 inches based on data provided by Statoil.

The excel sheet for Low pressure modification assuming the same flow out of each well is shown in Table C.1.

Table C.1: Liquid accumulation excel sheet.

East tank, temblate L, 4 wells

East tank, different units

year count	Calendar ye	qf	Gp	GP/G	PR	Z	qw	pwf	pwh	qw	qwh	pwh	Z	visc.	ρ_o	ρ_w	ρ_g	σ_wg	σ_og	vc_w	vc_o	qo_w	qo_o	Nre
		Sm3/d					Sm3/d	bara	bara	MMscfd	MMcfd	psia		ft^2/s	lbm/ft3	lbm/ft3	lbm/ft3	dyne/cm	dyne/cm	ft/s	ft/s	MMscfd	MMscfd	
0	2008	6,00E+06	0,00E+00	0,00	240,00	0,96	1,50E+06	219,69	173,17	52,97	0,40	2511,63	0,95	1,83E-06	38,89	58,19	7,24	61,37	4,12	4,42	2,00	13,26	5,99	1,41E+06
1	2009	6,00E+06	1,97E+09	0,04	231,29	0,95	1,50E+06	210,14	165,24	52,97	0,42	2396,63	0,94	1,89E-06	39,20	58,17	6,89	61,67	4,49	4,54	2,10	13,06	6,05	1,40E+06
2	2010	6,00E+06	3,94E+09	0,07	221,59	0,95	1,50E+06	199,42	156,32	52,97	0,44	2267,30	0,94	1,96E-06	39,55	58,14	6,49	62,00	4,95	4,69	2,23	12,81	6,09	1,40E+06
3	2011	6,00E+06	5,90E+09	0,11	211,98	0,94	1,50E+06	188,68	147,35	52,97	0,47	2137,15	0,94	2,05E-06	39,90	58,11	6,10	62,33	5,44	4,86	2,37	12,54	6,12	1,38E+06
4	2012	6,00E+06	7,87E+09	0,15	202,54	0,94	1,50E+06	178,01	138,41	52,97	0,50	2007,51	0,94	2,15E-06	40,25	58,08	5,71	62,67	5,96	5,04	2,52	12,24	6,13	1,37E+06
5	2013	7,60E+06	1,04E+10	0,19	191,01	0,94	1,90E+06	154,73	114,72	67,10	0,76	1663,90	0,93	2,50E-06	41,16	58,01	4,67	63,54	7,53	5,61	2,99	11,33	6,04	1,31E+06
6	2014	7,60E+06	1,29E+10	0,24	179,54	0,94	1,90E+06	140,33	101,91	67,10	0,85	1478,06	0,93	2,76E-06	41,65	57,97	4,12	64,00	8,48	6,00	3,31	10,76	5,93	1,71E+06
7	2015	7,70E+06	1,54E+10	0,28	168,15	0,93	1,93E+06	124,60	87,16	67,98	1,01	1264,18	0,94	3,17E-06	42,21	57,92	3,49	64,53	9,68	6,55	3,74	10,02	5,73	1,86E+06
8	2016	7,98E+06	1,80E+10	0,33	156,56	0,93	2,00E+06	105,71	67,58	70,46	1,36	980,15	0,94	4,01E-06	42,95	57,86	2,67	65,22	11,44	7,53	4,51	8,89	5,32	2,14E+06
9	2017	7,78E+06	2,06E+10	0,38	145,40	0,93	1,95E+06	90,65	52,61	68,72	1,72	763,05	0,95	5,09E-06	43,52	57,81	2,06	65,73	12,93	8,62	5,33	7,88	4,87	2,45E+06
9,6	2017,6	7,68E+06	2,21E+10	0,41	138,67	0,93	1,92E+06	80,76	41,59	67,79	2,15	603,28	0,95	6,38E-06	43,95	57,77	1,62	66,10	14,12	9,76	6,18	7,02	4,45	2,77E+06
11	2019	6,62E+06	2,51E+10	0,46	125,77	0,94	1,66E+06	72,47	39,33	58,49	1,97	570,44	0,95	6,74E-06	44,03	57,76	1,53	66,18	14,37	10,05	6,40	6,81	4,34	2,86E+06
12	2020	6,36E+06	2,72E+10	0,50	116,94	0,94	1,59E+06	60,23	25,13	56,18	2,98	364,47	0,96	1,05E-05	44,60	57,72	0,97	66,64	16,06	12,68	8,32	5,46	3,58	3,60E+06
13	2021	5,76E+06	2,91E+10	0,54	108,96	0,94	1,44E+06	54,82	23,24	50,84	2,93	337,04	0,96	1,13E-05	44,68	57,71	0,89	66,70	16,30	13,20	8,70	5,24	3,45	3,75E+06
14	2022	5,22E+06	3,08E+10	0,57	101,75	0,94	1,30E+06	50,18	21,83	46,05	2,83	316,68	0,97	1,20E-05	44,74	57,70	0,84	66,75	16,48	13,63	9,00	5,06	3,35	3,87E+06
15	2023	4,75E+06	3,24E+10	0,60	95,20	0,94	1,19E+06	45,81	20,09	41,90	2,80	291,44	0,97	1,30E-05	44,81	57,70	0,77	66,80	16,71	14,22	9,43	4,85	3,22	4,04E+06
16	2024	4,32E+06	3,38E+10	0,62	89,23	0,95	1,08E+06	42,11	18,91	38,13	2,72	274,31	0,97	1,38E-05	44,86	57,70	0,73	66,84	16,86	14,66	9,75	4,70	3,12	4,17E+06
17	2025	3,93E+06	3,51E+10	0,65	83,79	0,95	9,84E+05	38,87	17,95	34,74	2,61	260,34	0,97	1,46E-05	44,91	57,69	0,69	66,87	16,99	15,06	10,03	4,57	3,04	4,28E+06
18	2026	3,59E+06	3,62E+10	0,67	78,81	0,95	8,98E+05	35,94	17,01	31,73	2,52	246,73	0,97	1,54E-05	44,95	57,69	0,65	66,90	17,11	15,47	10,33	4,44	2,96	4,40E+06
19	2027	3,29E+06	3,73E+10	0,69	74,24	0,95	8,21E+05	33,40	16,29	29,00	2,41	236,24	0,98	1,60E-05	44,98	57,69	0,62	66,93	17,21	15,82	10,58	4,34	2,90	4,50E+06
20	2028	3,01E+06	3,83E+10	0,71	70,05	0,95	7,53E+05	31,07	15,55	26,58	2,32	225,52	0,98	1,68E-05	45,01	57,68	0,60	66,95	17,31	16,19	10,85	4,23	2,83	5,63E+05
21	2029	2,75E+06	3,92E+10	0,72	66,22	0,96	6,87E+05	29,50	15,64	24,25	2,11	226,82	0,98	1,67E-05	45,01	57,68	0,60	66,95	17,30	16,15	10,81	4,24	2,84	5,64E+05
22	2030	2,52E+06	4,00E+10	0,74	62,69	0,96	6,31E+05	27,68	15,06	22,29	2,01	218,42	0,98	1,73E-05	45,03	57,68	0,58	66,97	17,38	16,46	11,03	4,16	2,79	5,54E+05
23	2031	2,32E+06	4,08E+10	0,75	59,44	0,96	5,79E+05	26,30	14,89	20,45	1,87	215,90	0,98	1,75E-05	45,04	57,68	0,57	66,97	17,40	16,56	11,10	4,13	2,77	5,51E+05
24	2032	2,13E+06	4,15E+10	0,77	56,44	0,96	5,33E+05	25,00	14,60	18,82	1,76	211,75	0,98	1,79E-05	45,05	57,68	0,56	66,98	17,44	16,72	11,22	4,09	2,74	5,46E+05
25	2033	1,96E+06	4,21E+10	0,78	53,68	0,96	4,89E+05	24,09	14,66	17,28	1,61	212,57	0,98	1,78E-05	45,05	57,68	0,56	66,98	17,43	16,69	11,20	4,09	2,74	5,47E+05
26	2034	1,81E+06	4,27E+10	0,79	51,12	0,96	4,52E+05	22,98	14,30	15,97	1,53	207,36	0,98	1,82E-05	45,06	57,68	0,55	66,99	17,48	16,90	11,35	4,04	2,71	4,80E+06
27	2035	1,69E+06	4,33E+10	0,80	48,72	0,97	4,23E+05	21,32	13,19	14,94	1,55	191,27	0,98	1,98E-05	45,11	57,68	0,51	67,03	17,64	17,60	11,85	3,87	2,61	5,00E+06

West tank, template M, 3 wells

West tank, different units

year count	Calendar ye	qf	Gp	GP/G	PR	Z	qw	pwf	pwh	qw	qwh	pwh	Z	visc.	ρ_o	ρ_w	ρ_g	σ_wg	σ_og	vc_w	vc_o	qo_w	qo_o	Nre
		Sm3/d					Sm3/d	bara	bara	MMscfd		psia		ft^2/s	lbm/ft3	lbm/ft3	lbm/ft3	dyne/cm	dyne/cm	ft/s	ft/s	MMscfd	MMscfd	
0	2008	4,00E+06	0,00E+00	0,00	210,00	0,93	1,33E+06	177,53	145,98	47,09	0,42	2117,28	0,94	1,94E-06	40,46	58,94	6,34	62,87	5,66	4,79	2,36	12,28	6,04	1,36E+06
1	2009	4,00E+06	1,32E+09	0,08	194,16	0,92	1,33E+06	158,48	129,49	47,09	0,47	1878,14	0,93	2,12E-06	41,08	58,89	5,57	63,52	6,70	5,14	2,65	11,70	6,03	1,46E+06
2	2010	4,00E+06	2,64E+09	0,15	177,38	0,92	1,33E+06	137,41	111,11	47,09	0,55	1611,54	0,93	2,40E-06	41,78	58,84	4,73	64,24	8,02	5,61	3,04	10,97	5,93	1,60E+06
3	2011	4,00E+06	3,96E+09	0,23	161,04	0,92	1,33E+06	115,55	91,78	47,09	0,67	1331,14	0,94	2,83E-06	42,51	58,78	3,86	64,98	9,60	6,26	3,55	10,06	5,71	1,78E+06
4	2012	4,00E+06	5,28E+09	0,30	145,14	0,92	1,33E+06	92,10	70,49	47,09	0,88	1022,36	0,94	3,60E-06	43,32	58,72	2,91	65,78	11,59	7,25	4,33	8,89	5,31	2,06E+06
5	2013	2,40E+06	6,07E+09	0,35	135,83	0,92	8,00E+05	108,65	89,42	28,25	0,41	1297,00	0,94	2,90E-06	42,59	58,77	3,75	65,07	9,81	6,35	3,63	9,93	5,67	1,81E+06
6	2014	2,40E+06	6,86E+09	0,39	126,58	0,92	8,00E+05	96,84	79,22	28,25	0,47	1149,02	0,94	3,23E-06	42,98	58,74	3,30	65,46	10,74	6,80	3,98	9,38	5,49	1,93E+06
7	2015	2,30E+06	7,62E+09	0,44	117,79	0,92	7,67E+05	87,03	70,90	27,07	0,50	1028,27	0,95	3,58E-06	43,30	58,72	2,93	65,77	11,55	7,23	4,32	8,89	5,31	2,05E+06
8	2016	2,02E+06	8,29E+09	0,47	110,12	0,93	6,73E+05	82,29	67,35	23,77	0,47	976,90	0,95	3,75E-06	43,44	58,71	2,78	65,90	11,90	7,44	4,48	8,67	5,22	2,11E+06
9	2017	2,22E+06	9,02E+09	0,52	101,65	0,93	7,39E+05	65,69	52,34	26,09	0,66	759,15	0,96	4,77E-06	44,02	58,66	2,13	66,44	13,51	8,53	5,31	7,66	4,77	2,42E+06
9,6	2017,6	2,32E+06	9,50E+09	0,54	96,29	0,93	7,74E+05	53,84	41,27	27,33	0,89	598,52	0,96	6,00E-06	44,47	58,63	1,67	66,84	14,80	9,68	6,18	6,81	4,35	2,75E+06
11	2019	1,89E+06	1,04E+10	0,59	86,14	0,94	6,30E+05	49,87	39,11	22,26	0,76	567,30	0,97	6,32E-06	44,55	58,62	1,58	66,91	15,06	9,96	6,39	6,63	4,25	2,83E+06
12	2020	1,92E+06	1,10E+10	0,63	78,90	0,94	6,41E+05	34,43	24,46	22,64	1,25	354,74	0,97	1,00E-05	45,18	58,58	0,97	67,42	16,98	12,71	8,43	5,24	3,47	3,61E+06
13	2021	1,68E+06	1,15E+10	0,66	72,48	0,94	5,60E+05	31,63	22,91	19,77	1,17	332,24	0,98	1,07E-05	45,25	58,58	0,91	67,47	17,19	13,15	8,75	5,07	3,37	7,18E+05
14	2022	1,47E+06	1,20E+10	0,69	66,82	0,95	4,91E+05	29,24	21,54	17,34	1,09	312,46	0,98	1,14E-05	45,32	58,57	0,86	67,52	17,39	13,57	9,06	4,91	3,28	6,97E+05
15	2023	1,31E+06	1,25E+10	0,71	61,78	0,95	4,35E+05	26,68	19,83	15,37	1,06	287,60	0,98	1,23E-05	45,40	58,57	0,79	67,58	17,64	14,16	9,49	4,71	3,15	6,70E+05
16	2024	1,16E+06	1,28E+10	0,73	57,30	0,95	3,85E+05	24,81	18,68	13,61	0,99	270,92	0,98	1,31E-05	45,45	58,56	0,74	67,62	17,81	14,60	9,81	4,56	3,07	6,51E+05
17	2025	1,03E+06	1,32E+10	0,75	53,29	0,96	3,42E+05	23,27	17,74	12,09	0,93	257,37	0,98	1,38E-05	45,50	58,56	0,70	67,65	17,95	14,99	10,09	4,45	2,99	6,36E+05
18	2026	9,16E+05	1,35E+10	0,77	49,70	0,96	3,05E+05	21,84	16,83	10,78	0,88	244,12	0,98	1,45E-05	45,54	58,56	0,67	67,68	18,08	15,39	10,38	4,33	2,92	6,20E+05
19	2027	8,19E+05	1,38E+10	0,79	46,48	0,96	2,73E+05	20,70	16,13	9,64	0,82	233,95	0,98	1,51E-05	45,58	58,56	0,64	67,70	18,19	15,73	10,63	4,23	2,86	4,47E+06
20	2028	7,35E+05	1,40E+10	0,80	43,58	0,96	2,45E+05	19,61	15,41	8,65	0,77	223,51	0,99	1,58E-05	45,61	58,55	0,61	67,73	18,30	16,10	10,90	4,14	2,80	4,58E+06
21	2029	6,51E+05	1,42E+10	0,81	40,99	0,96	2,17E+05	19,46	15,52	7,67	0,68	225,13	0,99	1,57E-05	45,61	58,55	0,62	67,72	18,28	16,04	10,85	4,15	2,81	5,96E+05
22	2030	5,88E+05	1,44E+10	0,82	38,65	0,97	1,96E+05	18,64	14,96	6,93	0,63	216,98	0,99	1,63E-05	45,63	58,55	0,59	67,74	18,37	16,34	11,07	4,07	2,76	5,86E+05
23	2031	5,28E+05	1,46E+10	0,83	36,54	0,97	1,76E+05	18,29	14,80	6,21	0,58	214,64	0,99	1,65E-05	45,64	58,55	0,59	67,75	18,40	16,43	11,14	4,05	2,75	5,83E+05
24	2032	4,77E+05	1,47E+10	0,84	34,63	0,97	1,59E+05	17,84	14,52	5,61	0,53	210,66	0,99	1,68E-05	45,65	58,55	0,58	67,76	18,44	16,59	11,25	4,01	2,72	5,77E+05
25	2033	4,26E+05	1,49E+10	0,85	32,92	0,97	1,42E+05	17,80	14,59	5,02	0,47	211,66	0,99	1,67E-05	45,65	58,55	0,58	67,76	18,43	16,55	11,22	4,02	2,73	5,79E+05
26	2034	3,89E+05	1,50E+10	0,86	31,35	0,97	1,30E+05	17,32	14,24	4,58	0,44	206,55	0,99	1,71E-05	45,67	58,55	0,56	67,77	18,48	16,76	11,37	3,97	2,70	5,72E+05
27	2035	3,67E+05	1,51E+10	0,86	29,86	0,97	1,22E+05	15,99	13,13	4,32	0,45	190,51	0,99	1,85E-05	45,73	58,55	0,52	67,80	18,66	17,46	11,88	3,81	2,59	4,96E+06

Appendix E. Economic tables

Table E.1: Economic data sheet for the reference case

Revenue (/million USD)		Total (/million USD)	Expenditure (/million USD)			Net Cash Flow	Net Presnet Value	Net Presnet Value	Daily Gas Production (in
Gas	Oil		CAPEX	OPEX	DRILLEX	(/million USD)	(/million USD)	(/million NOK)	total)
0.00	0.00	-		0.33		(0.07)	(0.07)	(0.44)	10.0E+6
1,285.61	8.00	1,293.61		2		284.15	263.03	1,578.19	10.0E+6
1,311.32	7.89	1,319.21		2		289.79	511.48	3,068.86	10.0E+6
1,337.55	7.77	1,345.31		2		295.53	746.08	4,476.46	10.0E+6
1,364.30	7.64	1,371.94		2		301.39	967.60	5,805.63	10.0E+6
1,390.31	7.50	1,397.81		2		307.08	1,176.60	7,059.58	10.0E+6
1,418.12	7.35	1,425.47		2		313.16	1,373.94	8,243.66	10.0E+6
1,352.47	6.73	1,359.20		2		298.58	1,548.16	9,288.99	9.4E+6
1,327.65	6.33	1,333.98		2		293.04	1,706.48	10,238.89	9.0E+6
1,128.35	5.15	1,133.49		2		248.93	1,831.01	10,986.05	7.5E+6
935.96	4.08	940.04		2		206.37	1,926.60	11,559.58	6.1E+6
938.95	3.89	942.85		2		206.99	2,015.37	12,092.22	6.0E+6
806.04	3.18	809.22		2		177.59	2,085.89	12,515.36	5.1E+6
676.64	2.53	679.16		2		148.98	2,140.67	12,844.03	4.2E+6
686.33	2.42	688.75		2		151.09	2,192.11	13,152.66	4.1E+6
672.25	2.23	674.48		2		147.95	2,238.75	13,432.49	4.0E+6
492.27	1.53	493.80		2		108.20	2,270.33	13,621.98	2.8E+6

Table E.2: Economic data sheet for the subsea compressor system

Total (/million USD)	Expenditure (/million USD)				Net Cash Flow	Net Presnet Value	C NPV (/million USD)	Daily Gas Production
	CAPEX	Sørco (USD)	OPEX (NOK)	OPEX(USD)	(/million USD)	(/million USD)		(in total)
-			2	0.333	(0.33)	(0.07)	(0.07)	10.0E+6
1,289.59			2	0.333	283.64	262.63	262.55	10.0E+6
1,314.87			2	0.333	289.20	247.94	510.49	10.0E+6
1,340.68			2	0.333	294.88	234.08	744.58	10.0E+6
1,367.07	58.4	24.1666667	2.9	0.483	282.48	207.63	952.21	10.0E+6
1,393.02	37.5	24.1666667	2.65	0.442	292.80	199.28	1,151.48	10.0E+6
1,420.50	37.5	24.1666667	2.92	0.487	298.84	188.32	1,339.80	10.0E+6
1,448.51	107.5	24.1666667	31.03	5.172	288.57	168.38	1,508.18	10.0E+6
1,476.98			35.1	5.850	323.65	174.86	1,683.03	10.0E+6
1,506.40			37.5	6.250	330.03	165.10	1,848.13	10.0E+6
1,536.36			52.08	8.680	336.09	155.67	2,003.81	10.0E+6
1,334.35			33.66	5.610	292.32	125.37	2,129.18	8.5E+6
1,214.46			31.38	5.230	266.03	105.64	2,234.82	7.6E+6
1,106.26			45.93	7.655	241.69	88.87	2,323.69	6.8E+6
1,009.43			30.69	5.115	220.95	75.22	2,398.92	6.1E+6
922.72			30.18	5.030	201.89	63.64	2,462.56	5.4E+6
844.34			41.82	6.970	184.22	53.77	2,516.34	4.9E+6

Table E.3: Economic data sheet for the LPM

Total (/million USD)	Expenditure (/million USD)				Net Cash Flow	Net Presnet Value	C NPV (/million USD)	Daily Gas Production
	CAPEX	Sørco (USD)	OPEX (NOK)	OPEX(USD)	(/million USD)	(/million USD)		(in total)
-			2	0.333	(0.07)	(0.33)	(0.33)	10.0E+6
1,289.59			2	0.333	283.64	262.63	262.29	10.0E+6
1,314.87			2	0.333	289.20	247.94	510.23	10.0E+6
1,340.68			2	0.333	294.88	234.08	744.32	10.0E+6
1,367.07	58.4	24.1666667	2.9	0.483	282.48	207.63	951.95	10.0E+6
1,393.02	37.5	24.1666667	2.65	0.442	292.80	199.28	1,151.22	10.0E+6
1,420.50	37.5	24.1666667	2.92	0.487	298.84	188.32	1,339.54	10.0E+6
1,448.51	107.5	24.1666667	31.03	5.172	288.57	168.38	1,507.92	10.0E+6
1,476.96			35.1	5.850	323.64	174.85	1,682.77	10.0E+6
1,506.39			37.5	6.250	330.03	165.10	1,847.87	10.0E+6
1,536.34			52.08	8.680	336.09	155.67	2,003.54	10.0E+6
1,331.88			33.66	5.610	291.78	125.14	2,128.68	8.5E+6
1,326.36			31.38	5.230	290.65	115.42	2,244.10	8.3E+6
1,222.40			45.93	7.655	267.24	98.26	2,342.37	7.5E+6
1,113.78			30.69	5.115	243.91	83.04	2,425.41	6.7E+6
1,017.28			30.18	5.030	222.70	70.20	2,495.61	6.0E+6
951.13			41.82	6.970	207.72	60.63	2,556.24	5.5E+6

Table E.4: Economic data sheet for the topside compressor system.

Total (/million USD)	Expenditure (/million USD)				Net Cash Flow (/million USD)	Net Presnet Value (/million USD)	C NPV (/million USD)	Daily Gas Production (in total)
	CAPEX	Sørco (USD)	OPEX (NOK)	OPEX(USD)				
-			2	0.333	(0.07)	(0.33)	(0.33)	10.0E+6
1,289.59			2	0.333	283.64	262.63	262.29	10.0E+6
1,314.87			2	0.333	289.20	247.94	510.23	10.0E+6
1,340.68			2	0.333	294.88	234.08	744.32	10.0E+6
1,367.07	58.4	24.1666667	2.9	0.483	282.48	207.63	951.95	10.0E+6
1,393.02	37.5	24.1666667	2.65	0.442	292.80	199.28	1,151.22	10.0E+6
1,420.50	37.5	24.1666667	2.92	0.487	298.84	188.32	1,339.54	10.0E+6
1,448.51	107.5	24.1666667	31.03	5.172	288.57	168.38	1,507.92	10.0E+6
1,477.35			35.1	5.850	323.73	174.90	1,682.82	10.0E+6
1,506.71			37.5	6.250	330.10	165.13	1,847.95	10.0E+6
1,374.67			52.08	8.680	300.52	139.20	1,987.15	8.9E+6
1,257.09			33.66	5.610	275.33	118.08	2,105.23	8.0E+6
1,152.21			31.38	5.230	252.34	100.21	2,205.44	7.2E+6
1,058.14			45.93	7.655	231.11	84.98	2,290.42	6.5E+6
973.34			30.69	5.115	213.01	72.52	2,362.94	5.9E+6
896.54			30.18	5.030	196.13	61.83	2,424.77	5.3E+6
826.74			41.82	6.970	180.35	52.64	2,477.41	4.8E+6

Appendix F. Reservoir Optimization Cases

Table F1. Flow Calculation for Reference Case / No Compressors with blue color shows the end of natural plateau (2014)

		East tank, template L, 4 wells									West tank, template M, 3 wells																
year count	Calendar year	qf	dGp	Gp	GP/G	PR	Z	qw	pwf	pwh	qf,M	DGp	Gp	GP/G	PR	Z	qw	pwf	pwh	Psep	PtowheadL	P-outL	DpChookeL	PtowheadM	P-outM	DPchookeM	Qfield	Year
		Sm3/d						Sm3/d	bara	bara							Sm3/d	bara	bara	bara	bara							
0	2008	6,0E+6	000,0E+0	0,00E+00	-	240	0,957	1,5E+6	220	173,2	4,0E+6	000,00E+0	0,00E+00	0,00	210	0,926	1,3E+6	178	146	65 173,12	168,32	103,32	145,95	143,43	78,43	10,0E+6	2008
1	2009	6,0E+6	2,0E+9	1,97E+09	0,04	231	0,953	1,5E+6	210	165,2	4,0E+6	1,32E+9	1,32E+09	0,08	194	0,921	1,3E+6	158	129	65 165,18	160,15	95,15	129,46	126,62	61,62	10,0E+6	2009
2	2010	6,0E+6	2,0E+9	3,94E+09	0,07	222	0,948	1,5E+6	199	156,3	4,0E+6	1,32E+9	2,64E+09	0,15	177	0,918	1,3E+6	137	111	65 156,26	150,93	85,93	111,07	107,74	42,74	10,0E+6	2010
3	2011	6,0E+6	2,0E+9	5,90E+09	0,11	212	0,945	1,5E+6	189	147,3	4,0E+6	1,32E+9	3,96E+09	0,23	161	0,917	1,3E+6	116	92	65 147,29	141,62	76,62	91,73	87,67	22,67	10,0E+6	2011
4	2012	6,0E+6	2,0E+9	7,87E+09	0,15	203	0,942	1,5E+6	178	138,4	4,0E+6	1,32E+9	5,28E+09	0,30	145	0,918	1,3E+6	92	70	65 138,34	132,29	67,29	70,43	65,05	0,05	10,0E+6	2012
5	2013	7,5E+6	2,5E+9	1,03E+10	0,19	191	0,938	1,9E+6	156	115,7	2,5E+6	825,00E+6	6,11E+09	0,35	135	0,919	833,3E+3	107	87	65 115,62	103,96	38,96	87,40	85,76	20,76	10,0E+6	2013
6	2014	7,5E+6	2,5E+9	1,28E+10	0,24	180	0,936	1,9E+6	141	103,2	2,5E+6	825,00E+6	6,93E+09	0,40	126	0,921	833,3E+3	94	77	65 103,07	89,80	24,80	76,52	74,63	9,63	10,0E+6	2014
7	2015	7,0E+6	2,3E+9	1,51E+10	0,28	169	0,935	1,8E+6	132	96,2	2,4E+6	775,50E+6	7,71E+09	0,44	117	0,923	783,3E+3	85	69	65 96,09	83,68	18,68	68,75	66,90	1,90	9,4E+6	2015
8	2016	7,0E+6	2,3E+9	1,74E+10	0,32	159	0,934	1,8E+6	118	84,1	2,0E+6	660,00E+6	8,37E+09	0,48	109	0,926	666,7E+3	82	67	65 83,93	69,38	4,38	66,70	65,32	0,32	9,0E+6	2016
9	2017	6,0E+6	2,0E+9	1,94E+10	0,36	151	0,934	1,5E+6	116	84,7	1,5E+6	495,00E+6	8,86E+09	0,51	104	0,928	500,0E+3	84	70	65 84,60	74,28	9,28	69,62	68,88	3,88	7,5E+6	2017
10	2018	5,0E+6	1,6E+9	2,10E+10	0,39	143	0,934	1,3E+6	115	86,7	1,1E+6	363,00E+6	9,22E+09	0,53	99	0,930	366,7E+3	86	72	65 86,67	79,83	14,83	71,86	71,47	6,47	6,1E+6	2018
11	2019	5,0E+6	1,6E+9	2,26E+10	0,42	136	0,934	1,3E+6	106	79,0	1,0E+6	330,00E+6	9,55E+09	0,55	96	0,931	333,3E+3	83	70	65 78,88	71,30	6,30	69,66	69,33	4,33	6,0E+6	2019
12	2020	4,3E+6	1,4E+9	2,40E+10	0,44	130	0,935	1,1E+6	104	79,3	744,7E+3	245,75E+6	9,80E+09	0,56	93	0,933	248,2E+3	84	71	65 79,24	73,72	8,72	70,67	70,49	5,49	5,1E+6	2020
13	2021	3,5E+6	1,2E+9	2,52E+10	0,46	126	0,936	878,1E+3	105	81,5	643,6E+3	212,38E+6	1,00E+10	0,57	90	0,934	214,5E+3	83	70	65 81,46	77,94	12,94	69,77	69,64	4,64	4,2E+6	2021
14	2022	3,5E+6	1,2E+9	2,63E+10	0,49	121	0,937	878,1E+3	99	76,5	620,6E+3	204,79E+6	1,02E+10	0,58	88	0,935	206,9E+3	81	68	65 76,48	72,72	7,72	67,91	67,78	2,78	4,1E+6	2022
15	2023	3,5E+6	1,1E+9	2,75E+10	0,51	116	0,938	867,2E+3	93	71,9	500,6E+3	165,19E+6	1,04E+10	0,59	86	0,936	166,9E+3	81	68	65 71,88	67,97	2,97	67,76	67,67	2,67	4,0E+6	2023
16	2024	2,3E+6	770,2E+6	2,83E+10	0,52	113	0,939	587,1E+3	99	78,5	500,7E+3	165,23E+6	1,05E+10	0,60	84	0,937	166,9E+3	79	66	65 78,47	76,85	11,85	66,02	65,94	0,94	2,8E+6	2024
17	2025	2,3E+6	770,2E+6	2,90E+10	0,54	109	0,939	587,1E+3	95	75,4	300,7E+3	99,23E+6	1,06E+10	0,61	83	0,937	100,2E+3	80	67	65 75,40	73,72	8,72	67,46	67,43	2,43	2,6E+6	2025
18	2026	2,3E+6	770,2E+6	2,98E+10	0,55	106	0,940	587,1E+3	91	72,3	300,7E+3	99,23E+6	1,07E+10	0,61	82	0,938	100,2E+3	79	66	65 72,30	70,55	5,55	66,45	66,42	1,42	2,6E+6	2026
19	2027	2,3E+6	770,2E+6	3,06E+10	0,56	103	0,941	587,1E+3	88	69,2	300,7E+3	99,23E+6	1,08E+10	0,62	81	0,939	100,2E+3	78	65	65 69,17	67,33	2,33	65,44	65,41	0,41	2,6E+6	2027
20	2028	2,0E+6	671,8E+6	3,12E+10	0,58	100	0,942	512,1E+3	87	69,0	200,7E+3	66,23E+6	1,09E+10	0,62	80	0,939	66,9E+3	78	66	65 69,02	67,62	2,62	65,87	65,86	0,86	2,2E+6	2028
21	2029	1,8E+6	606,2E+6	3,18E+10	0,59	97	0,943	462,1E+3	86	68,3	200,7E+3	66,23E+6	1,10E+10	0,63	79	0,939	66,9E+3	77	65	65 68,27	67,12	2,12	65,21	65,19	0,19	2,0E+6	2029

Table F.2.1 Flow Calculation For Topside Compressor (the blue colour show the end of natural plateau (2015), and orange shows the end of driven plateau (2016,9).

		East tank, template L, 4 wells									West tank, template M, 3 wells								
year count	Calendar year	qf	dGp	Gp	GP/G	PR	Z	qw	pwf	pwh	qf,M	DGp	Gp	GP/G	PR	Z	qw	pwf	pwh
		Sm3/d						Sm3/d	bara	bara							Sm3/d	bara	bara
0	2008	6,0E+6	000,0E+0	0,00E+00	-	240	0,957	1,5E+6	220	173,2	4,0E+6	000,00E+0	0,00E+00	0,00	210	0,926	1,3E+6	178	146
1	2009	6,0E+6	2,0E+9	1,97E+09	0,04	231	0,953	1,5E+6	210	165,2	4,0E+6	1,32E+9	1,32E+09	0,08	194	0,921	1,3E+6	158	129
2	2010	6,0E+6	2,0E+9	3,94E+09	0,07	222	0,948	1,5E+6	199	156,3	4,0E+6	1,32E+9	2,64E+09	0,15	177	0,918	1,3E+6	137	111
3	2011	6,0E+6	2,0E+9	5,90E+09	0,11	212	0,945	1,5E+6	189	147,3	4,0E+6	1,32E+9	3,96E+09	0,23	161	0,917	1,3E+6	116	92
4	2012	6,0E+6	2,0E+9	7,87E+09	0,15	203	0,942	1,5E+6	178	138,4	4,0E+6	1,32E+9	5,28E+09	0,30	145	0,918	1,3E+6	92	70
5	2013	7,6E+6	2,5E+9	1,04E+10	0,19	191	0,938	1,9E+6	155	114,7	2,4E+6	792,00E+6	6,07E+09	0,35	136	0,919	800,0E+3	109	89
6	2014	7,6E+6	2,5E+9	1,29E+10	0,24	180	0,936	1,9E+6	140	101,9	2,4E+6	792,00E+6	6,86E+09	0,39	127	0,921	800,0E+3	97	79
7	2015	7,7E+6	2,5E+9	1,54E+10	0,28	168	0,934	1,9E+6	125	87,2	2,3E+6	759,00E+6	7,62E+09	0,44	118	0,923	766,7E+3	87	71
8,00761114	2016	7,6E+6	2,5E+9	1,79E+10	0,33	157	0,934	1,9E+6	110	74,2	2,4E+6	809,59E+6	8,43E+09	0,48	108	0,926	811,6E+3	71	56
8,99993832	2016,9	7,4E+6	2,4E+9	2,03E+10	0,37	146	0,934	1,9E+6	96	60,4	2,6E+6	836,29E+6	9,27E+09	0,53	99	0,930	851,3E+3	51	37
10	2018	6,8E+6	2,2E+9	2,25E+10	0,42	137	0,934	1,7E+6	89	56,5	2,2E+6	720,31E+6	9,99E+09	0,57	90	0,934	727,5E+3	48	36
11	2019	6,2E+6	2,0E+9	2,45E+10	0,45	128	0,935	1,5E+6	83	53,2	1,9E+6	617,31E+6	1,06E+10	0,61	83	0,937	623,5E+3	46	35
12	2020	5,6E+6	1,8E+9	2,64E+10	0,49	120	0,937	1,4E+6	77	50,3	1,6E+6	530,54E+6	1,11E+10	0,64	77	0,941	535,9E+3	44	35
13	2021	5,1E+6	1,7E+9	2,81E+10	0,52	113	0,938	1,3E+6	72	47,8	1,4E+6	457,03E+6	1,16E+10	0,66	72	0,944	461,7E+3	43	34
14	2022	4,7E+6	1,5E+9	2,96E+10	0,55	107	0,940	1,2E+6	68	45,7	1,2E+6	394,44E+6	1,20E+10	0,69	67	0,947	398,4E+3	42	34
15	2023	4,3E+6	1,4E+9	3,10E+10	0,57	101	0,942	1,1E+6	64	43,8	1,0E+6	340,88E+6	1,23E+10	0,70	63	0,949	344,3E+3	41	34
16	2024	3,9E+6	1,3E+9	3,23E+10	0,60	96	0,944	971,9E+3	61	42,2	893,6E+3	294,88E+6	1,26E+10	0,72	60	0,951	297,9E+3	41	34

Table F.2.2 Flow Calculation for Topside Compressor Case (Continued.)

							2*14											
Pscp	Ptwhead,L	P-ouL	DpChookL	Ptwhead,M	P-ouM	DPChookM	Psuc-L	Psuc-M									Qfield	Year
bara	bara						bara	bara									Sm3/day	
65	173,12	168,32	103,32	145,95	143,43	78,43											10,0E+6	2008
65	165,18	160,15	95,15	129,46	126,62	61,62											10,0E+6	2009
65	156,26	150,93	85,93	111,07	107,74	42,74											10,0E+6	2010
65	147,29	141,62	76,62	91,73	87,67	22,67											10,0E+6	2011
65	138,34	132,29	67,29	70,43	65,05	0,05											10,0E+6	2012
65	114,59	102,48	37,48	89,41	87,93	22,93			P suc av	errorsuc	delta p comp	rp					10,0E+6	2013
65	101,76	87,90	22,90	79,20	77,53	12,53			bara	bara^2	bara						10,0E+6	2014
65	86,99	69,77	4,77	70,88	69,16	4,16											10,0E+6	2015
65	74,04			56,09			53,63	53,63	53,63	6,19E-18	11,37	1,211924571					10,0E+6	2016
65	60,15			37,30			33,08	33,08	33,08	3,78E-14	31,92	1,964793197	Δp comp fixed	error comp		Total flow	10,0E+6	2016,9
65	56,31			36,14			33,00	33,00	33,00	1,05E-07	32,00	1,969688651	[bara]	[bara^2]			8,9E+6	2018
65	53,02			35,33			33,00	33,00	33,00	1,01E-05	32,00	1,969696969	32	3,59E-17		8,02E+06	8,0E+6	2019
65	50,17			34,74			33,00	33,00	33,00	4,96E-09	32,00	1,96969697	32	1,50E-18		7,21E+06	7,2E+6	2020
65	47,71			34,30			33,00	33,00	33,00	7,65E-10	32,00	1,969696974	32	4,14E-15		6,49E+06	6,5E+6	2021
65	45,58			33,97			33,00	33,00	33,00	2,14E-08	32,00	1,969696965	32	5,96E-15		5,86E+06	5,9E+6	2022
65	43,74			33,73			33,00	33,00	33,00	4,89E-09	32,00	1,969696952	32	8,69E-14		5,29E+06	5,3E+6	2023
65	42,15			33,55			33,00	33,00	33,00	1,18E-09	32,00	1,96969697	32	1,45E-18		4,78E+06	4,8E+6	2024

Table F.3.1The Flow Calculation for LPM (low pressure modification), the blue color shows the end of natural plateau (2015), and orange show the end of driven plateau flow (2017.6)

		East tank, template L, 4 wells										West tank, template M, 3 wells								
year count	Calendar year	qf	dGp	Gp	GP/G	PR	Z	qw	pwf	pwh		qf,M	DGp	Gp	GP/G	PR	Z	qw	pwf	pwh
		Sm3/d						Sm3/d	bara	bara								Sm3/d	bara	bara
0	2008	6,0E+6	000,0E+0	0,00E+00	-	240	0,957	1,5E+6	220	173,2		4,0E+6	000,00E+0	0,00E+00	0,00	210	0,926	1,3E+6	178	146
1	2009	6,0E+6	2,0E+9	1,97E+09	0,04	231	0,953	1,5E+6	210	165,2		4,0E+6	1,32E+9	1,32E+09	0,08	194	0,921	1,3E+6	158	129
2	2010	6,0E+6	2,0E+9	3,94E+09	0,07	222	0,948	1,5E+6	199	156,3		4,0E+6	1,32E+9	2,64E+09	0,15	177	0,918	1,3E+6	137	111
3	2011	6,0E+6	2,0E+9	5,90E+09	0,11	212	0,945	1,5E+6	189	147,3		4,0E+6	1,32E+9	3,96E+09	0,23	161	0,917	1,3E+6	116	92
4	2012	6,0E+6	2,0E+9	7,87E+09	0,15	203	0,942	1,5E+6	178	138,4		4,0E+6	1,32E+9	5,28E+09	0,30	145	0,918	1,3E+6	92	70
5	2013	7,6E+6	2,5E+9	1,04E+10	0,19	191	0,938	1,9E+6	155	114,7		2,4E+6	792,00E+6	6,07E+09	0,35	136	0,919	800,0E+3	109	89
6	2014	7,6E+6	2,5E+9	1,29E+10	0,24	180	0,936	1,9E+6	140	101,9		2,4E+6	792,00E+6	6,86E+09	0,39	127	0,921	800,0E+3	97	79
7	2015	7,7E+6	2,5E+9	1,54E+10	0,28	168	0,934	1,9E+6	125	87,2		2,3E+6	759,00E+6	7,62E+09	0,44	118	0,923	766,7E+3	87	71
8	2016	8,0E+6	2,6E+9	1,80E+10	0,33	157	0,934	2,0E+6	106	67,6		2,0E+6	666,44E+6	8,29E+09	0,47	110	0,925	673,2E+3	82	67
9	2017	7,8E+6	2,6E+9	2,06E+10	0,38	145	0,934	1,9E+6	91	52,6		2,2E+6	731,52E+6	9,02E+09	0,52	102	0,929	738,9E+3	66	52
9,619582136	2017,6	7,7E+6	1,6E+9	2,21E+10	0,41	139	0,934	1,9E+6	81	41,6		2,3E+6	474,65E+6	9,50E+09	0,54	96	0,931	773,8E+3	54	41
11	2019	7,0E+6	3,2E+9	2,53E+10	0,47	125	0,936	1,8E+6	66	26,5		2,1E+6	979,38E+6	1,05E+10	0,60	85	0,937	716,6E+3	37	26
12	2020	6,3E+6	2,1E+9	2,74E+10	0,50	116	0,938	1,6E+6	60	24,6		1,9E+6	619,19E+6	1,11E+10	0,63	78	0,940	625,4E+3	34	24
13	2021	5,7E+6	1,9E+9	2,92E+10	0,54	108	0,940	1,4E+6	54	22,7		1,6E+6	543,19E+6	1,16E+10	0,66	71	0,944	548,7E+3	31	22
14	2022	5,2E+6	1,7E+9	3,09E+10	0,57	101	0,942	1,3E+6	49	21,1		1,4E+6	478,00E+6	1,21E+10	0,69	66	0,948	482,8E+3	28	21
15	2023	4,7E+6	1,5E+9	3,25E+10	0,60	95	0,944	1,2E+6	45	19,7		1,3E+6	422,32E+6	1,25E+10	0,72	61	0,951	426,6E+3	26	19
16	2024	4,3E+6	1,4E+9	3,39E+10	0,63	89	0,946	1,1E+6	42	18,5		1,1E+6	374,08E+6	1,29E+10	0,74	57	0,954	377,9E+3	24	18
17	2025	3,9E+6	1,3E+9	3,52E+10	0,65	83	0,948	977,2E+3	38	17,6		1,0E+6	332,29E+6	1,32E+10	0,76	53	0,956	335,6E+3	23	17

Table F.3.2 The Flow Calculation for LPM (continued)

							2*14								
Psep	PtowheadL	P-outL	DpChookeL	PtowheadM	P-outM	DPChookeM	Ptowhead							Qfield	Year
bara	bara						bara								
65	173,12	168,32	103,32	145,95	143,43	78,43								10,0E+6	2008
65	165,18	160,15	95,15	129,46	126,62	61,62								10,0E+6	2009
65	156,26	150,93	85,93	111,07	107,74	42,74								10,0E+6	2010
65	147,29	141,62	76,62	91,73	87,67	22,67								10,0E+6	2011
65	138,34	132,29	67,29	70,43	65,05	0,05								10,0E+6	2012
65	114,59	102,48	37,48	89,41	87,93	22,93		P suc av	errorsuc	delta p comp	rp			10,0E+6	2013
65	101,76	87,90	22,90	79,20	77,53	12,53		bara	bara^2	bara				10,0E+6	2014
65	86,99	69,77	4,77	70,88	69,16	4,16								10,0E+6	2015
65	67,34			67,34			73,23	67,34	4,26E-15	5,89	1,087530845			10,0E+6	2016
65	52,32			52,32			73,23	52,32	8,58E-08	20,92	1,399792111	Δp comp fixed	error comp	10,0E+6	2017
65	41,23			41,23			73,23	41,23	1,53E-14	32,00	1,776091324	[bara]	[bara^2]	10,0E+6	2017,6
28	26,04			26,04			41,69	26,04	1,61E-06	15,65	1,600777489	15	4,16E-01	9,2E+6	2019
28	24,22			24,23			39,35	24,22	2,97E-06	15,13	1,624610084	15	1,70E-02	8,2E+6	2020
28	22,29			22,29			37,44	22,29	3,52E-10	15,15	1,679548722	15	2,23E-02	7,4E+6	2021
28	20,73			20,73			35,85	20,73	1,64E-10	15,12	1,72920214	15	1,42E-02	6,6E+6	2022
28	19,38			19,38			34,54	19,38	3,32E-10	15,16	1,782565983	15	2,66E-02	6,0E+6	2023
28	18,28			18,28			33,45	18,28	2,55E-10	15,16	1,829218651	15	2,63E-02	5,4E+6	2024
28	17,39			17,39			32,54	17,39	1,81E-10	15,16	1,87182543	15	2,46E-02	4,9E+6	2025

Table F.4.1Flow Calculation for Subsea Compressor Case (The blue color shows the end of the natural plateau (2015) and orange shows the end of the driven plateau (2017.6)

		East tank, template L, 4 wells										West tank, template M, 3 wells								
year count	Calendar year	qf	dGp	Gp	GP/G	PR	Z	qw	pwf	pwh		qfM	DGp	Gp	GP/G	PR	Z	qw	pwf	pwh
		Sm3/d						Sm3/d	bara	bara								Sm3/d	bara	bara
0	2008	6,0E+6	000,0E+0	0,00E+00	-	240	0,957	1,5E+6	220	173,2		4,0E+6	000,00E+0	0,00E+00	0,00	210	0,926	1,3E+6	178	146
1	2009	6,0E+6	2,0E+9	1,97E+09	0,04	231	0,953	1,5E+6	210	165,2		4,0E+6	1,32E+9	1,32E+09	0,08	194	0,921	1,3E+6	158	129
2	2010	6,0E+6	2,0E+9	3,94E+09	0,07	222	0,948	1,5E+6	199	156,3		4,0E+6	1,32E+9	2,64E+09	0,15	177	0,918	1,3E+6	137	111
3	2011	6,0E+6	2,0E+9	5,90E+09	0,11	212	0,945	1,5E+6	189	147,3		4,0E+6	1,32E+9	3,96E+09	0,23	161	0,917	1,3E+6	116	92
4	2012	6,0E+6	2,0E+9	7,87E+09	0,15	203	0,942	1,5E+6	178	138,4		4,0E+6	1,32E+9	5,28E+09	0,30	145	0,918	1,3E+6	92	70
5	2013	7,6E+6	2,5E+9	1,04E+10	0,19	191	0,938	1,9E+6	155	114,7		2,4E+6	792,00E+6	6,07E+09	0,35	136	0,919	800,0E+3	109	89
6	2014	7,6E+6	2,5E+9	1,29E+10	0,24	180	0,936	1,9E+6	140	101,9		2,4E+6	792,00E+6	6,86E+09	0,39	127	0,921	800,0E+3	97	79
7	2015	7,7E+6	2,5E+9	1,54E+10	0,28	168	0,934	1,9E+6	125	87,2		2,3E+6	759,00E+6	7,62E+09	0,44	118	0,923	766,7E+3	87	71
8	2016	8,0E+6	2,6E+9	1,80E+10	0,33	157	0,934	2,0E+6	106	67,6		2,0E+6	666,44E+6	8,29E+09	0,47	110	0,925	673,2E+3	82	67
9	2017	7,8E+6	2,6E+9	2,06E+10	0,38	145	0,934	1,9E+6	91	52,6		2,2E+6	731,52E+6	9,02E+09	0,52	102	0,929	738,9E+3	66	52
9,619582136	2017,6	7,7E+6	1,6E+9	2,21E+10	0,41	139	0,934	1,9E+6	81	41,6		2,3E+6	474,65E+6	9,50E+09	0,54	96	0,931	773,8E+3	54	41
11	2019	6,6E+6	3,0E+9	2,51E+10	0,46	126	0,936	1,7E+6	72	39,3		1,9E+6	861,52E+6	1,04E+10	0,59	86	0,936	630,4E+3	50	39
12	2020	6,0E+6	2,0E+9	2,71E+10	0,50	118	0,937	1,5E+6	67	38,1		1,6E+6	541,36E+6	1,09E+10	0,62	80	0,939	546,8E+3	48	38
13	2021	5,4E+6	1,8E+9	2,88E+10	0,53	110	0,939	1,3E+6	63	37,1		1,4E+6	469,58E+6	1,14E+10	0,65	75	0,942	474,3E+3	46	37
14	2022	4,8E+6	1,6E+9	3,04E+10	0,56	103	0,941	1,2E+6	60	36,3		1,2E+6	407,67E+6	1,18E+10	0,67	70	0,945	411,8E+3	45	36
15	2023	4,4E+6	1,4E+9	3,18E+10	0,59	97	0,943	1,1E+6	57	35,7		1,1E+6	354,29E+6	1,21E+10	0,69	66	0,948	357,9E+3	43	36
16	2024	3,9E+6	1,3E+9	3,31E+10	0,61	92	0,945	987,1E+3	54	35,1		934,7E+3	308,45E+6	1,24E+10	0,71	62	0,950	311,6E+3	43	35

Table F.4.2: Flow Calculation for Subsea Compressor (Continued)

							2*14								
Psep	PtowheadL	P-outL	DpChookeL	PtowheadM	P-outM	DPChookeM	Ptowhead							Qfield	Year
bara	bara						bara								
65	173,12	168,32	103,32	145,95	143,43	78,43								10,0E+6	2008
65	165,18	160,15	95,15	129,46	126,62	61,62								10,0E+6	2009
65	156,26	150,93	85,93	111,07	107,74	42,74								10,0E+6	2010
65	147,29	141,62	76,62	91,73	87,67	22,67								10,0E+6	2011
65	138,34	132,29	67,29	70,43	65,05	0,05								10,0E+6	2012
65	114,59	102,48	37,48	89,41	87,93	22,93		P suc av	errorsuc	delta p comp	rp			10,0E+6	2013
65	101,76	87,90	22,90	79,20	77,53	12,53		bara	bara^2	bara				10,0E+6	2014
65	86,99	69,77	4,77	70,88	69,16	4,16								10,0E+6	2015
65	67,34			67,34			73,23	67,34	4,26E-15	5,89	1,087530845			10,0E+6	2016
65	52,32			52,32			73,23	52,32	8,58E-08	20,92	1,399792111	Δp comp fixed	error comp	10,0E+6	2017
65	41,23			41,23			73,23	41,23	1,53E-14	32,00	1,776091324	[bara]	[bara^2]	10,0E+6	2017,6
65	39,05			39,09			71,07	39,07	1,00E-03	32,00	1,819015578	32	7,85E-06	8,5E+6	2019
65	37,85			37,89			69,87	37,87	8,67E-04	32,00	1,844883512	32	7,35E-07	7,6E+6	2020
65	36,94			36,89			68,92	36,92	1,00E-03	32,00	1,866799491	32	1,18E-06	6,8E+6	2021
65	36,18			36,15			68,15	36,16	5,73E-04	31,99	1,884532304	32	1,45E-04	6,1E+6	2022
65	35,52			35,57			67,54	35,54	9,37E-04	32,00	1,900292633	32	1,43E-07	5,4E+6	2023
65	35,03			35,08			67,05	35,06	9,12E-04	32,00	1,91283047	32	3,06E-07	4,9E+6	2024